

**MECHANICAL BEHAVIOR OF REINFORCED CONCRETE
SLAB RETROFITTED WITH CARBON FIBER SHEET**

March 2000

Hae-Geun PARK

ACKNOWLEDGEMENTS

I would like to express my sincere and profound gratitude to Dr. Koichi Ono, Professor of Department of Civil System Engineering at Kyoto University for his invaluable advice and encouragement during the doctoral course. His flexible ideas and rich scholarship were a matter of great importance for this research. I would like to bestow my best respect to his dedications to this dissertation.

I am also deeply indebted to Professor Takeshi Tamura and Professor Toyooki Miyagawa of Kyoto University for their advice and review of this dissertation.

I acknowledge the support from the Nippon oil Co.,Ltd, Konishi Co.,Ltd and Sunkit Co.,Ltd. I am indebted to all my colleagues and juniors of *Composite Structural Design Laboratory* at Kyoto University, for their warm affection to daily life in Japan.

I wish to express my appreciation and gratitude to Professor Young-Shik Shin, Professor Young-Bong Kwon, Professor Hyug-Moon Kwon, Professor Kwang-Sung Woo and Professor Jae-Hoon Lee, professors of Yeung Nam University, Korea.

Sincere thanks also go to Professor Soon-Tak Lee and Professor Hong-Kee Jee of Yeung Nam University, Professor Chung-Bang Yoon and Professor Jin-Keun Kim of KAIST, for their encouragement.

I acknowledge the useful help and encouragement from Dr. S.W. Kim of KICT, Professor K.H. Park and Professor J.K Seo of Kyung dong college, Professor J.H Kim of An Yang university, Professor Y.S. Park of AIT, Korea, Mr. S.Y. Bae, Dr. J.Y. Song and Mr. H.S.Son of Yeung Nam University, and Mr. D.G. Park of Yokohama National University.

I also appreciate the financial assistance from the International Rotary foundation, and special thanks go to Mr. Koichiro Kitaoku who was my counselor.

Finally, I am deeply grateful to all members of my families including my parents for their warm encourage and support during the stay in Japan and to my wife Ju-Hee, my daughter Hae-Jin for their understanding and encouragement.

CONTENTS

ACKNOWLEDGEMENT

Chapter 1 INTRODUCTION

1.1 GENERAL REMARKS	1
1.2 RESEARCH SIGNIFICANCE	2

Chapter 2 REVIEW OF PREVIOUS RESEARCH

2.1 INTRODUCTION	3
2.2 CHARACTERISTICS OF ADVANCED FIBER MATERIALS	
2.2.1 Carbon Fibers	5
2.2.2 Aramid Fibers	5
2.2.3 Glass Fibers	6
2.3 STRUCTURAL BEHAVIOR OF LAMINATED RC MEMBERS BY ADVANCED FIBER MATERIALS	
2.3.1 Flexural Strengthening	7
2.3.2 Shear Strengthening	13
2.3.3 FRP Confinement	18
2.3.4 Durability	21
2.3.5 Interfacial Bond Mechanism of FRP Sheets	23
2.3.6 FRP Strands and bar	26
2.4 SEISMIC RETROFIT OF HIGHWAY RC BRIDGE	
2.4.1 Damage of RC Bridge due to Earthquake	28

	2.4.2	Seismic Retrofit of Bridge Columns	28		4.3.3	Load - Strain Relationship	55
	2.4.3	Seismic Retrofit of Beam-Column Connections	34		4.3.4	Effect of Flexural Strength Improvement	56
	2.4.4	Other methods for Enhancing Seismic Behavior	34		4.3.5	Effect of Anchoring System	56
					4.3.6	Strain of Carbon Fiber Sheets at the Failure	57
Chapter 3	INTERFACIAL BOND BEHAVIOR BETWEEN CONCRETE SURFACE AND CARBON FIBER SHEET			4.4	ANALYTICAL STUDY		
	3.1	INTRODUCTION	36		4.4.1	Section Analysis	58
	3.2	EXPERIMENTAL PROGRAM			4.4.2	Finite Element Analysis	65
		3.2.1	Test Specimen	37	4.5	CONCLUSIONS OF CHAPTER 4	
		3.2.2	Loading Set-Up & Measurement	38			72
	3.3	TEST RESULTS AND DISCUSSION		Chapter 5	FATIGUE BEHAVIOR OF RC& CARBON FIBER SHEET COMPOSITE SLAB UNDER LARGE REPEATED LOADING		
		3.3.1	Experimental Results	39		5.1	INTRODUCTION
		3.3.2	Comparison With Finite Element Analysis	42		5.2	EXPERIMENTAL PROGRAM
	3.4	CONCLUSIONS OF CHAPTER 3		46			5.2.1
							Test Specimen
Chapter 4	STRENGTH IMPROVEMENT OF LAMINATED RC SLAB BY CARBON FIBER SHEET						76
	4.1	INTRODUCTION	47				5.2.2
	4.2	EXPERIMENTAL PROGRAM					Retrofitting of Carbon Fiber Sheets
		4.2.1	Test Specimen	47			5.2.3
		4.2.2	Material Properties	48			Loading Set Up & Measurement
		4.2.3	Strengthening of Carbon Fiber Sheets	50		5.3	TEST RESULTS AND DISCUSSION
		4.2.4	Loading Set Up	51			5.3.1
		4.2.5	Measurement & Test Procedure	52			Flexural Fatigue Test Results
	4.3	TEST RESULTS AND DISCUSSION					5.3.2
		4.3.1	Structural Behavior & Failure Mode	53			Loss of Flexural Stiffness due to Fatigue
		4.3.2	Load - Deflection Relationship	54			5.4
							ASSESSMENT OF CUMULATIVE FATIGUE DAMAGE
							5.4.1
							Total Dissipated Energy Capacity
							5.4.2
							Progressive Accumulation of Damage
							5.4.3
							Applications of Infrared Thermography
							5.4.4
							Retrofit Design Concept for RC Bridge Slab
							92
							5.5
							CONCLUSIONS OF CHAPTER 5
							93
Chapter 6	FLEXURAL STRENGTH EVALUATION OF A RC SLAB RETROFITTED WITH CARBON FIBER SHEET						

6.1 INTRODUCTION	94
6.2 PROPOSED NEW ANALYTICAL METHOD BASED ON BOND STRENGTH	
6.2.1 Strain, Stress and Curvature in Composite Cross Section	95
6.2.2 Estimation of the Ultimate Flexural Strength	98
6.2.3 Comparison of Analytical and Experimental Results	104
6.2.4 Parametric Study	105
6.2.5 Iterative procedures	108
6.3 CONCLUSIONS OF CHAPTER 6	111
Chapter 7 SUMMARY AND CONCLUSIONS	112
REFERENCES	119
ABSTRACT (IN JAPANESE)	135
AUTHOR'S RESEARCH ACTIVITY	137

Chapter 1

INTRODUCTION

1.1 GENERAL REMARKS

Reinforced Concrete (RC) has been widely used as a potential structural material for infrastructures. However, many RC structures have been damaged and deteriorated due to aggressive environments, increase of the traffic load, severe earthquakes and other reasons. Need for repair and retrofitting of damaged RC structures has become one of the important issues confronting the repair and rehabilitation industries worldwide.

Since 1960, as one of the primary retrofit techniques, externally bonded steel jacketing method has been widely used to retrofit these damaged RC structures. However, this method has some disadvantages due to handling of heavy materials, difficulties of construction, maintenance and corrosion. Particularly, corrosion has much influence on the bond strength between steel plate and bonded concrete surface, and finally causes the failure of structure.

From the last decade, the use of Fiber-Reinforced-Plastic (FRP) Composite materials such as Carbon fiber, Aramid fiber and Glass fiber for strengthening of damaged RC members has emerged as one of the most exciting and promising technologies in

material and structural engineering field owing to following advantages;

- ◆ High tensile strength
- ◆ Easy handling owing to lightweight and good flexibility
- ◆ Reduction of corrosion related problems
- ◆ Practically no increase of dead weight of the structure
- ◆ Little interruption in the use of the structure

1.2 RESEARCH SIGNIFICANCE

Through numerous researches and applications, Carbon Fiber Sheet (CFS) has been successfully played key roles as one of the feasible reinforcing composite materials due to its superior characteristics. However, the fatigue behavior of RC bridge slab retrofitted with CFS under large repeated loading has not been reported so much. *The main objective of this research is planed to clarify the mechanical behavior of RC slab retrofitted with CFS under static and fatigue loading.*

- ◆ Chapter 2 introduces review of previous researches on structural behavior of laminated RC members by FRP materials. This chapter also contains a brief review of seismic retrofitting techniques and experimental results of viaduct column retrofitted with CFS.
- ◆ Chapter 3 presents the results of experimental and analytical investigations on interfacial bond behavior between concrete and CFS. Bond strength between concrete surface and CFS (actually epoxy layer) is evaluated by laboratory test. A Finite Element (FE) analysis is also developed to simulate the shear stress distributions along the bonded length of CFS.
- ◆ Chapter 4 presents improvement of flexural strength of laminated RC bridge slab by CFS. An experimental investigation was conducted with test slabs under static

load. Section analysis based on the compatibility of deformations and equilibrium of forces, and 2-D (two-dimensional) FE analysis are developed to predict the structural behavior of strengthened RC slab.

- ◆ Chapter 5 presents experimental study of flexural fatigue behavior of RC slab retrofitted with CFS, particularly under very large repeated loading. The test slab is almost identical to an existing slab of a highway in terms of the amount of reinforcement, quality of concrete and thickness of the slab, which is 18cm. Only one directional flexural behavior of the slab was tested. Repeated loads corresponding to 3.0, 4.5 or 6.0 times of the design bending moment were applied to the test slab until failure. Normal type of CFS with 300g/m² (T300), 400g/m² (T400) and high-elastic modulus type of CFS with 300g/m² (HM300) were used for the strengthening. The test slabs are loaded in dry or wet condition. Some of the test slabs were pre-damaged under the repeated load and retrofitted by CFS, then loaded again to see the improvement of the fatigue life.

An energy dissipation characteristic is discussed to evaluate the cumulative fatigue damage of retrofitted RC slab. Finally, *Infrared Thermography*, one of the damage monitoring techniques in the *NDT* (Non-Destructive Testing) field, and retrofit design concept for existing RC bridge slab are also briefly introduced.

- ◆ Chapter 6 presents a proposed new analytical method based on bond strength between concrete and CFS to evaluate the flexural strength of RC bridge slab strengthened with CFS. The evaluation of the ultimate flexural strength of a strengthened slab is tried under the assumption that the failure occurs when the shear stress mobilized at the interface between the concrete bottom and the glued CFS reaches the bond strength. The shear stress is evaluated theoretically and the bond strength is obtained by a laboratory test. A parametric study is also conducted.
- ◆ Chapter 7 presents a summary of each chapter and some general conclusions.

Chapter 2

REVIEW OF PREVIOUS RESEARCH

2.1 INTRODUCTION

In recent years, Fiber Reinforced Plastics (FRP) material have been used to rehabilitate many types of structures including bridges, parking decks, smoke stacks, and buildings with its superior characteristics such as high strength and stiffness per unit weight, easier handling due to their lightweight, and corrosion resistance. Numerous research studies have revealed that FRP composite systems bonded to various structural members can significantly increase their stiffness and load carrying capacity beyond what can be achieved through conventional methods.

In this chapter, the previous researches of FRP retrofit systems are discussed. Material properties of FRP materials are investigated, and various researches on structural behavior of laminated RC members by FRP for flexure, shear, confinement, durability and seismic retrofit systems are also reviewed.

2.2 CHARACTERISTICS OF ADVANCED FIBER MATERIALS

2.2.1 CARBON FIBERS

Carbon fibers are produced from precursors of cellulose and polyacrylonitrile (PAN), producing high strength fibers, or a special hydrocarbon pitch producing high modulus fibers. Carbon fibers are produced by heating the precursor to temperatures up to 2600°C for high strength fibers or 3000°C for high modulus fibers.

These extremely thin fibers are aligned in strands, or tows. Containing 3,000 to 12,000 carbon filaments, tows are only as thick as a human hair. Despite their size and low weight, carbon fibers have very high tensile strength and stiffness. For reference, Carbon Fiber Reinforced Plastic (CFRP) laminates consist of unidirectional continuous carbon fibers impregnated with an epoxy resin. All carbon fibers offer relatively high strengths and stiffness, but are brittle and fail at reasonably low strain levels. Carbon fibers do not corrode themselves, but they may cause galvanic corrosion in other materials. Commercially available carbon fibers are generally classified into *Pitch carbon* and *PAN carbon* fibers.

Pitch carbon fibers are ordinary or high elastic modulus of fiber and the PAN carbon fibers are high strength or high elastic modulus of fiber. Both tensile strength and elastic modulus of the ordinary fiber of the Pitch are about 20% of those of the PAN type. On the other hand, high elastic modulus type provide an identical or higher elastic modulus than the PAN type.



Figure 2.1 Carbon Fiber Sheets

2.2.2 ARAMID FIBERS

Aramid fibers such as Kevlar 49 offer high tensile strength, low density and relatively high elongation to failure. This results in them being very good for absorbing large amounts of energy, for example in structures subject to impact forces. The fibers have

very low density and therefore results in extremely lightweight structures. Most FRP materials exhibit slightly lower strength in compression than tension, but this is particularly true for aramid reinforced FRP and any areas subject to significant compressive stress will require careful consideration. Aramid fibers have a negative coefficient of thermal expansion.

2.2.3 GLASS FIBERS

Two types of glass fibers are commercially available for use as continuous fiber materials; namely, *E-glass fibers* and *Alkali-resistant glass fibers*. The E-glass fibers contain large amounts of boric acid and aluminate, while the alkali-resistant glass fibers contain a considerable amount of zirconia, which serves to prevent corrosion by alkali attacks from cement matrices.

E-GLASS FIBERS

E-Glass fibers are of lower strength and stiffness than the other fibers being considered, but are also considerably lower in cost. Typically an E-Glass structure may be over twice the weight of a carbon or aramid reinforced composite structure, although this will still be dramatically lighter than a conventional structure in steel, concrete or even aluminum. E-Glass fibers are electrically non-conductive and offer good corrosion resistance.

It should be noted however that *E-Glass fibers can be attacked by strong alkaline solutions and needs to be protected with suitable resins or surface tissues in such situations.* Laminates produced with unidirectional E-Glass fibers exhibit ultimate strengths in excess of those provided by conventional structural steel, but with much reduced stiffness. Table 2.1 and Figure 2.1 show materials properties of fiber materials.

Table 2.1 Properties of advanced fiber materials

Advanced Fiber Materials		Tensile strength (N/mm ²)	Elastic modulus (N/mm ²)	Elongation (%)	Density (g/cm ³)	Diameter (μm)
Carbon Fiber	PAN	High Strength	3500	2.0 × 10 ⁵ ~ 2.4 × 10 ⁵	1.3~1.8	1.7~1.8
		High Elastic Modulus	2500 ~ 4000	3.5 × 10 ⁵ ~ 6.5 × 10 ⁵	0.4~0.8	1.8~2.0
	Pitch	Ordinary	780 ~ 1000	3.8 × 10 ⁵ ~ 4.0 × 10 ⁵	2.1~2.5	1.6~1.7
		High Elastic Modulus	3000 ~ 3500	4.0 × 10 ⁵ ~ 8.0 × 10 ⁵	0.4~1.5	1.9~2.1
Aramid Fiber	High Elastic Modulus	2800	1.3 × 10 ⁵	2.3	1.45	12
	High Strength	3500	7.4 × 10 ⁴	4.6	1.39	12
Glass Fiber	E-Glass	3500 ~ 3600	7.4 × 10 ⁴ ~ 7.5 × 10 ⁴	4.8	2.6	8~12
	Alkali resistant Glass	1800 ~ 3500	7.0 × 10 ⁴ ~ 7.6 × 10 ⁴	2.0~3.0	2.27	8~12

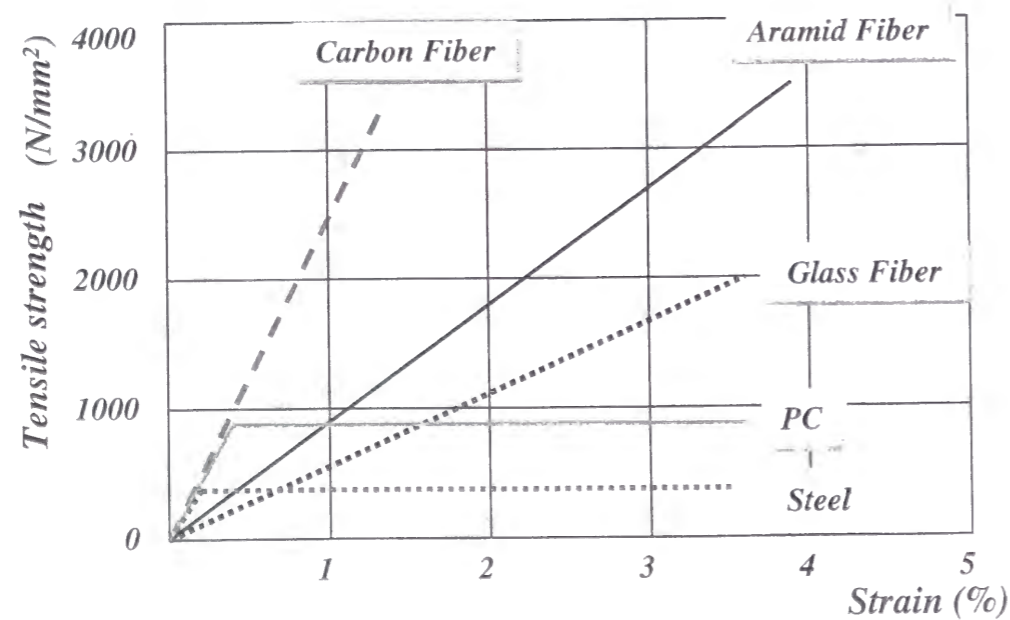


Figure 2.2 Relationship between tensile strength and strain in fiber materials

2.3 STRUCTURAL BEHAVIOR OF LAMINATED RC MEMBERS BY ADVANCED FIBER MATERIALS

Worldwide, a great deal of researches have been conducted concerning the use of Fiber Reinforced Plastic (FRP) composite materials in the repair and strengthening of damaged RC members. Experimental and analytical investigations on structural behavior of retrofitted RC members by FRP materials for flexure, shear, confinement and durability, etc are reviewed in this section.

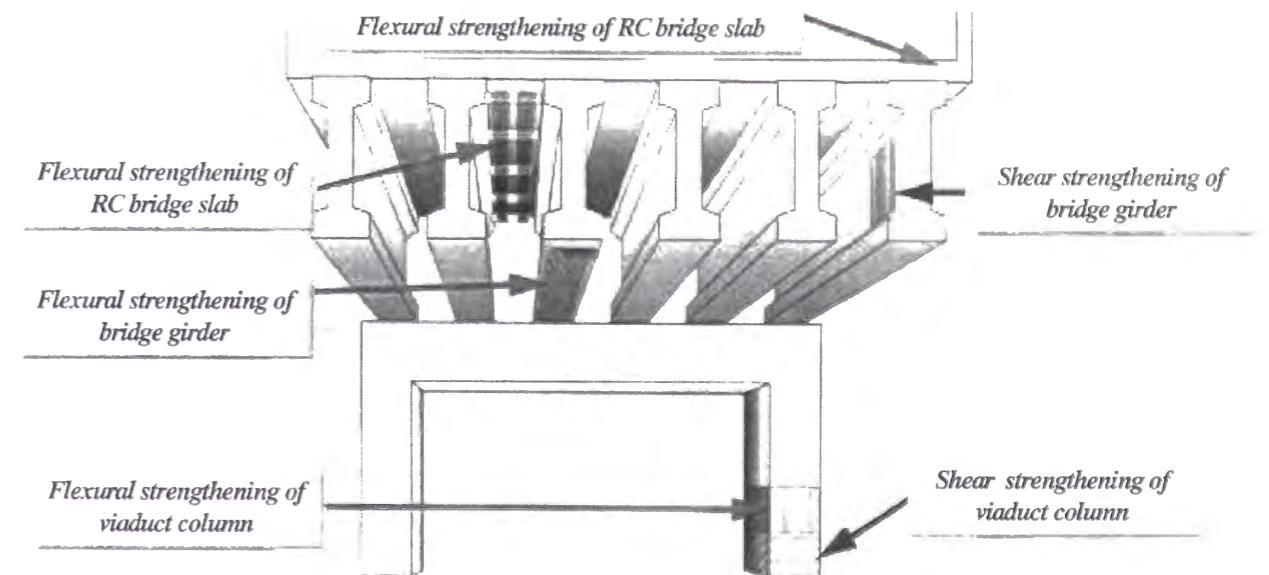


Figure 2.3 FRP retrofitting system

2.3.1 FLEXURAL STRENGTHENING

Many researchers have investigated the effectiveness of FRP materials for flexural strengthening of RC members.

FLEXURAL STATIC LOADING

- ◆ Meier (1987) presented the first study on the use of Carbon Fiber Reinforced Plastic (CFRP) laminates in strengthening applications, and he showed that advanced fiber composites could replace the conventional steel reinforcement.

- ◆ Kaiser (1989) successfully employed CFRP composites for the first time in loading tests for the strengthening of full-scale reinforced concrete beams. His work showed the validity of the strain compatibility method in the analysis of cross sections and suggested that inclined cracking may lead to a peeling-off the strengthening sheet.
- ◆ Saadatmanesh and Ehsani (1990) studied test results of reinforced concrete beam with Glass Fiber Reinforced Plastic (GFRP) sheets bonded to their tension zone, and emphasized that selection of the appropriate adhesive is of primary importance in the mechanical performance of the strengthened members. They also performed parametric studies to examine the effect of different design material properties and quantities on the strength of the retrofitted beams.



Figure 2.4 CFS retrofitting for flexure

- ◆ Ritchie et al (1991) investigated a series of concrete beams strengthened with composites made of Carbon, Aramid and Glass Fibers, and developed an analytical method based on strain compatibility to predict the strength and stiffness of the plated beams.
- ◆ Triantafillou and Plevris (1992,1995) used the strain-compatibility method and concepts of linear elastic-fracture mechanics to develop a model for the FRP peeling-off mechanism in order to provide a comprehensive study of the short-term flexural behavior of reinforced concrete beam strengthened with externally bonded

composite laminates. Their work also addressed the effect of different types and area fractions of unidirectional composites on the strength, stiffness, and ductility of the strengthened elements. Finally, their analytical results for the failure mechanisms and loads were validated through a series of experiments employing thin CFRP sheets.

- ◆ Sharif et al (1994) tested initially loaded reinforced concrete beams strengthened with epoxy bonded fiberglass plastic plates. They also proposed shear and normal stresses at the plate curtailment using Robert's approximate analytical solution assuming elastic behavior.

$$\tau = \left\{ V + \left[\frac{k_s}{E_p b_p d_p} \right]^{\frac{1}{2}} M \right\} \frac{b_p d_p}{I b_a} (h_p - X)$$

$$\sigma = \tau d_p \left[\frac{k_n}{4E_p I} \right]^{1/4}$$

Where, V is shear force at plate curtailment. k_s and k_n are shear and normal stiffness of epoxy/unit length. E_p , b_p and d_p are elastic modulus, width and thickness of FRP plate. h_p is location from top of concrete section to centroid of FRP plate. I_p is moment of inertia of FRP plate and I is moment of inertia of fully composite transformed equivalent to FRP section,

- ◆ Malek et al (1998) presented a method for calculating shear and normal stress concentration at the cutoff point of the FRP plate. This analytical method presented in this thesis can be used to predict the distribution of shear and normal stress at the interface of the FRP plate and the adhesive throughout the entire length of the plate and particularly the location of the cutoff point. This model has been developed based on linear elastic behavior of the concrete. The effect of the large flexural cracks along the beam has been investigated. The maximum values of these stresses, are given by the following simple equation.

At the cutoff point, the maximum value of shear stress is obtained as;

$$\tau_{\max} = t_{frp} (b_3 \sqrt{A} + b_2)$$

Where, $A = \frac{G_a}{t_{epoxy} t_{frp} E_{frp}}$, $b_{2,3}$ = parameters used in shear/normal stress equations

Also, the maximum value of normal stress is obtained as;

$$f_{n,\max} = \frac{K_n}{2\beta^3} \left(\frac{V_{frp}}{E_{frp} I_{frp}} - \frac{V_c + \beta M_o}{E_c I_c} \right) + \frac{q E_{frp} I_{frp}}{b_{frp} E_c I_c}$$

Where, K_n = normal stiffness per unit area of epoxy, β = coefficient used in normal stress definition, V_{frp} = shear force in the plate beam, I_{frp} = moment of inertia of plate beam

FLEXURAL FATIGUE LOADING

- ◆ Kaiser (1989) investigated a beam with a 2.0m span under fatigue loading. The cross section was 300mm wide and 250mm deep. The existing steel reinforcement consisted of 2rebars of 8mm diameter in the tension as well as the compression zones. This beam was post-strengthened with a hybrid sheet with the dimensions 0.3x200mm. The fatigue loading was applied with a frequency of 4Hz. The test set-up corresponded to a four-point flexure test with loading at the one-third points.

After 480,000cycles the first fatigue failure occurred in one of the two rods in the tension zone. After 560,000 cycles the second rod broke at another cross section. After 610,000 cycles further bread was observed in the first rod and after 720,000 cycles, in the second rod. After 805,000 cycles, the sheet finally failed. This test was executed with unrealistically high steel stresses. The goal of the test however was to gain insight into the failure mechanism after complete breaking of the steel reinforcement. It was remarkable to observe how much the hybrid sheet could withstand after failure of the steel reinforcement.

- ◆ Deuring (1990) performed a further fatigue test on a T section beam with a span of 6.0m under more realistic conditions. The total carrying capacity of this beam amounted to 610kN without the CFRP. Through the bonding of a CFRP sheet having the dimensions 200x1mm, the carrying capacity was increased by 32% to 815kN. The beam was subjected to four points bending from 126kN to 283kN for 10.7 million cycles. The temperature was raised from room temperature to 40 and the relative humidity to at least 95%. ***The goal of this test phase was to verify that the bonded CFRP sheet could withstand very high humidity with simultaneous fatigue loading.*** Already at the beginning of this test phase the CFRP sheet was nearly completely saturated with water. After a total of 12.0 million cycles the first reinforcement steel failed due to fatigue. Second fatigue test was conducted similar to the one described above; this time however, the CFRP plate was prestressed and 30.0million cycles were performed with no sign of any damage.
- ◆ Matsui et al (1997) conducted a wheel trucking fatigue test with damaged RC deck slab strengthened by CFS. From the results, the damaged RC deck slab prolonged its fatigue life more than 5 to 17 times owing to the CFS, and also the high elastic modulus of CFS was considered as more effective for extending fatigue life of existing bridge slab.



Figure 2.5 Wheel trucking fatigue test

- ◆ Barnes (1999) examined the fatigue performance of CFRP strengthened concrete beams. Five reinforced concrete beams were tested. From the limited number of test

specimens, it would be appeared that fatigue fracture of the internal reinforcement steel is the dominant factor governing failure in RC beams strengthened in flexure with CFRP plates. It was recommended that the criteria for the fatigue design of CFRP plated beams should be to limit the stress range in the rebars to that permitted in an unplated beam.

2.3.2 SHEAR STRENGTHENING

The nominal shear strength of a RC beam may be computed by the basic design equation as

$$V_n = V_{con} + V_{steel}$$

The nominal shear strength V_n is the sum of the shear strength of concrete V_{con} (which for a cracked section is attributable to aggregate interlock, dowel action of the longitudinal reinforcement and the diagonal tensile strength of the uncracked portion of concrete) and the shear strength of the steel reinforcement V_{steel} . In case of beam strengthened with externally bonded FRP sheets, the nominal shear strength may be computed by the addition of a FRP term to account for the contribution of FRP sheet to the shear strength of beams.

$$V_n = V_{con} + V_{steel} + V_{frp}$$

The contribution of FRP reinforcement to shear capacity (V_{frp}) of RC members depends on several parameters, including the stiffness of FRP, the quality of the resin, the compressive strength of concrete, the number of piles of FRP sheets, the wrapping scheme and the fiber orientation angle. However, it has been difficult to establish certain formula to compute V_{frp} because the parameters are numerous and studies on shear strengthening of RC beams using fiber composite materials have been limited.

- ◆ Berset (1992) at the Massachusetts Institute of Technology performed the first research. He tested RC beams with and without shear strengthening reinforcement

in the form of GFRP laminates epoxy-bonded to vertical sides in the shear critical zones, and developed a simple analytical model for the contributing of the external reinforcement to shear capacity. In Berset's model the FRP shear reinforcement is treated in analogy with steel stirrups, reaching a maximum allowable strain, which is determined by experiments.

- ◆ Uji (1992) tested reinforced concrete beams strengthened in shear with either wrapped-around carbon fabrics or CFRP laminates bonded to the vertical sides (with the fibers either vertical or inclined). His model for the FRP contribution to shear capacity is based on rather arbitrarily defined FRP-concrete bonding interfaces, which, during peeling-off. (debonding) of the fabrics, carry average shear stresses (bonding stresses) determined by experiments (to be about 1.3MPa). The upper limit to the FRP contribution is given by its tensile strength.
- ◆ In another study, Dolan et al (1992) tested prestressed concrete beams with externally applied aramid fabric reinforcement, and concluded that AFRP fabrics perform quite well as shear retrofit reinforcement.



Figure 2.6 FRP retrofitting for shear

- ◆ The work of Al-Sulaimani et al (1994) dealt with shear strengthening using GFRP laminates in the form of plates or strips. Their model for the contribution of composites to shear capacity is based on the assumption of FRP concrete interfaces, which carry average shear stresses during peeling-off equal to 0.8 MPa and 1.2

MPa for the case of plates and strips, respectively.

- ◆ Ohuchi et al (1994) carried out an extensive series of experiments on reinforced concrete beams strengthened in shear with wrapped-around carbon fabrics. They modeled the CFRP contribution to shear capacity in analogy with steel stirrups, assuming a limiting strain for the external reinforcement equal to either the tensile failure strain of CFRP or 2/3 of it, depending on the thickness of the fabrics.
- ◆ Chajes et al (1995) reported on FRP-strengthened concrete beams using composites with various types of fibers, namely glass, aramid, and carbon. In this work, the FRP contribution to shear capacity is modeled in analogy with steel stirrups and assumes a limiting FRP strain, which was determined by experiments to be approximately equal to 0.005.
- ◆ Malvar et al (1995) also tested reinforced concrete beams strengthened in shear with CFRP fabrics and verified the high effectiveness of the technique. In terms of analysis, they stated that the contribution of the fabrics to shear capacity could be obtained in analogy with steel stirrups by considering the limiting FRP strain equal to that at tensile fracture of the material.
- ◆ Norris et al (1997) proposed simple equation to evaluate the contribution of the FRP to the shear strength of RC beam as follows,

$$V_{frp} = F_{frp} \cdot t_{frp} \cdot d$$

Where, F_{frp} = tensile strength of FRP, t_{frp} = thickness of FRP,

d = distance from compression flange to centroid of tension steel

However, the above equation is only used to the failure mode of FRP rupture.

- ◆ An experimental investigation was performed at the University of Missouri-Rolla (Khalifa et al 1998) to investigate the shear performance and mode of failure of RC

beams strengthened with CFRP sheets. Full-scale RC beams were tested with some variables, which are a/d ratio, steel stirrups, amount and configurations of CFRP and anchoring. The experimental results indicated that the shear contribution of CFRP was significant and dependent on the variable investigated.

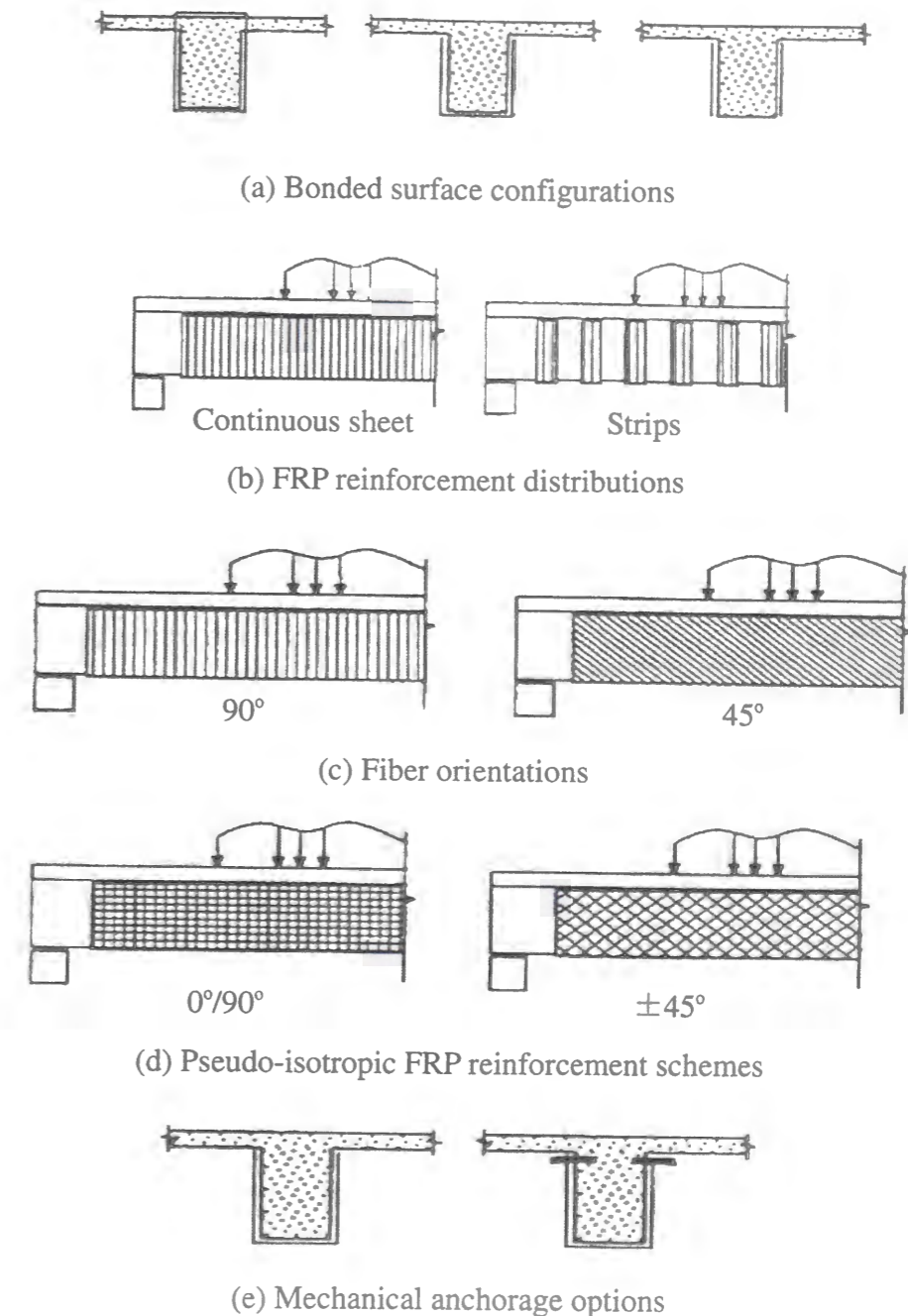


Figure 2.7 FRP retrofitting for shear (by Khalifa, 1998)

- ◆ Triantafillou (1998) noted that CFRP sheets used for shear strengthening rupture as stress levels below their ultimate strength due to stress concentrations, and if the level of strain at rupture is considered as the effective strain ε_{fe} , the contribution of FRP reinforcement to shear capacity (V_{frp}) of a RC beam can be evaluated by

$$V_{frp} = \rho_f E_f \varepsilon_{fe} b_w 0.9d (1 + \cot\beta) \sin\beta$$

Here, ρ_f = FRP shear reinforcement ratio = $(2t_f w_f / b_w s_f)$, β = angle between principal fiber orientation and longitudinal axis of beam, b_w = width of beam cross section, w_f = width of FRP strip, s_f = spacing of FRP strips, E_f = elastic modulus of FRP.

This equation may be rewritten by

$$V_{frp} = \frac{A_f f_{fe} (\sin \beta + \cos \beta) df}{s_f}$$

Here, the modulus of elasticity times the effective strain is replaced with the effective stress. The area of FRP shear reinforcement is the total thickness of the sheet times the width of the FRP strip W_f . If continuous sheets are used, the width of the strip and the spacing of the strip S_f should be equal.

2.3.1 FRP CONFINEMENT

Several researchers have demonstrated that the ductility and strength of concrete columns can be increased by lateral confinement with the use of FRP composite wrapping materials.

- ◆ Fardis et al (1981) conducted the experimental study on the behavior concrete-encased FRP tubes. Four types of glass fiber were used with the number of FRP layers varying from 1 to 5. The failure mode of specimens was a simultaneous fracture with concrete crushing of FRP. The ultimate strength and the corresponding strain of concrete were significantly increased with the number of FRP layers. They also proposed new equations;

$$f'_{cc} = f'_c [1 + 4.1(\frac{f_{FRP} \cdot t}{d \cdot f'_c})]$$

$$\varepsilon_{cc} = 0.002 + 0.001 \frac{E_{FRP} \cdot t}{d \cdot f'_c}$$

Where, f'_{cc} and ε_{cc} are the maximum strength and the corresponding strain of confined concrete

f'_c is the maximum strength of unconfined concrete

f_{FRP} and t is the tensile strength and the thickness of FRP

d is the diameter of concrete core

- ◆ Ahmad et al (1991) presented experimental & analytical results on the strength and deformation of concrete transversely reinforced with fiberglass filament (wires). A total of 33 concrete cylinder confined with fiberglass wires were tested to obtain complete stress-strain curves in compression. The stress-strain curves for confined concrete can be represented by

$$f_c = \left\{ \frac{A(\varepsilon_c / \varepsilon'_c) + (B-1)(\varepsilon_c / \varepsilon'_c)^2}{1 + (A-2)(\varepsilon_c / \varepsilon'_c) + B(\varepsilon_c / \varepsilon'_c)^2} \right\} f'_c$$

Where, f'_c , ε'_c is the maximum stress and the corresponding strain, respectively

f_c is the stress at strain ε_c , and A and B are constants

The above equation can be used to predict the stress-strain curve of confined concrete, by using f'_{cc} and ϵ'_{cc} in place of f'_c and ϵ' , where f'_{cc} and ϵ'_{cc} are the peak stress and the corresponding strain for confined concrete.

The peak stress and strain can be determined by

$$\frac{f'_{cc}}{f'_c} = 1 + \frac{k}{4^{ns_p}}, \quad \text{here, } k = \begin{cases} 1.9 \\ 1.6 \\ 1.2 \end{cases} \quad \text{and } n = \begin{cases} 5 \\ 6 \\ 8 \end{cases} \quad \text{for } f'_c = \begin{cases} 38.9\text{MPa} \\ 50.5\text{MPa} \\ 64.2\text{MPa} \end{cases}$$

$$\frac{\epsilon'_{cc}}{\epsilon'_c} = 1 + \frac{k}{4^{ns_p}}, \quad \text{here, } k = \begin{cases} 3.9 \\ 3.9 \\ 3.5 \end{cases} \quad \text{and } n = \begin{cases} 6 \\ 6 \\ 6 \end{cases} \quad \text{for } f'_c = \begin{cases} 38.9\text{MPa} \\ 50.5\text{MPa} \\ 64.2\text{MPa} \end{cases}$$

Where, s_p is the spacing of the fiberglass.

- ◆ Demers et al (1994) investigated the use of advanced composite material wrappings for strengthening plain concrete cylinders using one or three layers of carbon or glass fiber sheets. Round columns (152x305mm) as well as square columns (150x150x500mm) were used. Their results showed that a significant increases in strength up to 70% were observed and ductility was 7 times higher than that of unwrapped plain concrete cylinders. Increases were negligible for square columns because the high stress concentrations at the corners resulted in premature failure of the sheets before significant confining pressure could be induced.
- ◆ Other experimental investigations on confinement of concrete with FRP have been carried out (Karbhari et al 1993, Miyauchi et al 1997), and they proposed new confinement equations.

$$f'_{cc} = f'_c \left[1 + 2.1 \left(\frac{f_{FRP} \cdot t}{d \cdot f'_c} \right)^{0.87} \right]$$

$$\epsilon_{cc} = 0.002 + 0.01 \left(\frac{f_{FRP} \cdot 2t}{d \cdot f'_c} \right)$$

(By Karbhari et al 1993)

$$f'_{cc} = f'_c \left[1 + 3.5 \left(\frac{f_{FRP} \cdot 2t}{d \cdot f'_c} \right) \right]$$

$$\epsilon_{cc} = 0.002 \left[1 + 10.6 \left(\frac{f_{FRP} \cdot 2t}{d \cdot f'_c} \right)^{0.373} \right]$$

(By Miyauchi et al 1997)

$$f'_{cc} = f'_c \left[1 + 2.2 \left(\frac{f_{FRP} \cdot 2t}{d \cdot f'_c} \right)^{0.84} \right]$$

(By Saafi et al 1999)

$$\epsilon_{cc} = \epsilon_{co} \left[1 + (537 \epsilon_{FRP} + 2.6) \left(\frac{f'_{cc}}{f'_c} - 1 \right) \right]$$

Where, f'_{cc} and ϵ_{cc} are the maximum strength and the corresponding strain of confined concrete

f'_c and ϵ_{co} are the maximum strength and the corresponding strain of unconfined concrete

f_{FRP} and t is the tensile strength and the thickness of FRP

ϵ_{FRP} is the ultimate strain of the FRP, d is the diameter of concrete core

- ◆ To study the stiffness degradation of concrete confined with FRP tubes, Mirmiran et al (1997) performed a **uni-axial compression test under cyclic loading**. Glass fiber was used and the number of FRP layers was 5,10, and14. They reported that the failure mode of cylinder specimens was similar to specimens under monotonic loading, and the stiffness degradation was no as severe as that of steel-encased concrete.
- ◆ Ono et al (1997) conducted experimental investigations on concrete cylinder specimen (100x200mm) confined by CFS, as shown in Figure 2.8. They demonstrated that both the compressive strength and the strain at maximum stress were enhanced in proportion to the number of layers of the carbon fiber sheets.

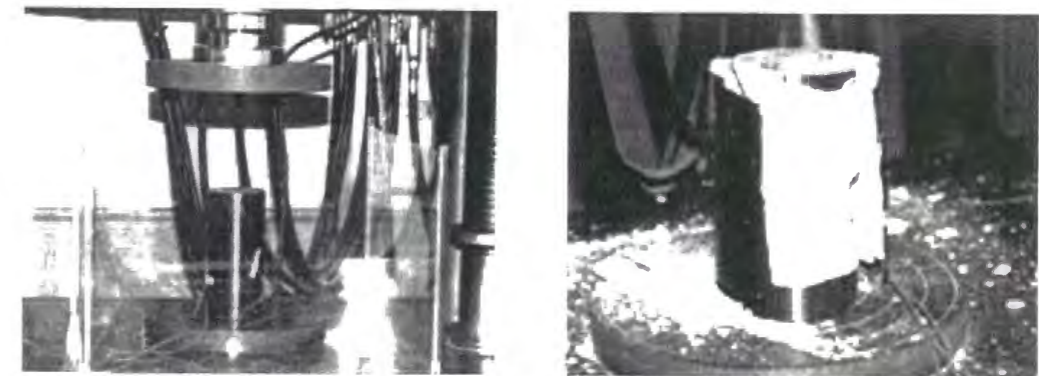


Figure 2.8 Uni-axial compression test of concrete cylinder confined by CFS

2.3.2 DURABILITY

Durability of composites and composite-reinforced systems against environmental factors such as extreme temperature cycles, moisture, chemical attack, and ultraviolet radiation is of major concern in structural retrofitting. Early research has indicated that many polymer-matrix composites can absorb moisture from the surrounding environment, resulting in dimensional changes as well as adverse internal stresses within the system (Jang, 1994). Additionally, the composite materials alone are inherently corrosion resistant and can show substantial cost benefits when used in aggressive environments (Schwartz, 1997). To date, limited studies have been conducted on the long-term behavior and environmental durability of concrete structures retrofitted with FRP laminates.

- ◆ Baumert et al (1996) studied *low temperature behavior of concrete beams* strengthened with FRP sheets. The test was made by investigating the flexural behavior of post-strengthened beams at room temperature (21 °C) and low temperature (-27°C). The beams were subjected to four points loading at the two different temperatures and the results indicated that the reduced temperature did not affect the flexural behavior.
- ◆ Soudki and Green (1996, 1997) conducted an experimental study on the performance of circular plain and reinforced concrete cylinders (150x300mm) strengthened with CFRP wraps in *cold weather conditions*. Their experimental results showed that the use of CFRP sheets to strengthen concrete columns in cold regions is feasible and appeared to be efficient in terms of strength, stiffness and ductility. An increase up to 3 times in strength was obtained in CFRP wrapped columns exposed to freeze/thaw cycling when compared to unwrapped cylinders subjected to freeze/thaw cycling. The authors reported that low temperature exposure and under water exposure did not affect significantly the strength, but affected the mode of failure.
- ◆ Arockiasamy and Thayer (1998) reported a study on the damage process of CFRP composite-concrete interface *under fatigue loading at low temperatures*. The

experimental work included investigations on fatigue strength, ultimate capacity and failure modes of repaired reinforced concrete beams in cold environment and room temperature. The study also included investigations of thermal response of repaired plain concrete beams with CFRP laminates subjected to thermal cycles. With regard to ultimate strength, the study concluded that no noticeable difference in the general trend of the load-deflection curves of the repaired beams, which were subjected to fatigue loads at room temperature and low temperature, could be observed.

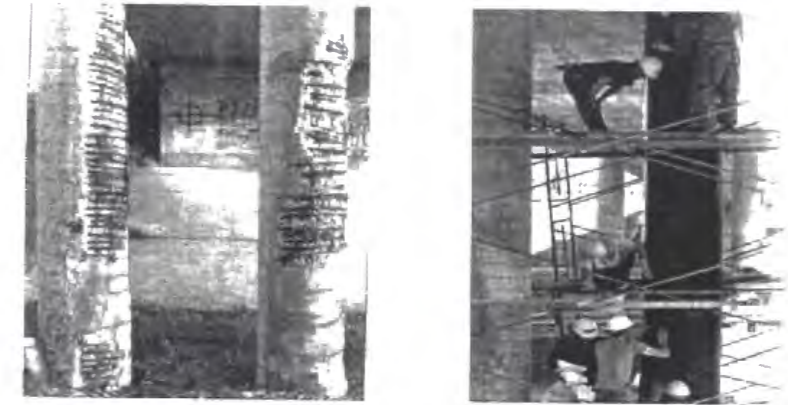


Figure 2.9 CFS retrofit of bridge column damaged by corrosion

- ◆ Toutanji and Rey (1997, 1998) conducted an experimental study on the performance of concrete columns (76x305mm) wrapped with carbon and glass FRP composite sheets subjected to *wet-dry and freeze-thaw conditions*. Their experimental results showed that CFRP is superior to glass when exposed to harsh environments. The authors reported that when the effect of freezing and thawing on the exposed concrete was minimized, the degradation in strength in both carbon and glass fiber wrapped specimens was significantly reduced. No loss in ductility was observed for CFRP wrapped cylinders exposed to wet/dry environments, while a loss in ductility was observed in GFRP wrapped cylinders. Both CFRP and GFRP wrapped cylinders exposed to freeze/thaw environment exhibited a significant reduction in ductility. All wrapped cylinders subjected to freeze/thaw cycling exhibited more catastrophic failure behavior as compared to unconditioned and wet/dry conditioned specimens.

- ◆ The effect of environmental conditions on concrete cylinders wrapped with FRP sheets was studied by EL-Hacha et al (1999). Thirty-six plain concrete cylinders (150x300 mm) were tested. Cylinders were subjected to *high temperatures* (45°C) to heat-cool cycles (23°C to 45°C) and to prolonged heat exposure (45°C). The results indicated that confining concrete cylinders with a CFRP sheet was a very effective and efficient method for improving the strength and ductility of concrete columns under severe environmental conditions.

2.3.3 INTERFACIAL BOND MECHANISM OF FRP SHEET

In order to develop rehabilitation procedures for concrete structures involving externally applied composite material, a good understanding of the bond mechanism is need.

- ◆ Saadatmanesh et al. (1990) conducted an experimental study to evaluate the performance of four different adhesive used to composite plates to the tension face of RC beams. They concluded that the success of such a strengthening technique strongly depends on the suitability of the epoxy. The epoxy should have sufficient stiffness and strength to transfer the shear force between the concrete beam and composite plates. The epoxy should also be tough enough to prevent brittle bond failure caused by cracking of the concrete. They also found that rubber-toughened epoxies are particularly suited for this application.
- ◆ According to the conclusions of Chase's Single-lap shear bond test (1996), surface preparations of the concrete can influence in ultimate bond strength. To achieve the best possible bond, the concrete surface should be mechanically abraded or sandblasted, and a primer should be applied. They also implied that in addition to the stiffness of the CFRP sheets, the bond strength depends on the concrete compressive strength. The average bond strength between concrete and CFS was increased with the increase of compressive strength of concrete. Finally, additional experimental and analytical investigation is needed to develop a relationship for the bond properties.

- ◆ Van Gemert et al (1997) reported special shear test results. In this study, they presented the experimental test results, and proposed new method for evaluating bond strength between concrete and CFRP laminates based on non-linear fracture mechanics. Also, they stressed that at higher loads, the maximum shear stress τ shifted to the right (Figure 2.10) and attained higher values. When the direct tensile strength, which is larger than the pull-off strength, is reached, the crack will extend and the sheet will peel off in a brittle way.

$$P_{max} = b \sqrt{\frac{2E_{CFRP} t_{CFRP} G_f}{1 + \alpha}}$$

$$\alpha = \frac{E_{CFRP} t_{CFRP}}{E_{Concrete} t_{Concrete}}$$

Where, G_f = fracture energy (Nmm/mm^2), b = width of CFRP laminates(mm)

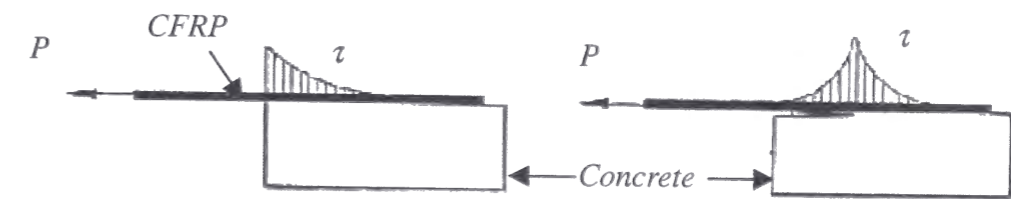


Figure 2.10 Shear stress distribution before and after cracking

- ◆ Maeda et al (1997) studied the bond mechanism of CFRP sheets with concrete by performing simple tension tests. The authors described the concept of the average bond strength and the effective bond length based on the experimental results. Also, they proposed new equation for calculating the ultimate load P_{max} as follows,

$$P_{max} = L_{e-cal} b \tau_{bu}$$

Where, L_{e-cal} is calculated by the equation obtained from the least squares method ($= \exp [6.134 - 0.58 \ln (t \times E_{cfs})]$), τ_{bu} is the average bond strength calculated by the following equation, $\tau_{bu} = E_{cfs} t (d\varepsilon / dx)$, ($d\varepsilon / dx$) is gradient for effective bond length ($=110\mu/mm$).

- ◆ In order to understand the adhesive characteristics of CFRP sheet, tension test were conducted by Takao et al (1998). From the results, the effective adhesion length of CFRP sheet was about 100mm, and ultimate load was in direct proportion to tension stiffness of CFRP sheet.

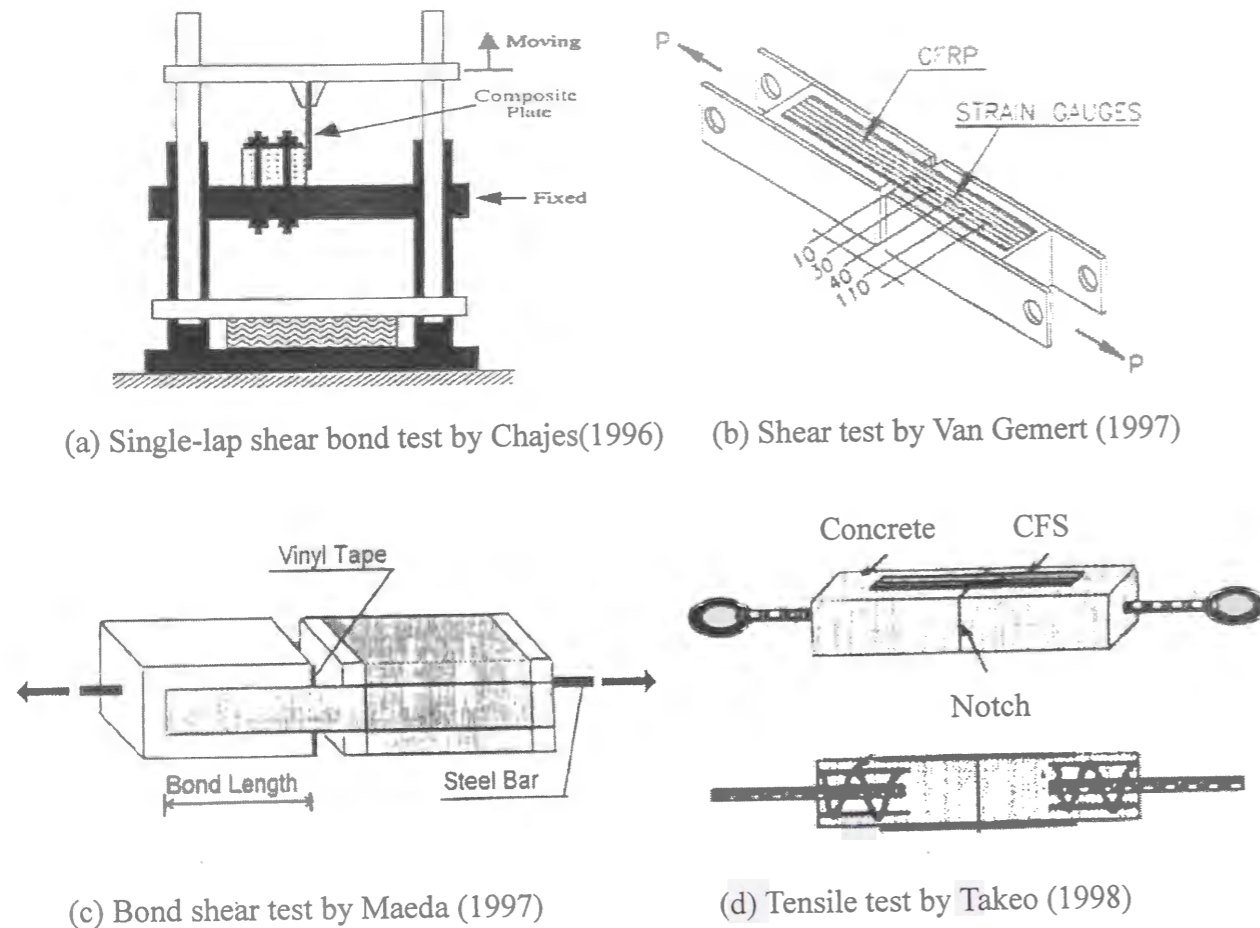


Figure 2.11 Interfacial bond tests

- ◆ Izuno et al (1998) carried out Uni-axial tensile test with three parameters, which were compressive strength of concrete, two different fibers (Carbon, Aramid) and bond length of sheet. Here, they proposed new equation to calculate the ultimate load P_{max}

$$P_{max} = (3.4f_c^{2.3} + 69.0) \cdot L \cdot E_f \cdot B_f \cdot t_f \times 10^{-6} \quad \text{for Aramid sheet}$$

$$P_{max} = (3.8f_c^{2.3} + 15.2) \cdot L \cdot E_f \cdot B_f \cdot t_f \times 10^{-6} \quad \text{for Carbon sheet}$$

Where, f_c = Compressive strength of concrete at 28days, L = Bonded length of sheet, E_f =Elastic modulus of sheet, B_f = width of sheet, t_f = thickness of sheet, They also noted that the effective bond length of sheet was 100mm.

- ◆ Dolan et al (1998) developed a push-apart test to define the interface shear between FRP and concrete, as shown in Figure 2.12. This test was designed to determine lower-bound bond strength for the test specimen, that is the force required to separate the CFRP and the concrete. The failure mode was shearing of the concrete below the CFRP/epoxy interface.



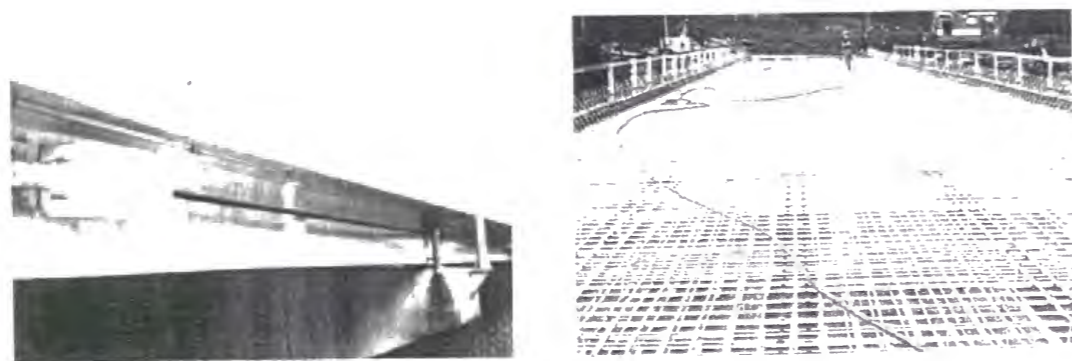
Figure 2.12 Push-apart bond test

2.3.4 FRP STRANDS & BAR

- ◆ The effect of fatigue loading on the use of external AFRP strands was examined by Saeki et al (1993, 1995) and Mutsuyoski et al (1993). They determined that fatigue loading applied at 33 percent of the ultimate load for 2 million cycles had an insignificant effect on the rigidity of the tested beams. In addition, they indicated that the loss in pre-stressing force was about 10 percent.
- ◆ Kumar (1998) conducted the fatigue test of four concrete decks reinforced with fiber-reinforced plastic (FRP) bar. The test results showed no loss of bond between FRP rebars and concrete in any of the test specimens. The major crack patterns were in the direction parallel to the stringers. The deck specimen reinforced with

FRP rebars had a linear variation in stiffness degradation even after 2.0million cycles; thus 2.0million fatigue cycles could be conservatively assumed as 80% of the fatigue life of these decks. Also, fatigue failure in concrete decks is influenced by crack formation at the bottom of the deck. Therefore, the span-to-depth ratios in the concrete slab should be proportioned such that the extreme fiber tensile stress in the deck is less than 50% of the modulus of rupture of concrete.

- ◆ Michaluk and Rizkalla (1998) presented test results of eight one-way concrete slabs, with clear spans of 3000mm, reinforced with glass-fiber, carbon fiber and conventional steel reinforcement. The slabs were tested under static loading conditions to determine their flexural and shear limit states. The slab behavior exhibited adequate warning prior to failure through large and deep cracks, accompanied by large deformations for slabs reinforced by GFRP bars.
- ◆ Hemanth and Gangarao (1998) investigated the application results of GFRP reinforcing bar to McKinleyville (U.S) Bridge deck slabs. They conducted extensive laboratory testing of GFRP bar reinforced concrete beams under static and fatigue loads before implementing GFRP bars in full-scale concrete bridge deck construction. Truck loading test results after implementing indicated that the bridge superstructure deflection and stress of GFRP bar are well within their allowable limits.



(a) CFRP strands in concrete bridge

(b) Implement of GFRP bar

Figure 2.13 Application of FRP Strands & Reinforcing bar to bridge

2.4 SEISMIC RETROFIT OF HIGHWAY RC BRIDGE

2.4.1 DAMAGE OF RC BRIDGE DUE TO EARTHQUAKE

Recent earthquakes in urban areas of the United States (1989 Loma Prieta, 1994 Northridge) and Japan (1995 Kobe) have demonstrated the inadequacy of old seismic design codes as shown in Figure 2.14. Through the investigation of RC columns for bridge piers that failed in Kobe earthquake, two kinds of typical damages such as Flexural or Shear cracking were observed. The summaries of these damage classifications for RC column are shown in Table 2.2 and 2.3, respectively. Thus, there is an urgent need for development of effective, durable, and cost-efficient repair & retrofit materials and methodologies.



Figure 2.14 Damages to bridges in recent earthquakes


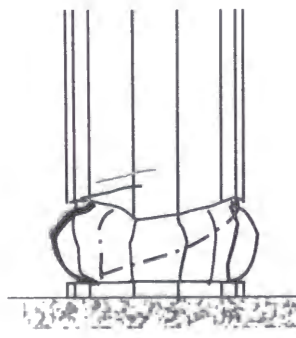
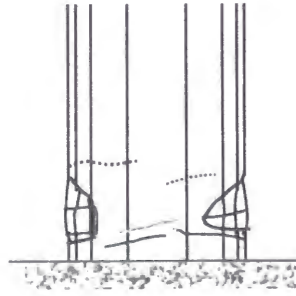
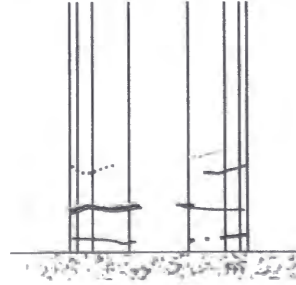
2.4.2 SEISMIC RETROFIT OF BRIDGE COLUMNS

Concrete columns are commonly deficient in flexural ductility, shear and flexural strength when affected by inadequate lap splice length or longitudinal reinforcement. A number of column retrofit techniques have been developed and tested.

◆ Concrete Jacketing

Additional of relatively thick layer of reinforced concrete around the columns can be used to enhance flexural strength, ductility, and shear strength of columns. Although this method has been used more frequently for building columns than for bridge column.





Table 2.2 Classification of seismic damage levels by flexure

Overview	Estimated displacement	Description
	More than the ultimate state	<ul style="list-style-type: none"> ■ Falling off of the cover concrete ■ Crushing of the inner concrete ■ Buckling or cut off of the main re-bars ■ Cut off of hoop re-bar ■ Loss of the axial alignment <p>→ <i>Demolition and reconstruction</i></p>
	More than $3 \delta_y$	<ul style="list-style-type: none"> ■ Falling off of the cover concrete ■ Segregation of the inner concrete into blocks ■ Buckling of the main re-bars ■ Cut off of hoop re-bar ■ A large amount of residual displacement <p>→ <i>Demolition and reconstruction or Strengthening</i></p>
	δ_y to $3 \delta_y$	<ul style="list-style-type: none"> ■ Many cracking on the surface ■ Partial falling off the cover concrete ■ Almost no bend of the main re-bar ■ Almost no residual displacement <p>→ <i>Strengthening</i></p>
	Less than δ_y	<ul style="list-style-type: none"> ■ No damage or only small cracking on the surface <p>→ <i>Repair</i></p>

* Reference: ONO. K (1998) "Record of RC Bridge Piers Damaged during the Great Hansin-Awaji earthquake and the Analysis"

* δ_y : displacement of longitudinal steel reinforcement at yielding

Table 2.3 Classification of seismic damage levels by shear

Overview	Estimated displacement	Description
	More than the ultimate state	<ul style="list-style-type: none"> ■ Crushing of the inner concrete at the diagonal fracture surface ■ Loss of the alignment or cut off of the main re-bar at the shear failure surface ■ Loss of the axial alignment <p>→ <i>Demolition and reconstruction</i></p>
	More than $2 \delta_y$	<ul style="list-style-type: none"> ■ Clear diagonal cracking ■ Falling off of the cover concrete ■ Exposure of the main re-bar <p>→ <i>Demolition and reconstruction or Strengthening</i></p>
	δ_y to $2 \delta_y$	<ul style="list-style-type: none"> ■ Visible diagonal cracking ■ Almost no falling off of the concrete <p>→ <i>Strengthening</i></p>
	Less than δ_y	<ul style="list-style-type: none"> ■ Discontinued small diagonal cracking <p>→ <i>Repair</i></p>

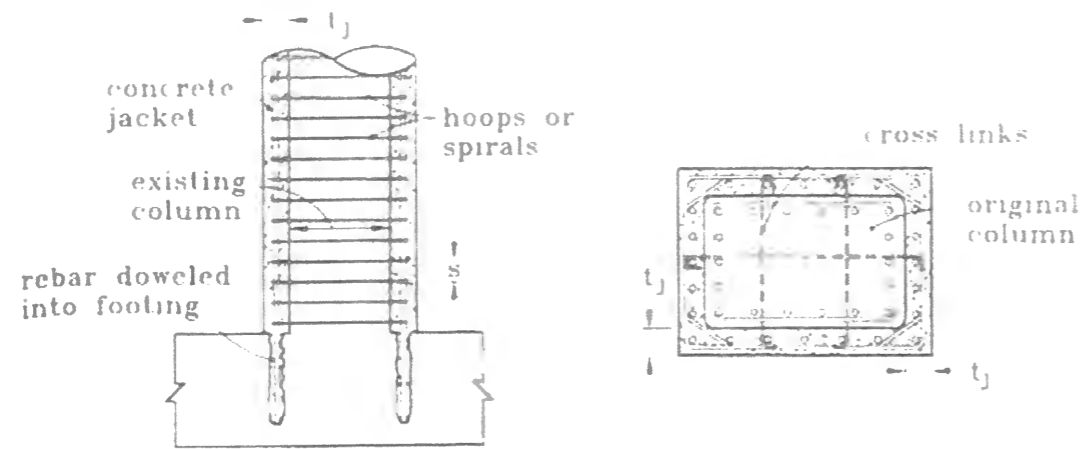


Figure 2.15 Concrete jacketing method

◆ **Steel Jacketing**

Steel jacketing requires installation of a steel plate around the existing column. In order to create a bond between the concrete and the steel plate, the steel jacket would be approximately 40 mm from the surface of the column. The gap between the column and the steel would then be filled with grout. The steel jacket would have to be painted or galvanized to prevent corrosion.

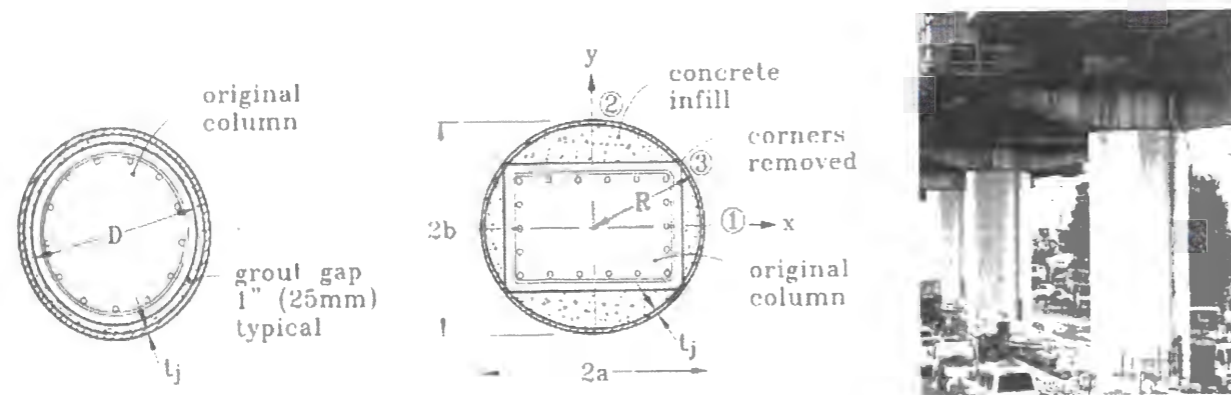


Figure 2.16 Steel jacketing method

◆ **FRP Wrapping**

Considerable researches have been performed to establish the effectiveness of viaduct column retrofit using Fiber Reinforced Polymer (FRP) wrapping such as Carbon, Aramid or Glass fiber sheets. In this technique, FRP sheets are generally impregnated

with epoxy resin for flexural ductility enhancement and flexural or shear strengthening of existing concrete columns.



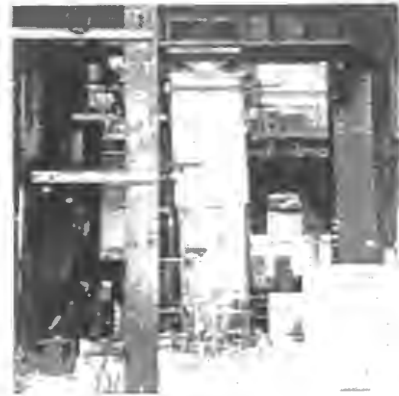
Figure 2.17 FRP wrapping method

Many experimental investigation have been conducted the seismic behavior of viaduct column strengthened by FRP materials.

- ◆ The first study on retrofitting with FRP composites was performed at the University of California at San Diego where 0.4 scale columns were retrofitted with fiberglass/epoxy jackets and tested under cyclic loading (Priestley et al., 1991). Successful results obtained from the test study resulted in immediate implementation of the method in pilot field applications.
- ◆ ONO et al (1997) reported experimental test results on bridge pier model subjected to cyclic loading. Ten column specimens (Shear model 5, Bending model 5) were loaded statically in the horizontal direction at the top under constant uniaxial compression force. From the test results, the modified shear reinforcement q may be used to evaluate shear strength improvement by the JSCE method.

$$q = P_s f_{wy} + \alpha P_{cfs} f_{cfs} \quad (\alpha < 1)$$

Where, P_s : Shear steel ratio, P_{cfs} : Shear CFS ratio α : Strength reduction factor
 f_{wy} : Yield strength of shear steel, f_{cfs} : Tensile strength of CFS

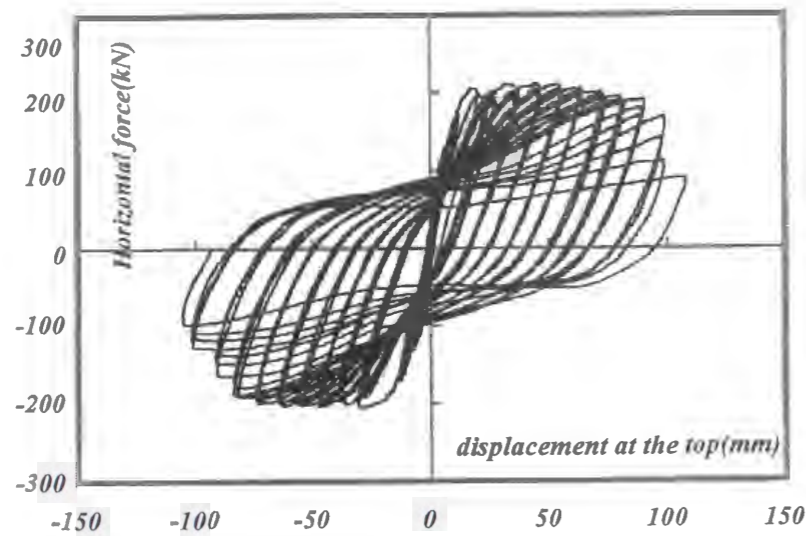


(a) Retrofitting with CFS

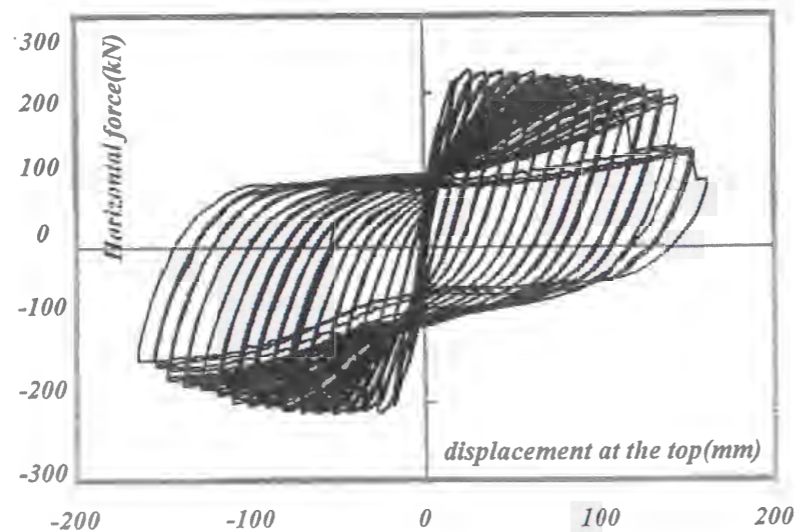


(b) Failure by CFS fracture

Figure 2.18 Testing of viaduct column strengthened by CFS (at the Kyoto Univ.)



(a) Control column (No CFS)



(b) Retrofitted with 4 layers of CFS

Figure 2.19 Load-displacement relation

2.4.3 SEISMIC RETROFIT OF BEAM-COLUMN CONNECTIONS

- ◆ Experimental investigation of Adin et al (1993) have shown satisfactory structural behavior of the beam-column connections by steel plate in terms of strength improvement and energy absorption capacity.
- ◆ More recently, seismic retrofitting of beam-column connections using FRP composites have been investigated and successfully tested in laboratory and field studies (Gergely et al 1998, Geng et al 1998).
- ◆ ONO et al (1998) have conducted experimental investigation of RC beam-column connections confined by different configurations of carbon fiber sheets. From the test results, it was concluded that the cross-confined connections with carbon sheets as shown in Figure 2.20(a) exhibited enhanced ductility and strength if sufficient amount of sheets and proper anchoring was suffered.



(a) Cross type



(b) Normal + Anchor Type

Figure 2.20 Testing of beam-column connections strengthened by CFS

2.4.4 OTHER METHODS FOR ENHANCING SEISMIC BEHAVIOR

RETROFIT OF SUPERSTRUCTURE

One of the series damages in superstructure is associated with unrestrained movement

joints. There have been many examples of bridge failure caused by movement of spans in the longitudinal direction, resulting in unseating at movement joints. To avoid this failure pattern, PC or FRP cable restrainer can be installed in order to transfer longitudinal seismic forces to adjacent frames as shown in Figure 2.21.



Figure 2.21 Cable restrainer for superstructure movement joint

SEISMIC ISOLATION IN BRIDGE RETROFIT

The basic principle of these techniques is to reduce the earthquake force by bearing and to suppress excessive displacement by damping. After KOBE earthquake (1995), the seismic base isolation and dissipation devices like rubber bearing have been widely used and adopted to new bridges in Japan in order to improve their seismic performance as shown in Figure 2.22.

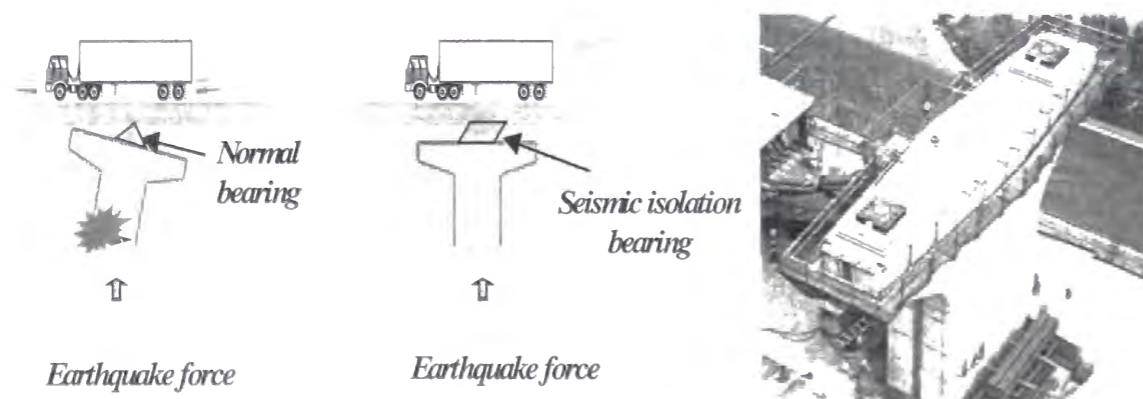


Figure 2.22 Seismic isolation bearing system

Chapter 3

INTERFACIAL BOND BEHAVIOR BETWEEN CONCRETE SURFACE AND CARBON FIBER SHEET

3.1 INTRODUCTION

Application of Carbon Fiber Sheets (CFS) to damaged RC structures to improve their strength has become popular owing to its easy handling and its non-corrosive structural characteristic. However, many experimental results show that flexural failure of RC members glued by CFS at the tensile side are apt to occur by sudden delamination of CFS from the concrete surface if the applied amount of CFS is enough. This phenomenon indicates that the bond strength between concrete and CFS is considered as one of the important factors to determine the actual strength of retrofitted RC members by CFS. Therefore, more researches are necessary for a good understanding of the interfacial bond behavior of laminated RC members by CFS.

This chapter summarizes the results of experimental and analytical investigation on the interfacial bond characteristic between concrete surface and CFS. The concept of the

average bond strength and the effective bond length based on the experimental results is described. Bond behavior between concrete surface and CFS is evaluated by laboratory test. A Finite Element [FE] analysis is conducted to simulate the strain distributions along the bonded length of CFS.

3.2 EXPERIMENTAL PROGRAM

3.2.1 TEST SPECIMEN

Interfacial bond behavior between concrete surface and CFS (actually epoxy layer) was evaluated by laboratory test. Each rectangular concrete prism specimen had 100mm width x 100mm depth x 200mm length. The two bonding faces of each prism specimen were prepared by grinding and cleaned, and then primer was applied to the concrete surface. Unidirectional CFS (100mm length x 37mm width) was glued with epoxy resin to bonding surfaces as shown in Figure 3.1.

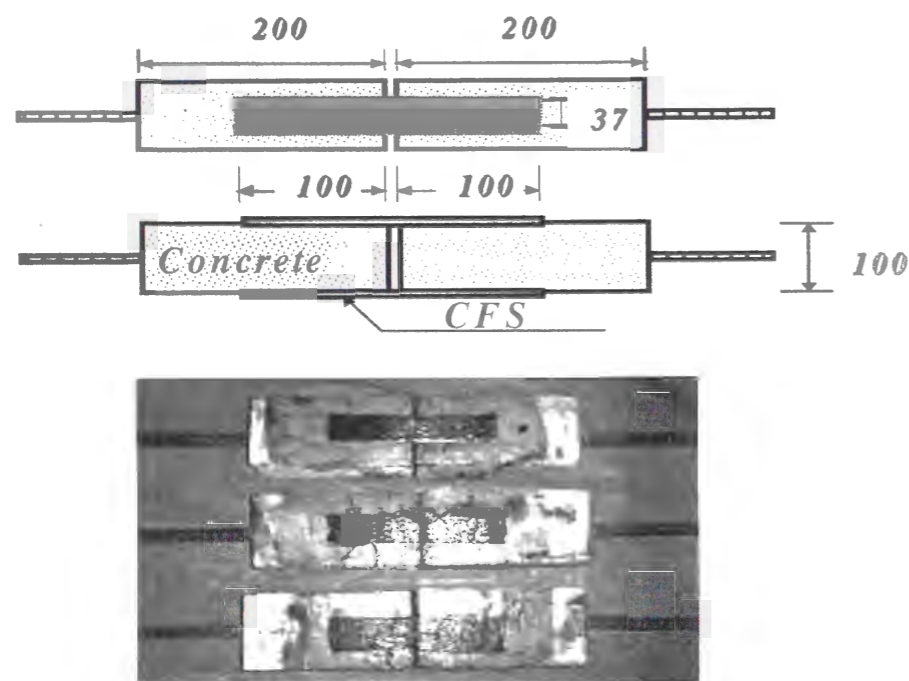


Figure 3.1 Bond test specimen (mm)

Three different types of CFS and amount of CFS were considered as main variables in this bond test. Table 3.1 shows the properties of the materials used.

3.2.2 LOADING SET-UP & MEASUREMENT

Figure 3.2 shows the loading set up. All specimens were statically loaded by load control, and strains of CFS were recorded during the test. The strain distribution in the CFS was measured by strain gages mounted on CFS at spacing of every 20mm.

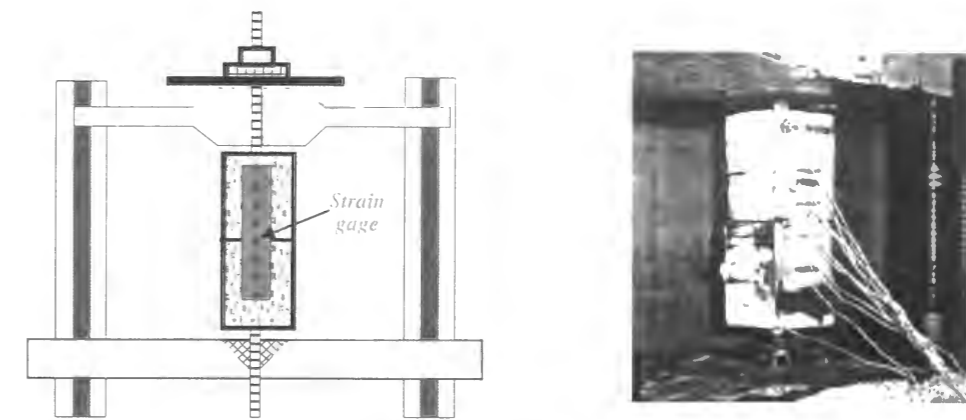


Figure 3.2 Loading set up

Table 3.1 Properties of the materials used

Material	Material Properties						
Concrete	Compressive strength : 32.5 N/mm ²		Elastic modulus: 2.4 × 10 ⁴ N/mm ²				
	Poisson's ratio : 0.2						
Epoxy	Tensile strength : 55.3 N/mm ²		Elastic modulus : 2.3×10 ³ N/mm ²				
	Poisson's ratio : 0.35						
CFS	Weight (g/m ²)	Density (g/cm ³)	Thickness (mm)	Tensile strength (N/mm ²)	Elastic modulus (N/mm ²)	Rupture strain (μ)	Poisson's ratio
T 300	300	1.8	0.167	3430	2.53 × 10 ⁵	14900	0.22
T 400	400		0.222				
HM 300	300	1.82	0.165	2940	3.92 × 10 ⁵	7500	0.18

3.3 TEST RESULTS & DISCUSSION

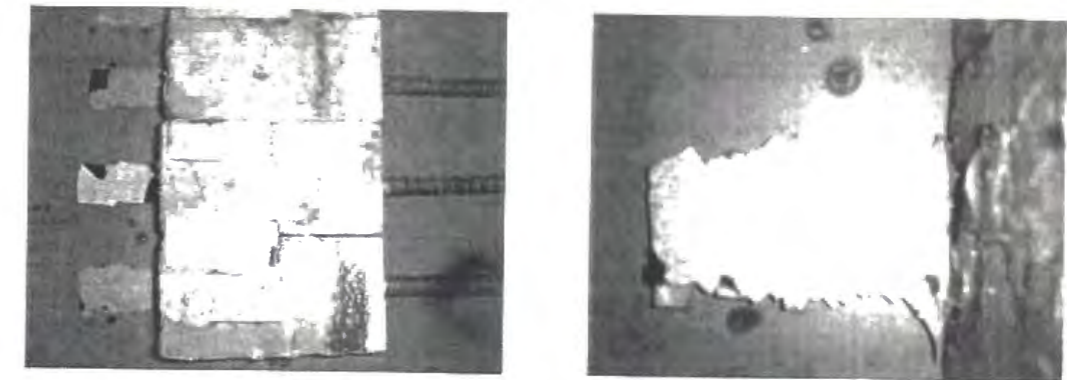
3.3.1 EXPERIMENTAL RESULTS

Table 3.2 is the summary of the bond test results. A total of eight rectangular concrete prism specimens were tested. Two specimens were tested for each case and 100mm-bond length was applied to all specimens. The failure of test specimens mainly occurred by sudden delamination of CFS from the concrete surface before reaches its rupture strain as shown Figure 3.3. Figure 3.4 shows the failure load versus thickness of the bonded CFS.

It is found that the failure load increases as the thickness of bonded CFS increases. However, the test specimens bonded by 2 layers of HM300 CFS have about 37% larger load carrying capacity than T300 CFS even its almost same thickness. Figure 3.5 shows measured strain distributions developed in the CFS along the bonded length. It can be seen that strain distributions between concrete and CFS is not uniform along the bonded length.

Table 3.2 Bond test results

Test specimen	CFS	Bond Length (mm)	Section Area (mm ²)	P_{max} (kN)	Bond Strength (N/mm ²)	
					*Method 1	*Method 2
A-1	T300×2	100	12.36	9.1	1.23	1.14
A-2				12.5	1.69	1.62
A-3	T400×1		8.24	12.0	1.62	1.57
A-4				12.5	1.69	1.65
A-5	T400×2		16.48	14.0	1.89	1.38
A-6				16.0	2.16	1.63
A-7	HM300×2		12.21	13.0	1.76	1.23
A-8				16.5	2.23	1.45



(a) Debonding failure

(b) CFS surface after debonding

Figure 3.3 Typical failure pattern of bond test specimen

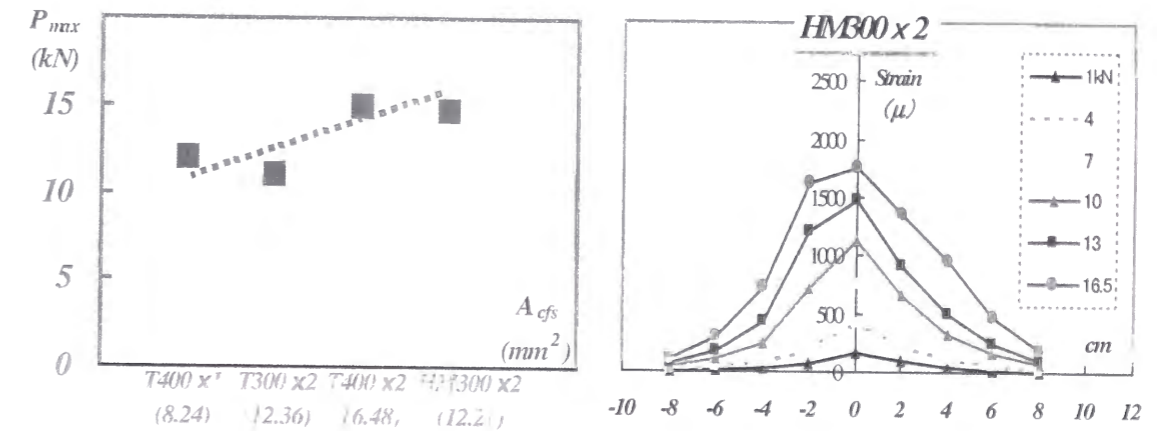


Figure 3.4 Failure load vs thickness of CFS Figure 3.5 Measured strain distribution in CFS

The bond strength f_b is evaluated by the following two methods in this study.

*Method 1

The average bond strength is defined as

$$f_b = P_{max} / 2A \quad (3-1)$$

Where, P_{max} : Maximum pull load, A : Attached area of CFS ($= b \cdot L$)

L : Bonded length ($=100\text{mm}$), b : Bonded width ($=37\text{mm}$)

If the bonded length increases, the maximum load increases in this method. However, the average bond strength decreases as the bonded length increases, because the maximum load is not increases in proportion to the bonded length.

***Method 2**

Figure 3.6 shows measured strain distributions between concrete surface and CFS just before the slipping. From the measured strains of the CFS at the surface, bond stresses are evaluated. The bond strength is defined by the average of the bond stresses just before slipping.

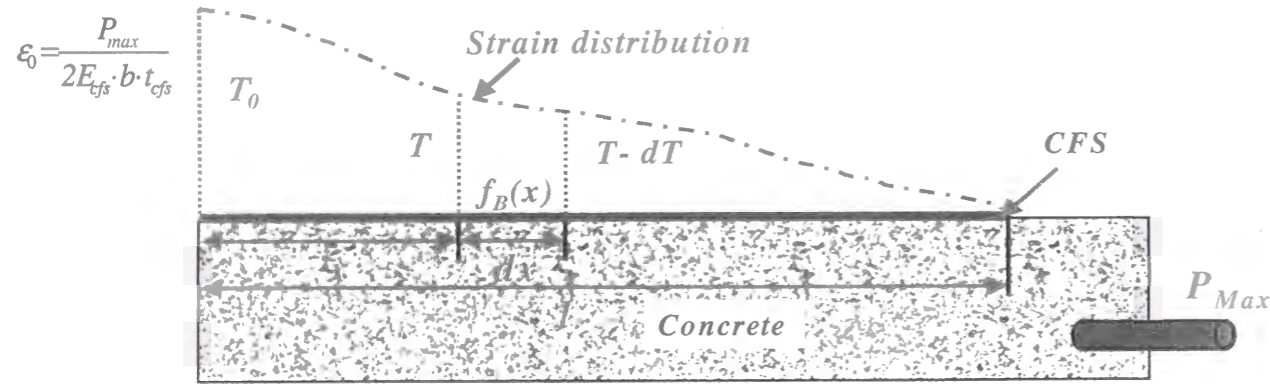


Figure 3.6 Measured strain distributions in CFS

$f_B(x)$ is bond stress occurring at x and T_{cfs} is the tensile force occurring in the CFS at x .

$$T_{cfs} = E_{cfs} \cdot \epsilon_{cfs} \cdot b \cdot t_{cfs}$$

$$dT/dx = E_{cfs} \cdot (d\epsilon/dx) \cdot b \cdot t_{cfs}$$

$$dT = f_B(x) \cdot b \cdot dx$$

$$f_B(x) = (dT/dx) / b$$

Therefore, the average bond strength f_B is

$$f_B = \int_0^l E_{cfs} \cdot t_{cfs} \left(\frac{d\epsilon}{dx} \right) dx / l$$

3.3.2 COMPARISON WITH FINITE ELEMENT ANALYSIS

Finite Element [FE] analysis using the commercial FE program *ABAQUS/Standard* (Version. 5.8 1998) was conducted to simulate the shear stress distributions along the bonded length of CFS. The concrete and epoxy resin between concrete and CFS were modeled using two-dimensional (2D) solid elements (*CPS4; 4-node bilinear plane stress quadrilateral solid element*), and CFS was modeled using one-dimensional (1D) beam elements (*B21, 2-node linear beam in a plane*) as shown in Figure 3.7.

Because the failure of concrete prism specimens occurred by sudden debonding of CFS from the concrete surface as shown in Figure 3.3, this FE analysis does not take into account the non-linearity of the bond behavior between concrete and CFS, that is, perfect bond is assumed between concrete and CFS. Thickness of the epoxy resin is 0.5mm. The properties of the materials used in this analysis are also listed in Table 3.1.

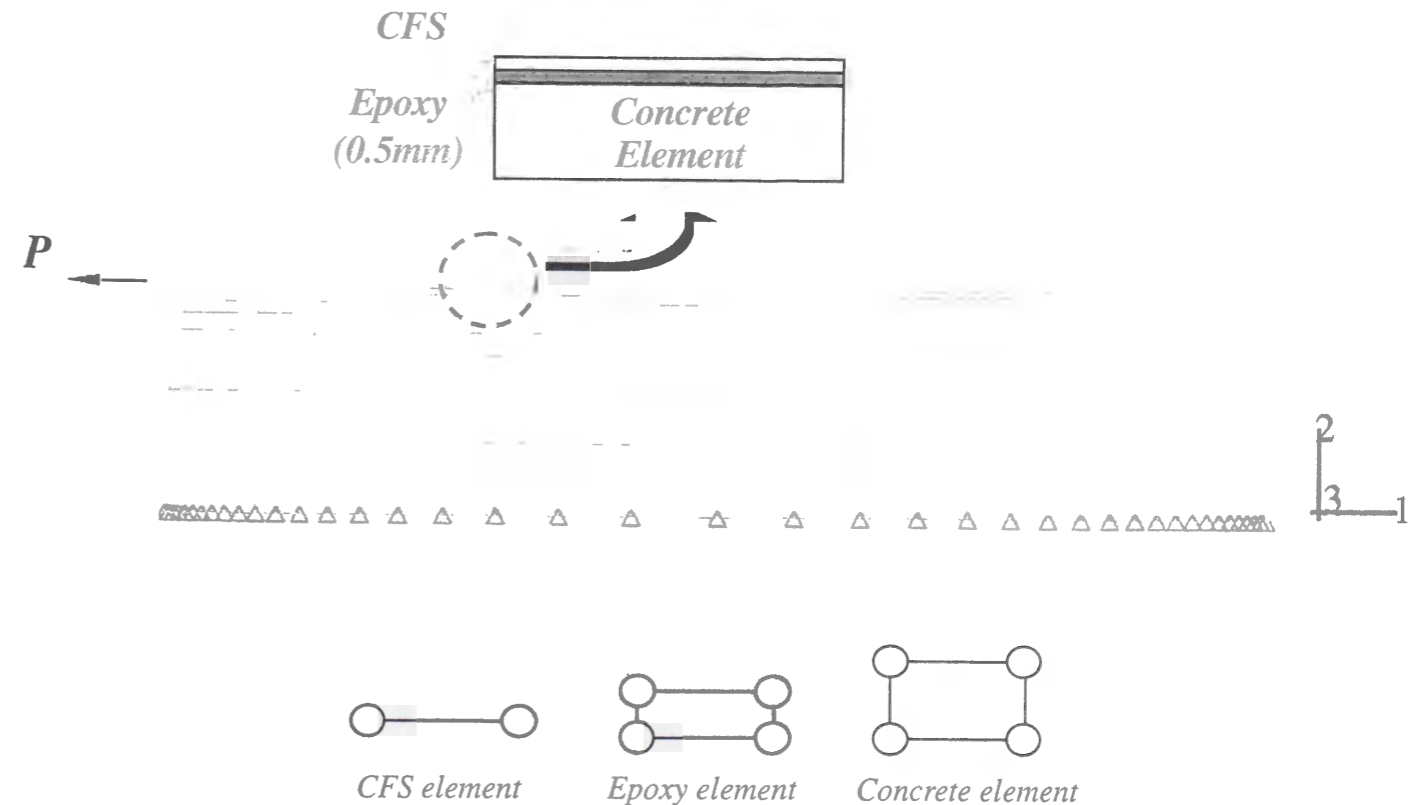


Figure 3.7 Modeling of test specimen (by ABAQUS 5.8)

Figure 3.8 shows horizontal strain distributions of test specimen bonded 2layers of T400 CFS obtained by FE analysis. Figure 3.9~3.11 show comparison of strain distributions and shear stress distributions in measured and FE results just before slipping, respectively. From the results, it can be concluded that a good correlation can be observed between analytical and experimental studies. However, the measured strains just before slipping show slightly larger than the FE results. This phenomenon seems that the nonlinear behavior due to the cracking of concrete or slipping of CFS may happen just before the failure of specimen.

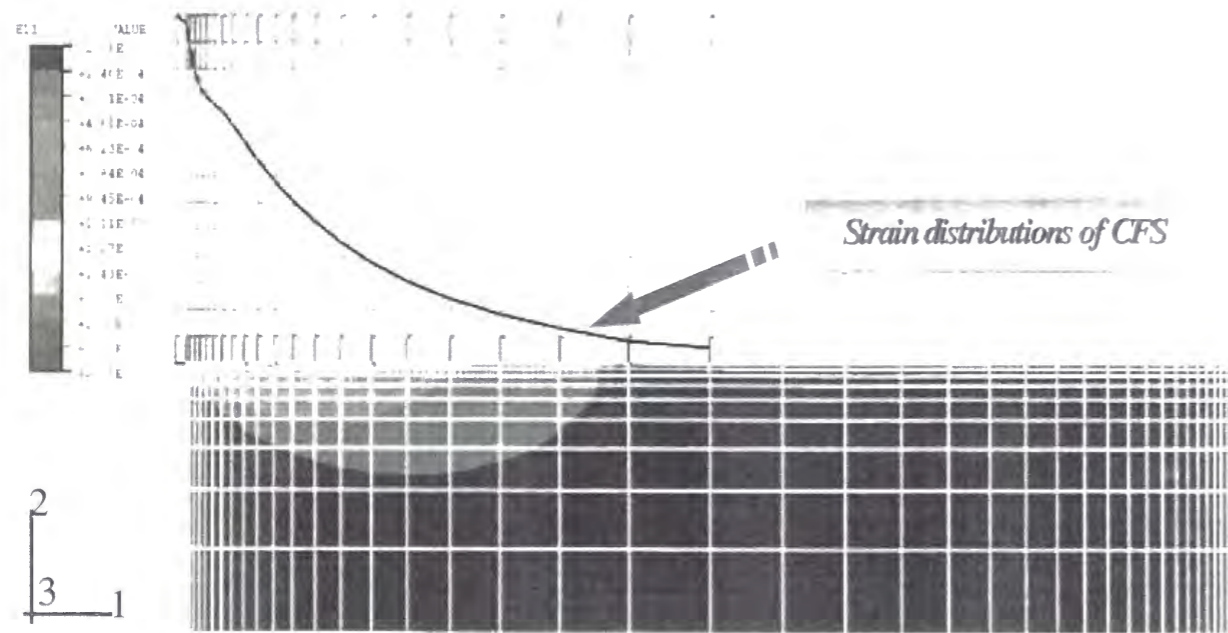


Figure 3.8 Horizontal strain E11 developed at maximum load by FEM (T400x2layers)

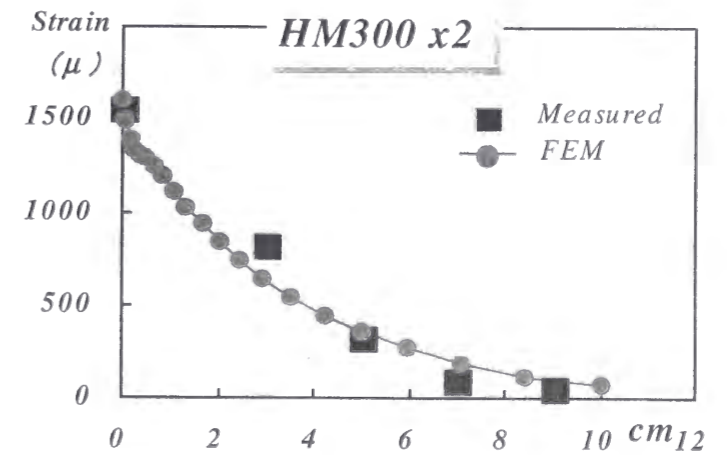
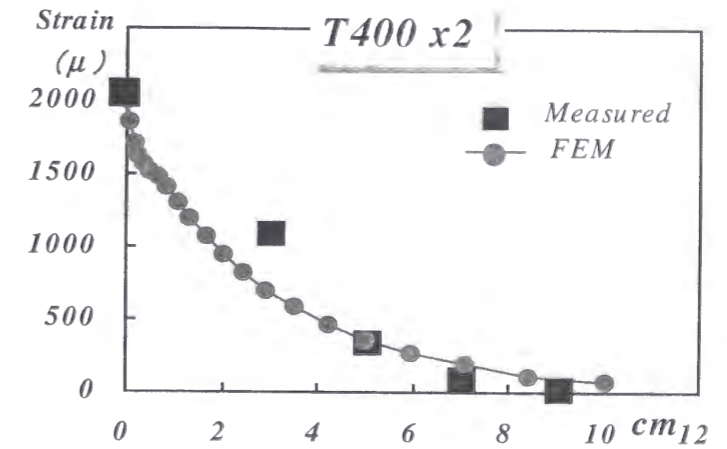
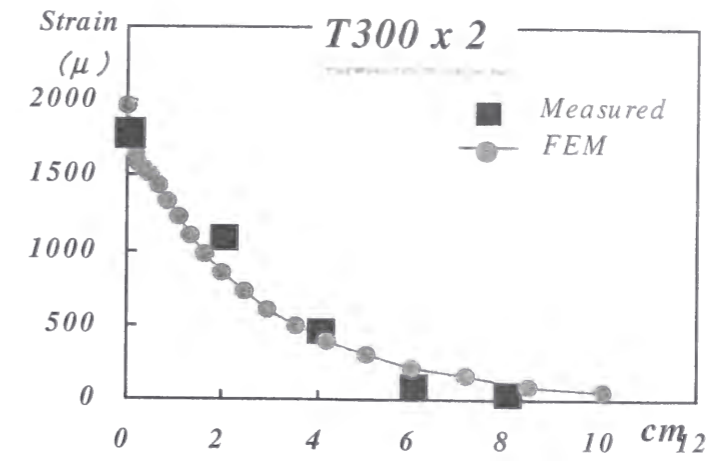


Figure 3.9 Comparison of strain distribution in measured and FEM just before slipping

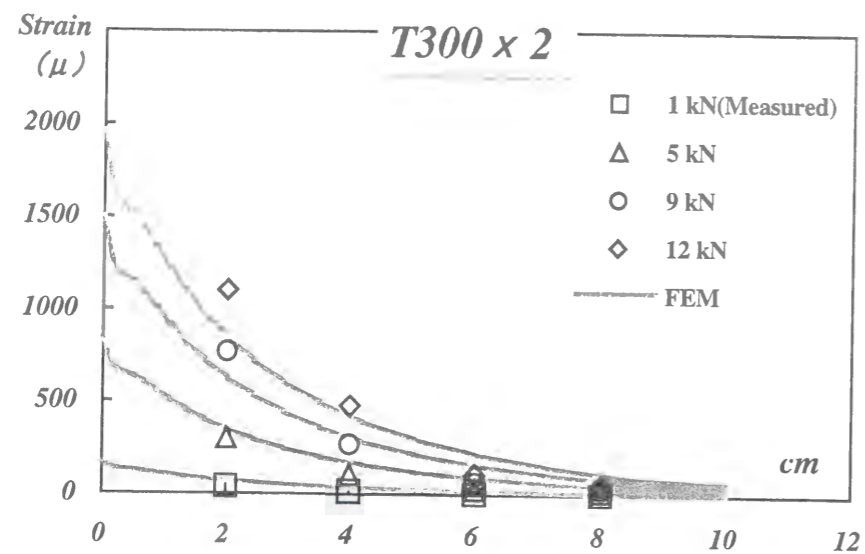


Figure 3.10 Comparison of strain distribution in measured and FEM at each load level

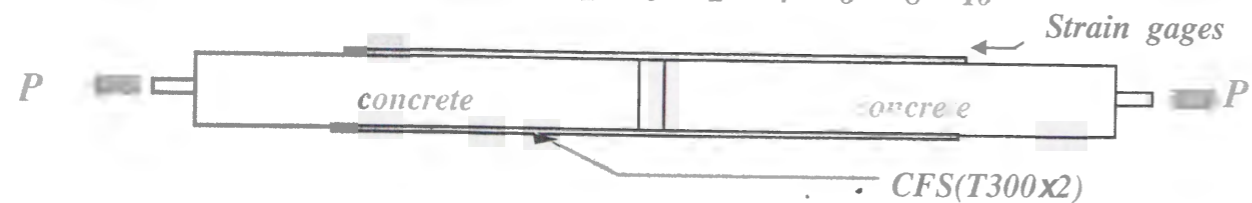
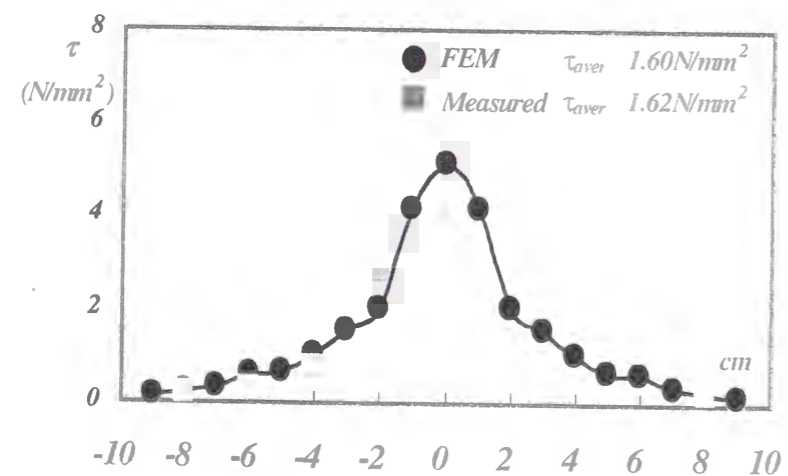


Figure 3.11 Comparison of shear stress distribution in measured and FEM just before slipping

3.4 CONCLUSIONS OF CHAPTER 3

Experimental and analytical investigations concerning the interfacial bond behavior between concrete surface and CFS were discussed. The following conclusions can be drawn from the study reported herein:

- The failure of test specimens mainly occurs by sudden delamination of CFS from the concrete surface before reaches its rupture strain.
- The maximum pull load increases as the thickness of bonded CFS increases. Also, test specimens bonded by high elastic modulus of CFS show better load capacity.
- Finite Element [FE] analysis was conducted to simulate the strain distributions along the bonded length of CFS. The FE analysis shows good accordance to the experimental results, and also within the scope of this bond test, 100mm length is considered as an effective bond length of CFS.

Chapter 4

STRENGTH IMPROVEMENT OF LAMINATED RC SLAB BY CARBON FIBER SHEET

4.1 INTRODUCTION

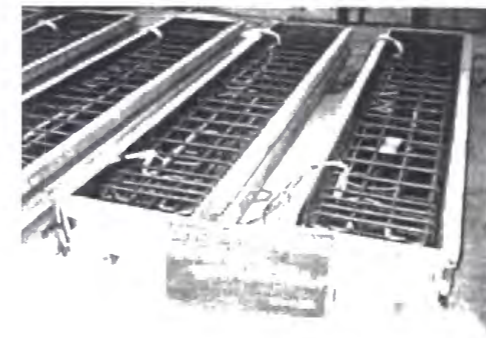
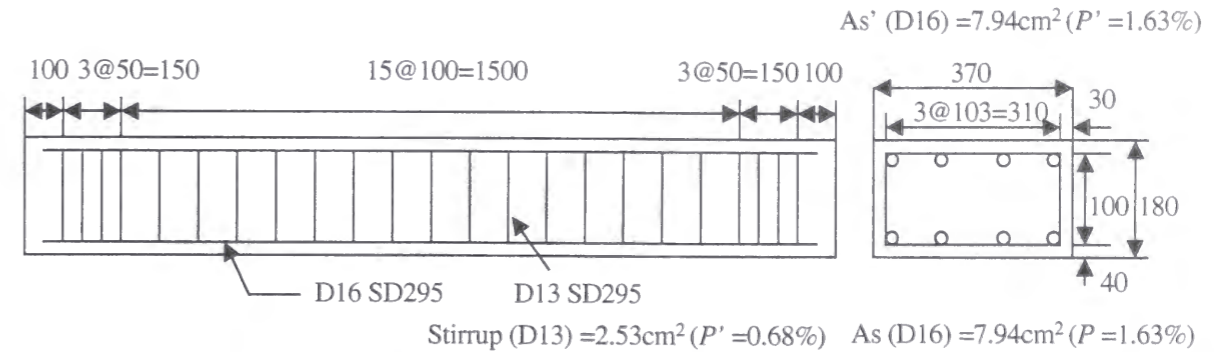
This chapter presents flexural strength improvement of laminated RC bridge slab by CFS. An experimental investigation was conducted with RC bridge slab specimens under static loading. Section analysis based on the compatibility of deformations and equilibrium of forces and 2-dimensional Finite Element (FE) analysis are developed to predict the structural behavior of composite RC slab.

4.2 EXPERIMENTAL PROGRAM

4.2.1 TEST SPECIMEN

Sixteen slab specimens were constructed. Each test slab has a rectangular cross-section of 370mm width, 180mm depth, and overall length of 2000mm. The test slab is almost identical to the real slab of a highway viaduct in terms of the amount of steel reinforcement, quality of concrete and the thickness of the slab. This test slab represents a part of the real

slab with the same flexural moment capacity. Two different types of anchor were used in this test. Details of the test slabs are shown in Figure 4.1.



(a) Before casting



(b) After casting

Figure 4.1 Detail of test specimen (mm)

4.2.2 MATERIAL PROPERTIES

- ◆ Concrete: Ready-mixed concrete was used for all test slabs. The concrete had a water-cement ratio of 0.45 by weight, and the maximum aggregate size was 20mm. The average 28-day concrete compressive strength was 39.2 N/mm² and elastic modulus was 2.52×10⁴N/mm². All test slabs were cured over 28 days prior to testing.
- ◆ Steel reinforcement: Three samples of each material were tested under uniaxial tension. The average mechanical properties are shown in Table 4.1.

Table 4.1 Properties of steel reinforcement

Steel reinforcement	Section area (cm ²)	Yield strength (N/mm ²)	Yield strain (μ)	Elastic modulus (N/mm ²)
Longitudinal reinforcement D16	1.986	341	1820	2.06×10 ⁵
Stirrup D13	1.267	374	1950	1.96×10 ⁵

- Adhesive: The adhesive used was composed of two-component, which are primer and epoxy.

Table 4.2 Properties of primer

Contents	Test method	Test condition	Unit	Standard value	Measured value
Viscosity	JIS K 6833	25°C	mPa·s	1500±300	1500
Specific gravity	JIS K 7112	20°C		1.10±300	1.15
Compressive strength	JIS K 7208	20°C, 7 日	N/mm ²	Over 58.8	72.2
Elastic modulus	JIS K 7208	20°C, 7 日	N/mm ²	9.8 × 10 ³	15.8 × 10 ³
Flexural strength	JIS K 7203	20°C, 7 日	N/mm ²	Over 19.6	31.4
Tensile strength	JIS K 7113	20°C, 7 日	N/mm ²	Over 19.6	23.1

Table 4.3 Properties of epoxy

Contents	Test method	Test condition	Unit	Standard value	Measured value
Viscosity	JIS K 7117	20°C	mPa·s	20000±7000	24000
Specific gravity	JIS K 7112	20°C		1.15±0.05	1.18
Compressive strength	JIS K 7208	20°C, 7 日	N/mm ²	Over 68.6	90.0
Elastic modulus	JIS K 7208	20°C, 7 日	N/mm ²	1.95 × 10 ³	2.65 × 10 ³
Flexural strength	JIS K 7203	20°C, 7 日	N/mm ²	Over 58.8	79.5
Tensile strength	JIS K 7113	20°C, 7 日	N/mm ²	Over 29.4	47.0

- Carbon Fiber Sheets [CFS]: The unidirectional CFS was used for strengthening provided by Nippon oil company. The CFS has a linear stress-strain behavior and its

material properties, as supplied by the manufacturer, are shown in Table 4.4.

Table 4.4 Properties of CFS

CFS Type	Weight (g/m ²)	Density (g/cm ³)	Thickness (mm)	Tensile strength (N/mm ²)	Elastic modulus (N/mm ²)	Rupture strain (μ)
T 200	200		0.111			
T 300	300	1.8	0.167	3430	2.53 × 10 ⁵	14900
T 400	400		0.222			
HM 300	300	1.82	0.165	2940	3.92 × 10 ⁵	7500

4.2.3 STRENGTHENING OF CFS

To ensure a good bond between concrete and CFS, the surface of the test slabs were cleaned and sanded to obtain a rough surface, and then primer was applied in the bonding surface of the beam with roller brush. After the primer cured, a coat of epoxy resin was applied onto the concrete surface. The CFS, previously cut to the required dimensions, was positioned on the prepared concrete surface, and an epoxy resin was applied. A similar procedure was repeated while applying additional layers. The CFS was glued at the bottom of the test slab with normal (NA) or perfect anchoring (PA) as shown Figure 4.2. After the CFS was bonded, 7-day resin curing was performed at ambient conditions.

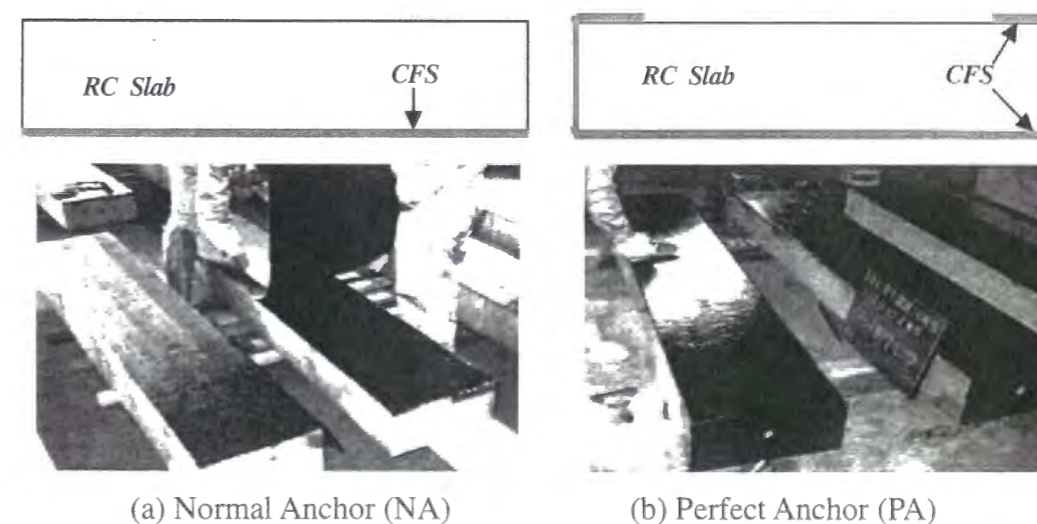


Figure 4.2 Anchoring type

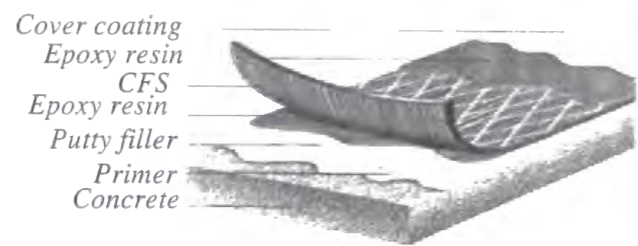


Figure 4.3 Strengthening procedure of a test slab

4.2.4 LOADING SET UP

Figure 4.4 shows the loading set up. Flexural static test with 6.1 shear-span ratio (a/d) was conducted under four-point flexural load. All test slabs were simply supported and subjected to two concentrated loads symmetrically placed about the mid-span. The load was applied using a 2000kN capacity universal testing machine. Load-cell connected to the data acquisition system was used to measure the applied load.

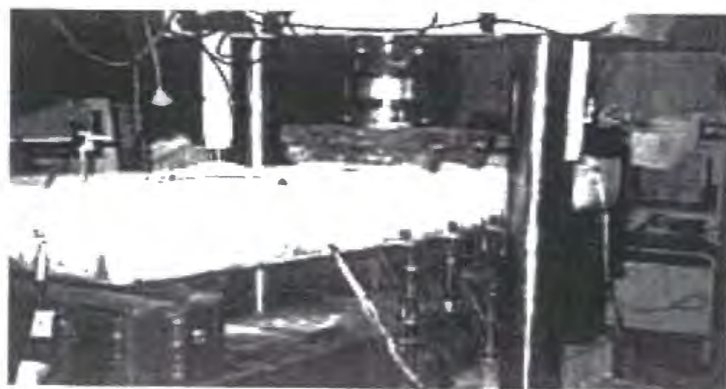
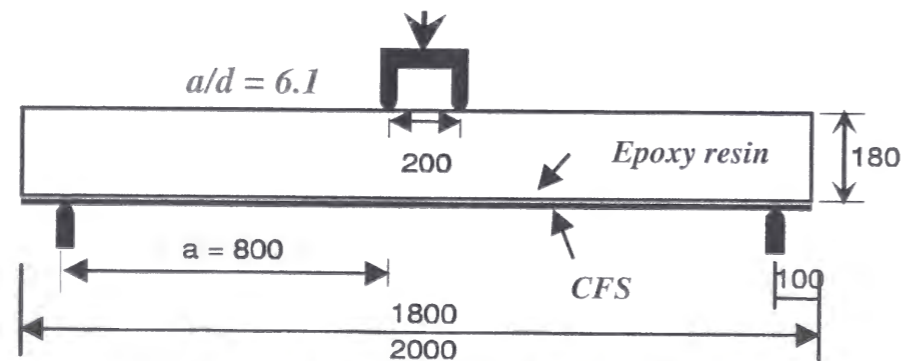


Figure 4.4 Loading set-up

4.2.5 MEASUREMENT & TEST PROCEDURE

Measurement of the strain and displacement of the test slab was performed throughout the experiments. At various positions along the slabs span, electrical resistance strain gauges were attached to measure the strains on the tensile reinforcement, the bottom of the CFS and the extreme compression face of the test slab as shown in Figure 4.5.

The deflection was also measured by Linear Variable Displacement Transducer (LVDT) placed at the center of the slab. The all test slabs were incrementally loaded with a uniform rate ($\cong 10\text{kN/minute}$) up to failure and after each increment of load, the strains and deflections were measured by a data acquisition system. The test slabs were painted before testing to facilitate the observation and marking of crack propagation during the test. After each load increment, the cracks were marked for failure pattern.

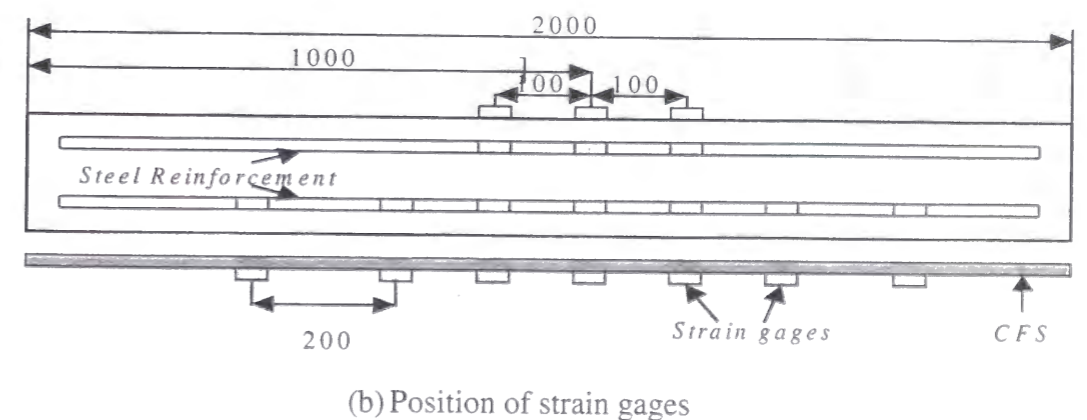
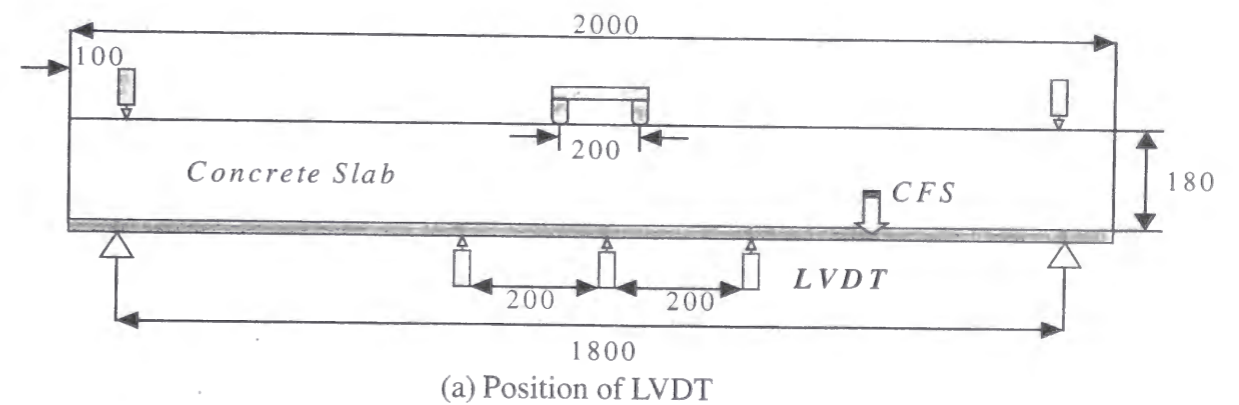


Figure 4.5 Position of gages

4.3 TEST RESULTS & DISCUSSION

Table 4.5 shows the static test results obtained from experimental study.

Table 4.5 Summary of the static test results

Test slab	CFS		Ancho-ring	P_{max} (kN)	Strength Improvement	Strain of CFS at failure (μ)	δ_y (mm)	δ_u (mm)	Ductility δ_u / δ_y
	Type	Layer							
Control	No CFS			91.7	1.0		8.0	35	4.4
SA-1			PA	136.2	1.49	5760 (38.7)*	9.8	32	3.3
SA-2				136.5	1.49	5990 (40.2)	10.3	40	3.9
SA-3		1	NA	124.5	1.36	6600 (44.3)	9.1	28	3.1
SA-4	T300				127.4	1.39	5650 (37.9)	9.1	30
SA-5			PA	161.7	1.76	7820 (52.5)	10	60	6.0
SA-6		2	NA	165.6	1.81	7310 (49.1)	9.4	30	3.2
SA-7					157.8	1.72	6000 (40.1)	10	28
SB-1	T400	1	PA	162.7	1.78	9950 (66.8)	10.6	85	8.0
SB-1*	T200	2		161.7	1.76	7400 (49.7)	11.0	55	5.0
SB-2			PA	189.1	2.06	9420 (63.2)	9.1	72	7.9
SB-3	T400	2		190.1	2.07	8800 (59.1)	8.6	82	9.5
SB-4				NA	198.0	2.16	Not available	9.2	30
SC-1	HM300	2	NA	218.0	2.38	5730 (76.4)	10.1	32	3.2

() : the ratio of CFS strain at failure to its rupture strain in %.

4.3.1 STRUCTURAL BEHAVIOR & FAILURE MODE

Figure 4.6 shows the typical failure pattern. When loaded, the control slab developed flexural cracks in the constant moment region at loads slightly below 25kN. At loads near

75kN, the tensile steel reinforcement yielded. Finally, the control slab failed in flexure due to crushing of the compression concrete at loads of nearly 91kN. The failure procedures of retrofitted test slab by CFS are regarded as follows. First, after occurring the first cracks in the concrete, the stiffness was reduced. From that time, the tensile steel and CFS were beginning to receive the additional load directly, and the behavior of these materials were almost linearly continued until the tensile steel was yielded nearly the strain of 2000μ (2000×10^{-6}). After yielding of the tensile steel, with the additional changes of stiffness and deflection, CFS only received the additional tension stress.

After all, the failure of retrofitted slabs mainly occurred by debonding of interface between concrete and CFS, and the large deflections were continuously taken place in the slabs. While, the place where shear force is zero, CFS was still attached in the concrete. From the test results, it seems that the bond strength between concrete and CFS is one of the important factors to decide the actual behavior of the retrofitted RC members by CFS.

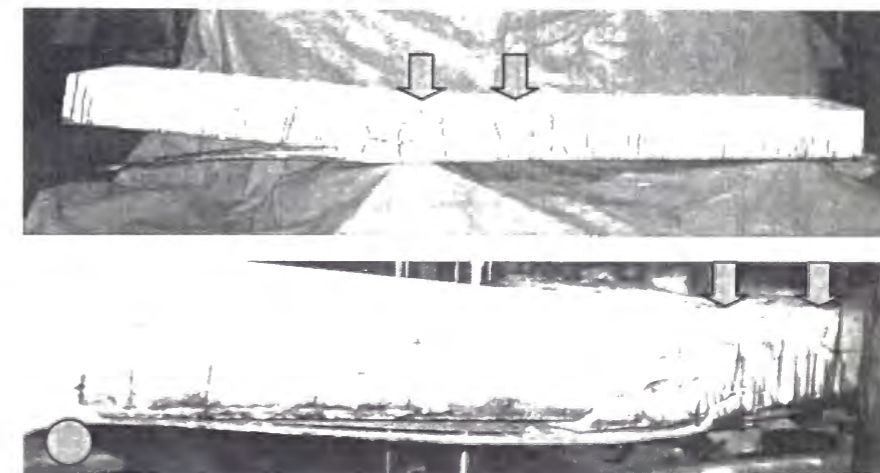


Figure 4.6 Typical failure pattern of laminated test slab

4.3.2 LOAD - DEFLECTION RELATIONSHIP

Figure 4.7 shows the load-deflection curve for the slabs tested.

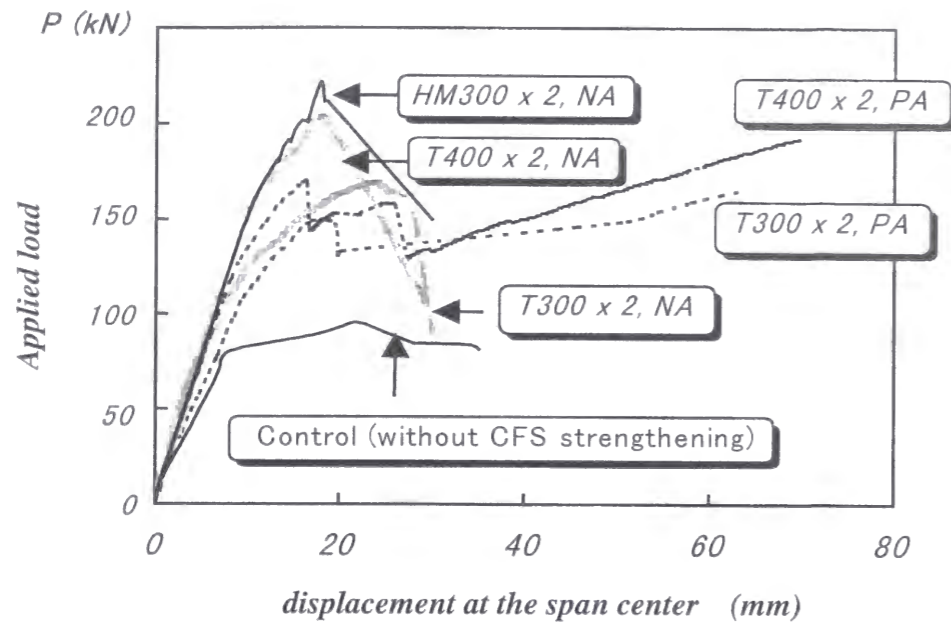


Figure 4.7 Load-displacement relationship

4.3.3 LOAD - STRAIN RELATIONSHIP

Figure 4.8 shows the variation of compressive strain in concrete and tensile strain of steel reinforcement and CFS at the span center.

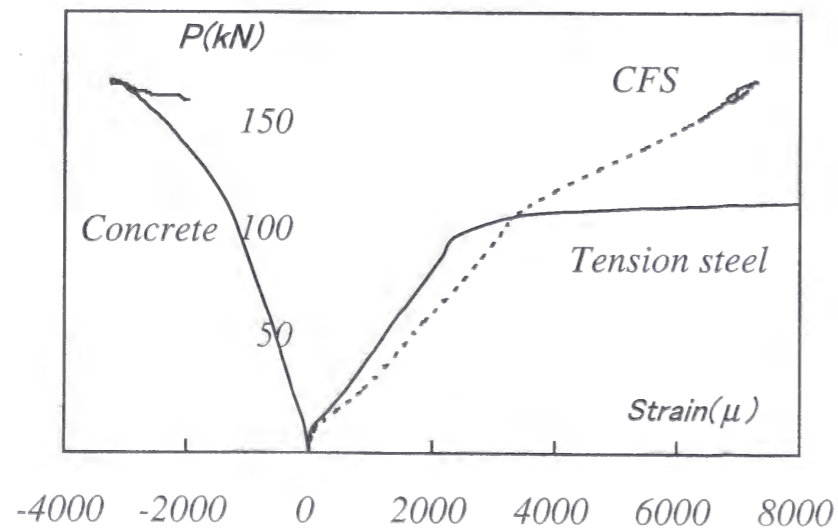


Figure 4.8 Load-strain relationship (SA-6 slab; T300 x 2layers)

4.3.4 EFFECT OF FLEXURAL STRENGTH IMPROVEMENT

Figure 4.9 shows strength improvement due to CFS. Strength ratio is the ratio of flexural strength of retrofitted slab to control slab. All test slabs retrofitted with CFS show significant increases in ultimate flexural strength as compared to the control slab. Retrofit of the test slab with 2 layers of T400 CFS improved the flexural strength over 2 times.

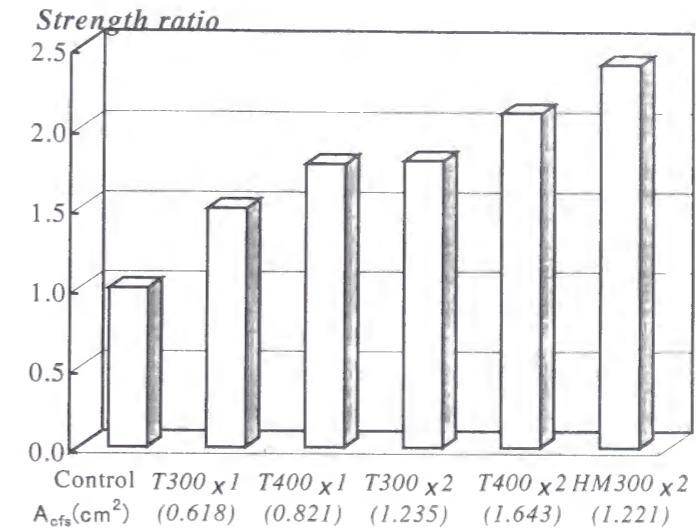


Figure 4.9 Strength improvement due to CFS

4.3.5 EFFECT OF ANCHORING SYSTEM

Energy-absorbing characteristics of test slab denoted by ductility is developed to investigate the structural behavior between two anchoring styles. In this research, the Ductility Index (DI) is obtained by following definition.

$$Ductility\ Index(DI) = \frac{Deflection\ ductility\ of\ retrofitted\ slab}{Deflection\ ductility\ of\ control\ slab}$$

Here, $Deflection\ ductility = \delta_u / \delta_y$

δ_y is the deflection at the span center when the re-bar yielded

δ_u is the deflection at the span center when the applied load dropped down to the level of yielding load from the maximum

From the results, Perfect Anchoring (PA) contributes to the improvement of the slab ductility as shown in Figure 4.10. This fact should be taken into consideration for the practical application. However, there was almost no difference in load carrying capacity between two anchoring types.

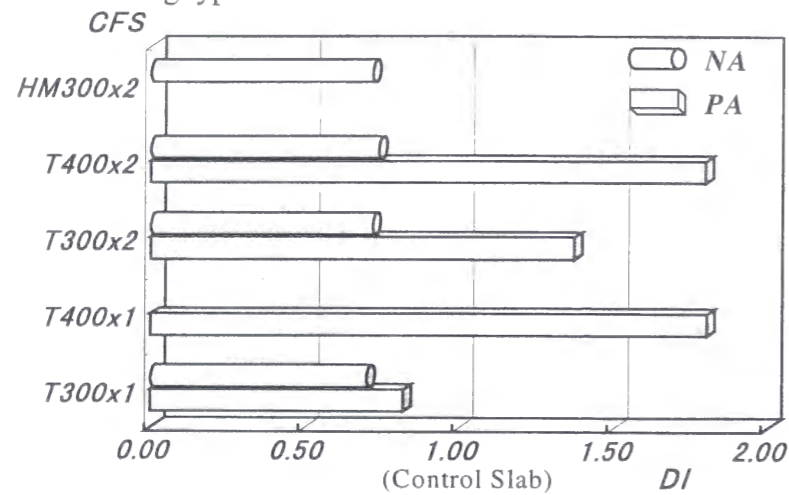


Figure 4.10 Ductility improvement due to anchoring

4.3.6 STRAIN OF CFS AT THE FAILURE

In proportion to the amount of CFS, the strain of CFS at the failure was increased. However, the strain level developed in CFS at the failure was much lower than its rupture strain. Therefore, the improvement of bond strength between concrete and CFS may increase the flexural strength of the slab more.

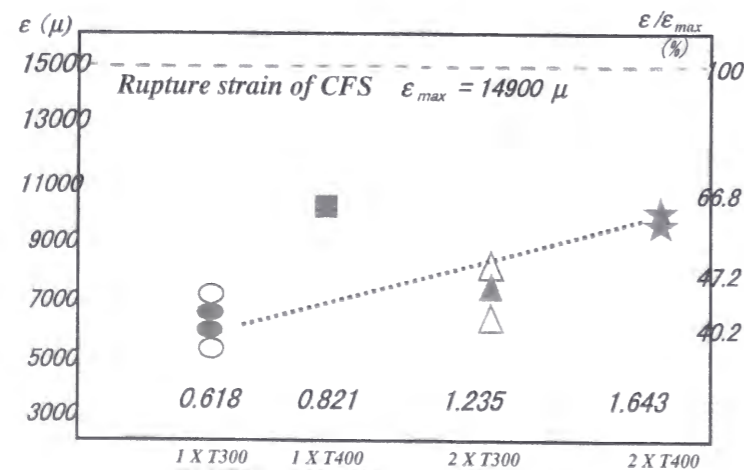


Figure 4.11 Strain of CFS at the failure

4.4 ANALYTICAL STUDY

4.4.1 SECTION ANALYSIS

Analytical model (R. Park, 1975) based on the compatibility of deformations, equilibrium of forces and rational stress-strain relationship for materials is investigated to predict the structural behavior of laminated RC slab by CFS. This model takes into account the nonlinear properties of concrete in compression, the tensile strength of concrete.

ASSUMPTIONS

The following assumptions are used in this analytical investigation.

1. Linear strain distribution through the depth of the cross section
2. Perfect bond between steel reinforcement and concrete, and concrete and CFS

STRESS-STRAIN RELATIONSHIPS FOR MATERIALS USED

The stress-strain relations for the concrete, steel reinforcement and CFS are shown in Figure 4.12.

■ CONCRETE

The stress-strain curve defined by the Japanese Society of Civil Engineers (JSCE) Design Code 1996 is used for compressive portion of concrete. The compressive strength of concrete f'_c is 39.2Mpa. For the tension portion of the concrete is assumed linear up to a tensile strength f_{tc} which is 3.3Mpa. The elastic modulus of concrete in compression and tension is 25.2Gpa.

■ STEEL REINFORCEMENT

The stress-strain curve for the steel reinforcement is assumed to be elastic-plastic and similar in both tension and compression. The yield strength and elastic modulus of steel reinforcement in compression and tension are 341Mpa and 206Gpa, respectively.

■ CFS

The stress-strain curves for the CFS is assumed to be linear elastic until failure stress. The tensile strength and elastic modulus of CFS are 3430Mpa and 253Gpa, respectively.

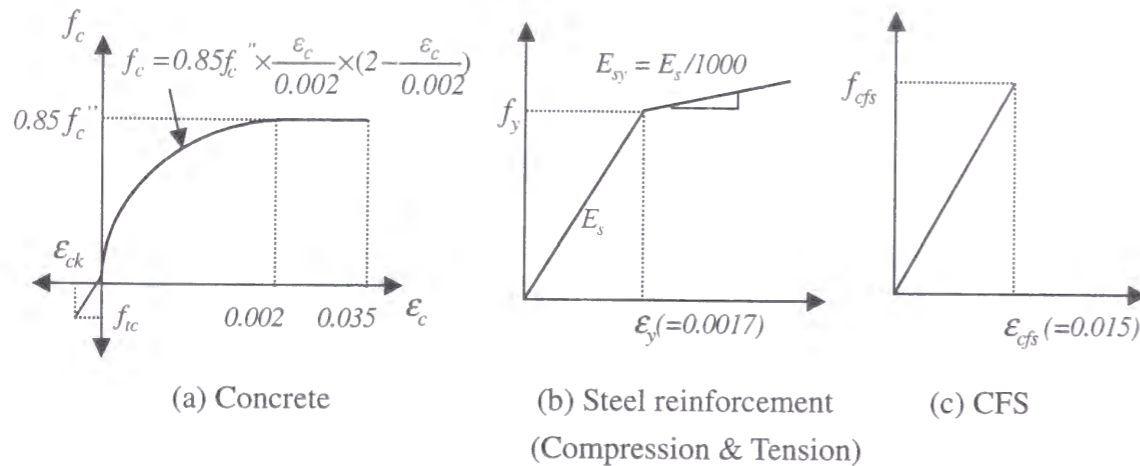


Figure 4.12 Stress-strain relations for materials used

SECTION ANALYSIS PROCEDURE

Figure 4.13 shows cross section of composite slab with strain, stress and force distribution. This theoretical approach assumes that failure is reached when either the strain in the extreme fiber of concrete in compression ϵ_{cc} is reached the value of 0.0035 or the CFS reaches its ultimate strain. The full calculation procedure is summarized as follows;

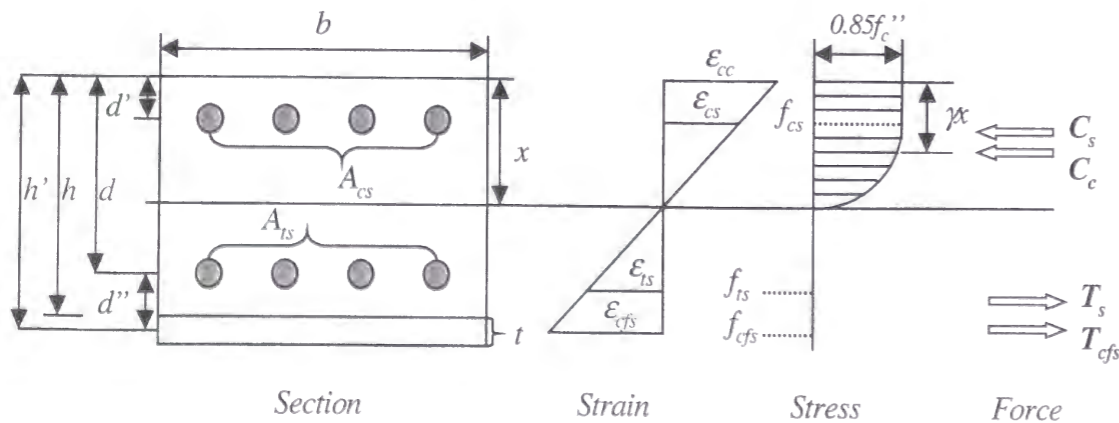


Figure 4.13 Cross section with strain, stress and force distribution

1. The strain in the extreme fiber of concrete in compression ϵ_{cc} is increased until failure is reached.
2. The strains in tensile concrete, steel reinforcements and CFS are determined from the strain distribution along the slab depth.

Strain of concrete in tension ϵ_{tc}	$\epsilon_{tc} = \epsilon_{cc} (h - x) / x$
Strain of steel in compression ϵ_{cs}	$\epsilon_{cs} = \epsilon_{cc} (x - d') / x$
Strain of steel in tension ϵ_{ts}	$\epsilon_{ts} = \epsilon_{cc} (d - x) / x$
Strain of CFS ϵ_{cfs}	$\epsilon_{cfs} = \epsilon_{cc} (h' - x) / x$

3. The stresses in concrete, steel reinforcement and CFS are then calculated using the stress-strain relationships for each material.

Stress of concrete in compression f_{cc}

$$\text{If, } \epsilon_{cc} \leq 0.002 \Rightarrow f_{cc} = 0.85f_c'' \times \frac{\epsilon_{cc}}{0.002} \times (2 - \frac{\epsilon_{cc}}{0.002})$$

$$\text{If, } 0.002 < \epsilon_{cc} \leq 0.0035 \Rightarrow f_{cc} = 0.85f_c''$$

Here, $0.85f_c''$ is strength of concrete in a member

Stress of concrete in tension f_{tc}

$$\text{If, } \epsilon_{tc} \leq \epsilon_{ck} \Rightarrow f_{tc} = E_c \epsilon_{tc}$$

$$\text{If, } \epsilon_{tc} > \epsilon_{ck} \Rightarrow \text{Crack happen}$$

Stress of steel in compression f_{cs}

$$\text{If, } \epsilon_{cs} \leq \epsilon_{ycs} \Rightarrow f_{cs} = E_{cs} \epsilon_{cs}$$

$$\text{If, } \epsilon_{cs} > \epsilon_{ycs} \Rightarrow f_{cs} = f_{ycs} + E_{csy} (\epsilon_{cs} - \epsilon_{ycs})$$

Stress of steel in tension f_{ts}

$$\text{If, } \epsilon_{ts} \leq \epsilon_{yts} \Rightarrow f_{ts} = E_{ts} \epsilon_{ts}$$

$$\text{If, } \epsilon_{ts} > \epsilon_{yts} \Rightarrow f_{ts} = f_{yts} + E_{cty} (\epsilon_{ts} - \epsilon_{yts})$$

Stress of CFS f_{cfs} $\Rightarrow f_{cfs} = E_{cfs} \epsilon_{cfs}$

4. Therefore, the forces acting on the cross section of composite slab are found by multiplying the each stress by their corresponding area.

$$\text{Compressive force in concrete } C_c \quad C_c = \alpha 0.85 f_c'' b x$$

$$\text{Tensile force in concrete } T_c \quad T_c = E_c \epsilon_{cc} b (h - x)^2 / 2x$$

$$\text{Compressive force in steel } C_t \quad C_t = E_{cs} \epsilon_{cc} A_{cs} (x - d') / x$$

$$\text{Tensile force in steel } T_s \quad T_s = E_{ts} \epsilon_{cc} A_{ts} (d - x) / x$$

$$\text{Tensile force in CFS } T_{cfs} \quad T_{cfs} = E_{cfs} \epsilon_{cc} b t (h' - x) / x$$

For any given concrete strain in the extreme compression fiber ϵ_{cc} , the compressive force in concrete and its position can be defined by mean stress factor α and centroid factor γ . The α is used to convert the nonlinear stress-strain relationship of concrete into an equivalent rectangular stress-strain relationship. This value can be calculated by using the area under stress-strain curve of concrete as follows;

$$\alpha (0.85 f_c'') \epsilon_{cu} = \int_0^{\epsilon_{cu}} f_{cc} d\epsilon_{cc}$$

$$\text{if } 0 \leq \epsilon_{cc} < 0.002$$

$$\alpha = \frac{1}{\epsilon_{cu}} \left[\frac{1}{0.002} \left(\epsilon_{cc}^2 - \frac{\epsilon_{cc}^3}{3 \cdot 0.002} \right) \right]_0^{\epsilon_{cu}} = \frac{\epsilon_{cu}}{0.002} \left(1 - \frac{\epsilon_{cu}}{3 \cdot 0.002} \right)$$

$$= \frac{1}{\epsilon_{cu}} \left[\frac{1}{0.002} \left(\epsilon_{cc}^2 - \frac{\epsilon_{cc}^3}{3 \cdot 0.002} \right) \right]_0^{\epsilon_{cu}} = \frac{\epsilon_{cu}}{0.002} \left(1 - \frac{\epsilon_{cu}}{3 \cdot 0.002} \right)$$

$$\text{if } 0.002 \leq \epsilon_{cc} < 0.0035$$

$$\alpha = \frac{\int_0^{\epsilon_{cu}} 0.85 f_c'' d\epsilon_{cc}}{0.85 f_c'' \epsilon_{cu}} = \frac{\int_0^{\epsilon_{cu}} d\epsilon_{cc}}{\epsilon_{cu}} = 1$$

On the other hand, the position of concrete compressive force C_c acting at distance γx can be calculated as follows;

The first moment of area about origin of area under stress-strain curve

$$\int_0^{\epsilon_{cu}} f_{cc} \epsilon_{cc} d\epsilon_{cc} = (1 - \gamma) \epsilon_{cu} \int_0^{\epsilon_{cu}} f_{cc} d\epsilon_{cc}$$

$$\gamma = 1 - \frac{\int_0^{\epsilon_{cu}} f_c'' \epsilon_{cc} d\epsilon_{cc}}{\epsilon_{cu} \int_0^{\epsilon_{cu}} f_c'' d\epsilon_{cc}} = 1 - \frac{\int_0^{\epsilon_{cu}} 0.85 f_c'' \frac{\epsilon_{cc}}{0.002} \left[2 - \frac{\epsilon_{cc}}{0.002} \right] \epsilon_{cc} d\epsilon_{cc}}{\epsilon_{cu} \int_0^{\epsilon_{cu}} 0.85 f_c'' \frac{\epsilon_{cc}}{0.002} \left[2 - \frac{\epsilon_{cc}}{0.002} \right] d\epsilon_{cc}}$$

$$\text{if } 0 \leq \epsilon_{cc} < 0.002$$

$$\gamma = 1 - \frac{\frac{\epsilon_{cu}^3}{0.002} \left(\frac{2}{3} - \frac{\epsilon_{cu}}{4 \cdot 0.002} \right)}{\frac{\epsilon_{cu}^3}{0.002} \left(1 - \frac{\epsilon_{cu}}{3 \cdot 0.002} \right)} = \frac{1}{3} - \left(\frac{\epsilon_{cu}}{12 \cdot 0.002} \right) \bigg/ \left(1 - \left(\frac{\epsilon_{cu}}{3 \cdot 0.002} \right) \right)$$

$$\text{if } 0.002 \leq \epsilon_{cc} < 0.0035$$

$$\gamma = 1 - \frac{\int_0^{\epsilon_{cu}} 0.85 f_c'' \epsilon_{cc} d\epsilon_{cc}}{\epsilon_{cu} \int_0^{\epsilon_{cu}} 0.85 f_c'' d\epsilon_{cc}} = \frac{1}{2}$$

5. The location of the neutral axis x is obtained from the equilibrium of internal forces acting on the cross section.

$$C_c + C_s + T_s + T_{cfs} = 0$$

6. The resisting moment is calculated as follows;

$$M_n = C_c (d - \gamma x) + C_s (d - d') + T_{cfs} d''$$

7. The curvature at center span is

$$\phi = \frac{\epsilon_{cc}}{x}$$

8. The flexural stiffness is

$$EI = \frac{M}{\phi}$$

9. The deflection of center span loaded as shown in Figure 4.5 is

$$\delta = \frac{P}{EI} \left(\frac{aL^2}{16} - \frac{a^3}{12} \right)$$

Here, L : Length of the span (=1800 mm), a : Shear span (= 800 mm)

10. The concrete strain, at the extreme compression fiber ϵ_{cc} is increased incrementally and the previous steps are repeated to obtain above values.

COMPARISON BETWEEN ANALYTICAL AND EXPERIMENTAL RESULT

A comparison of measured and analytical results based on the compatibility of deformations and equilibrium of forces indicated that the behavior of retrofitted slab can be predicted with reasonable accuracy as shown in Figure 4.14~4.16.

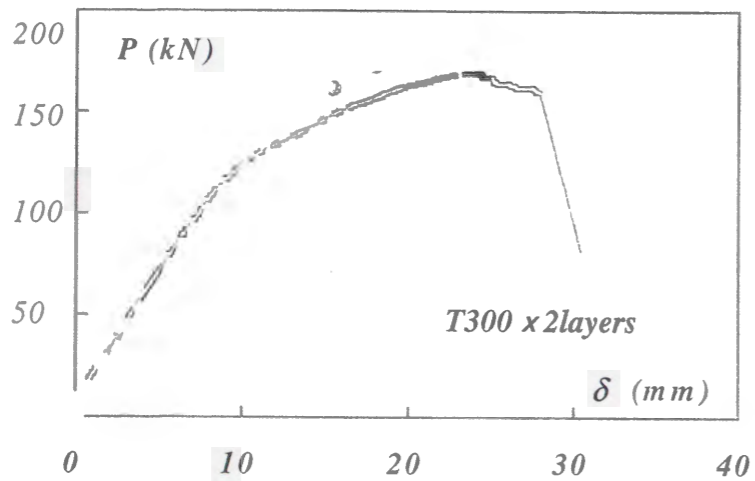
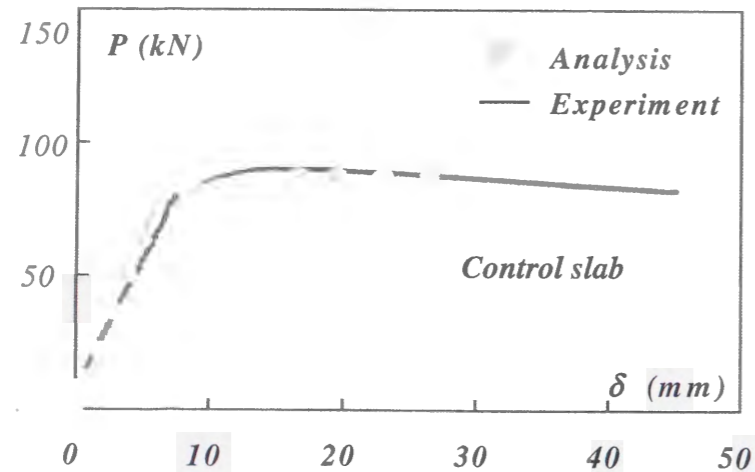


Figure 4.14 Load- deflection curves at the span center

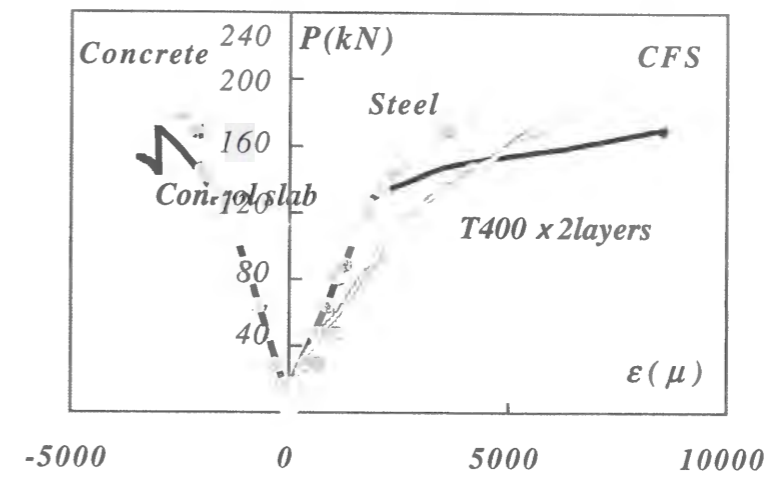
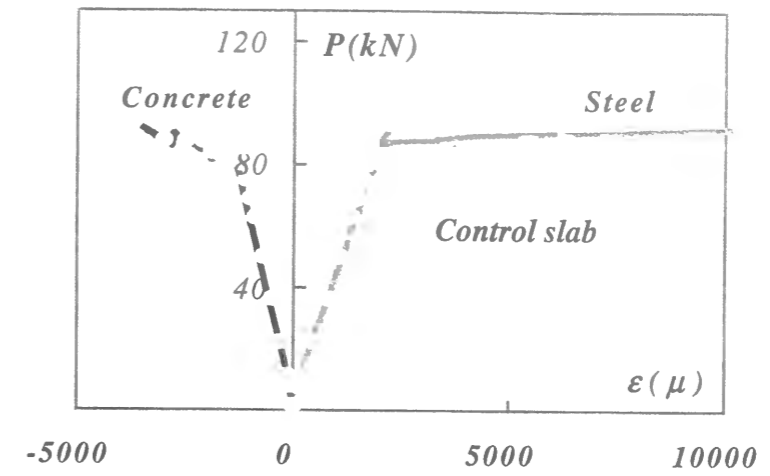


Figure 4.15 Load- strain curves at the span center

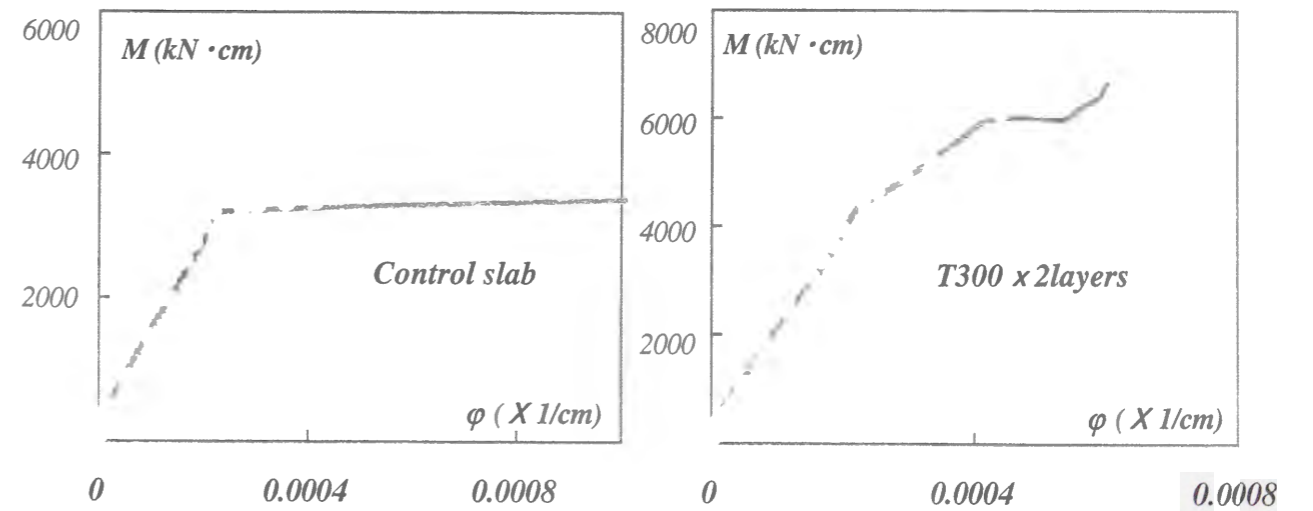


Figure 4.16 Moment- curvature curves at the span center

4.4.2 FINITE ELEMENT ANALYSIS

A numerical analysis using Finite Element Method (FEM) was performed to compare the experimentally obtained data. The *ABAQUS / Standard (Ver. 5.8, 1998)* FE commercial analysis program was used to simulate the structural behavior of laminated composite slab.

MATERIAL PROPERTIES

The mechanical properties of concrete, steel reinforcement, epoxy resin and CFS are reported in Table 4.6.

Table 4.6 Properties of materials used in FE analysis

Material properties	Concrete	Steel reinforcement	Epoxy resin	CFS
Elastic modulus (N/mm ²)	2.52×10^4	2.06×10^5	2.5×10^3	2.53×10^5
Poisson's ratio	0.2	0.3	0.35	0.26
Compressive strength (N/mm ²)	40	—	—	—
Yield strength (N/mm ²)	—	341	—	—
Tensile strength (N/mm ²)	—	—	30	3430

FINITE ELEMENT MODELING

◆ Concrete

In order to perform the nonlinear behavior of RC structure, the concrete model in *ABAQUS* requires three sub-options, which are *ELASTIC*, *CONCRETE* and *TENSION STIFFENING* options. The *ELASTIC* and *CONCRETE* options are used to define elastic and plastic properties of concrete, respectively.

The behavior of RC structure after cracking, *TENSION STIFFENING* option can be used. Effects associated with the interface between steel reinforcement and concrete, such as bond slip and dowel action, are also approximately modeled by this option. The concrete was modeled using two-dimensional (2D) solid elements (*CPS4; 4-node bilinear plane stress quadrilateral solid element*) in this study.

◆ Steel reinforcement

In *ABAQUS* steel reinforcement in concrete member can be defined by *REBAR* option. This option defines the steel reinforcement as uniformly spaced layers, which are treated as a smeared layer with a constant thickness equal to the area of each steel bar divided by the spacing of steel bar. In this analysis elasto-plastic material behavior was assumed.

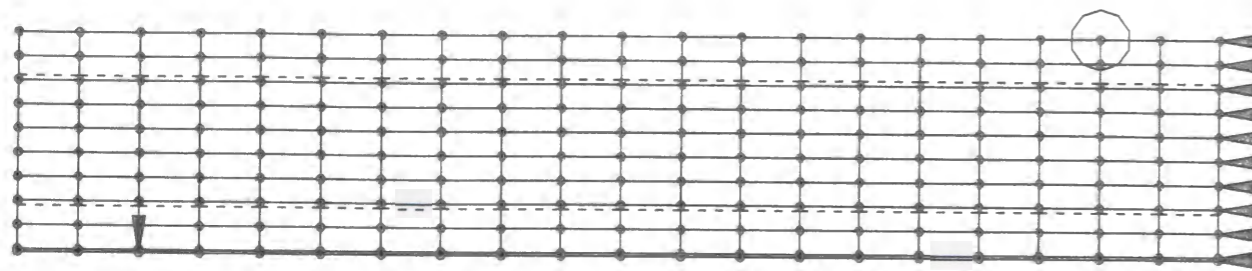
◆ Epoxy resin

The epoxy resin between concrete and CFS was modeled using two-dimensional (2D) solid elements (*CPS4; 4-node bilinear plane stress quadrilateral solid element*).

◆ CFS

The CFS was modeled using one-dimensional (1D) beam elements (*B21, 2-node linear beam in a plane*), and a linear-elastic material behavior was assumed.

Due to the symmetry of the slab, only half of the slab was analyzed with appropriate constraints at the centerline as shown in Figure 4.17. Also, a perfect bond between concrete and CFS was assumed in this study. A numerical simulation was conducted in accord with the theory of the smeared crack approach.



ABAQUS

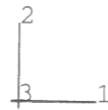
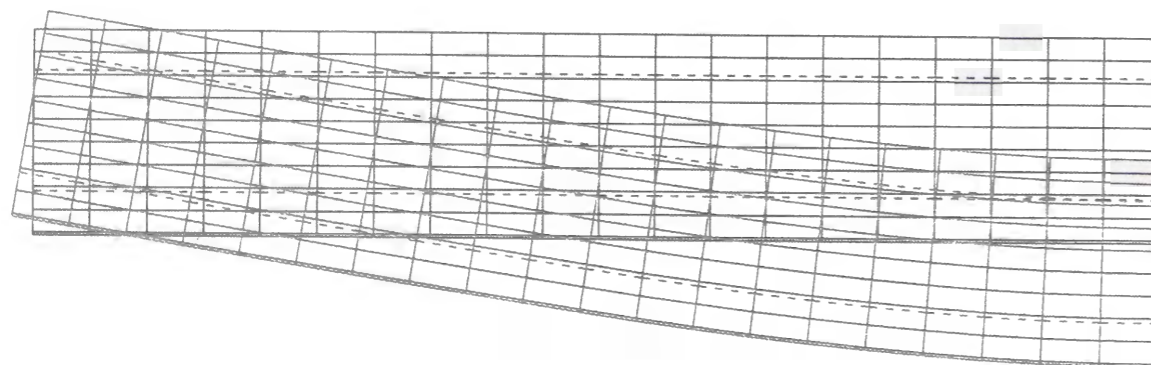


Figure 4.17 FEM modeling of retrofitted slab

COMPARISON WITH EXPERIMENTAL RESULTS

The load-displacement and strain curves obtained from *ABAQUS* are compared with the experimental results as shown in Figure 4.19~4.21.



DISPLACEMENT MAGNIFICATION FACTOR = 10.0 ORIGINAL MESH DEFORMED MESH
 RESTART FILE = cfs3g STEP 1 INCREMENT 19
 TIME COMPLETED IN THIS STEP 0.758 TOTAL ACCUMULATED TIME 0.758
 ABAQUS VERSION: 5.8-1 DATE: 15-DEC-1999 TIME: 17:40:04

Figure 4.18 Configuration of displacement obtained from *ABAQUS*

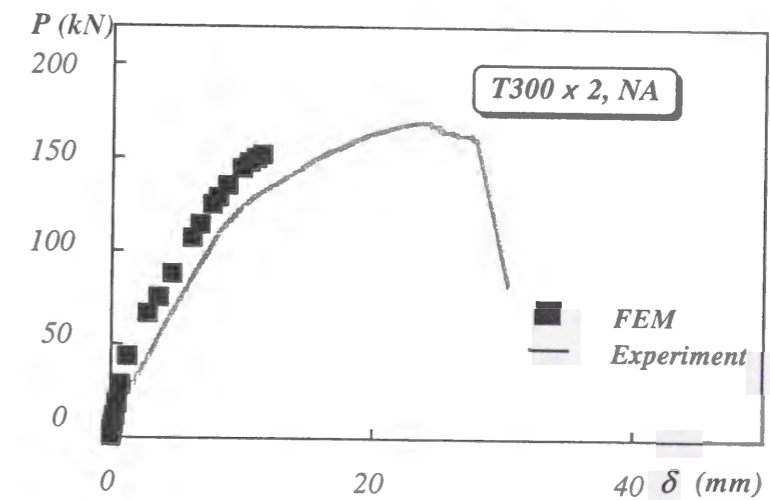
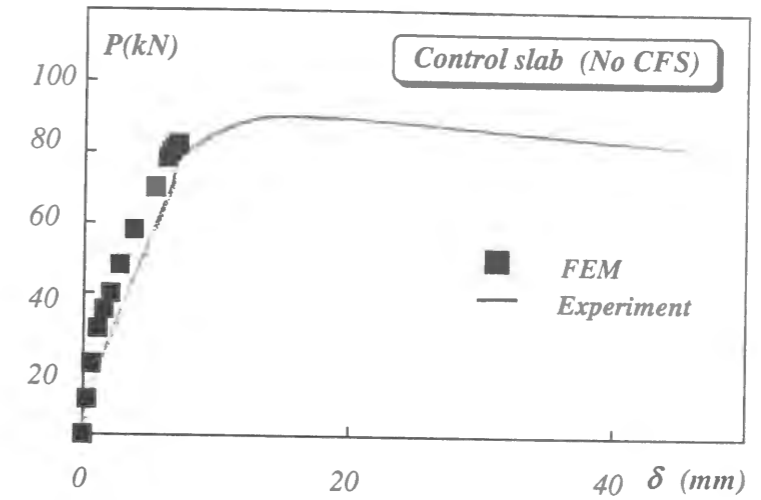


Figure 4.19 Comparison of experimental and FEA results in load-displacement

From the results, the numerical solution is slightly stiffer than the experimental values. The differences in the experimental and analytical results may be result of *ABAQUS* approach to RC modeling. Cracking is a major factor contributing to the nonlinear property of RC members. In experiment, cracks propagated and widened as the load was increased. However, micro cracks happened in experiment are can not modeled in *ABAQUS*.

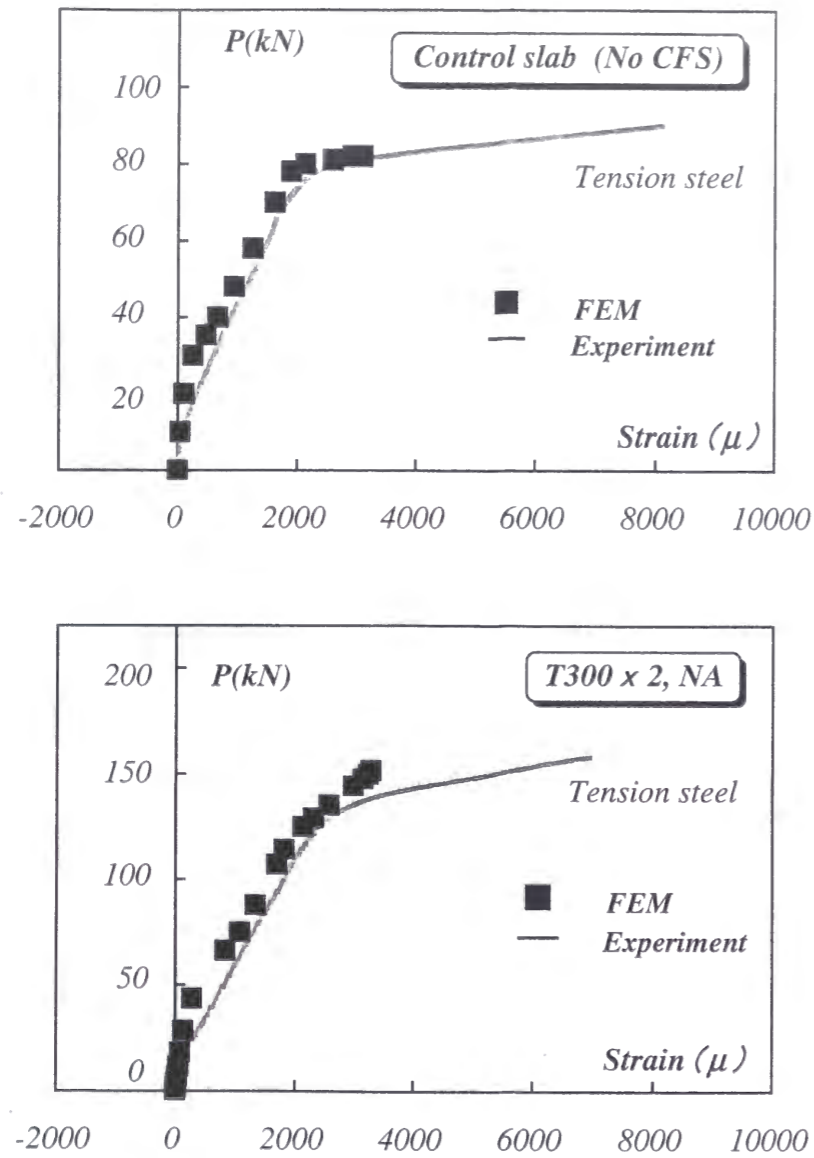


Figure 4.20 Comparison of load-strain curves in tension steel reinforcement

Also, the transfer of forces between the concrete and steel by bond is of fundamental importance to RC behavior since the location, spacing and width of cracks, internal distribution of forces, and the effective stiffness and strength of the member relate directly to the characteristics of the interface. *ABAQUS* assumes perfect bond between the concrete and internal steel reinforcement.

Effects associated with the interface are considered by modifying some aspects of the concrete behavior, for example by reducing the amount of stress transferred by the reinforcement to the concrete between flexural cracks. However, it has been found that this makes more complicated to obtain converged analytical solutions.

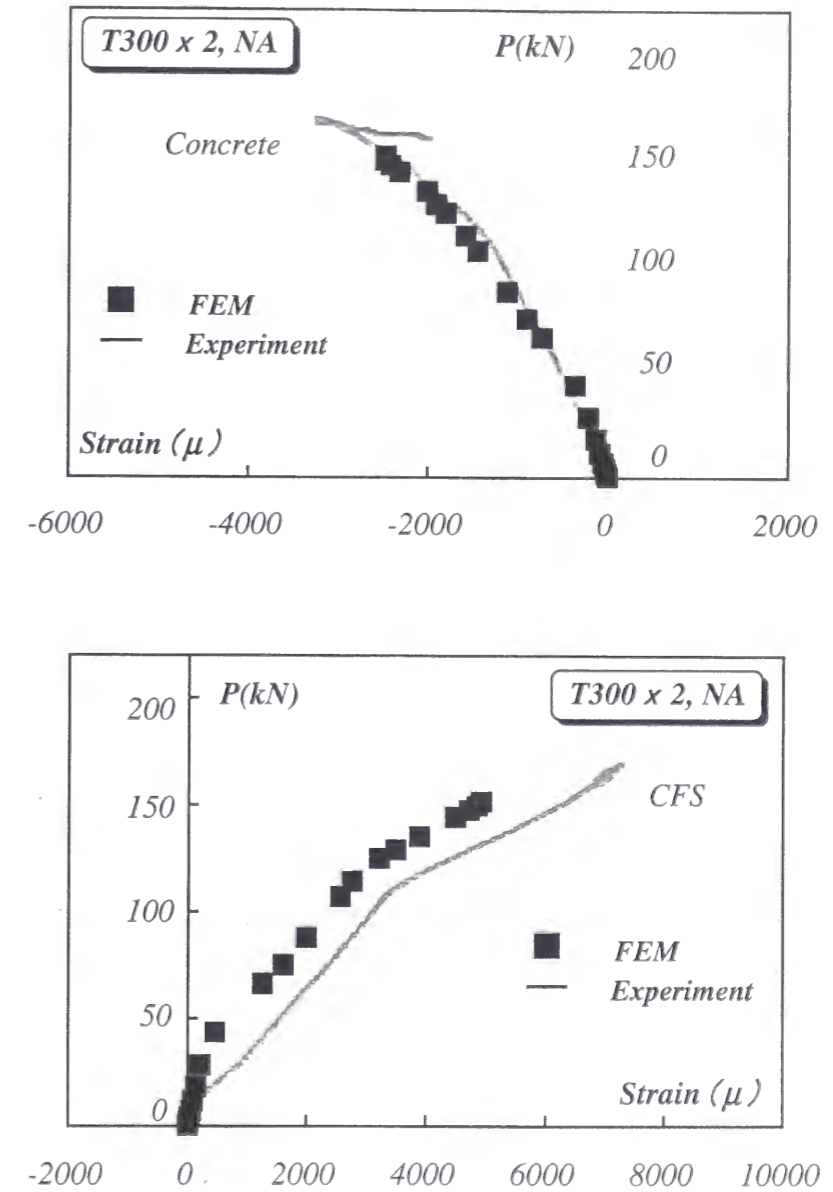


Figure 4.21 Comparison of load-strain curves in compressive concrete and CFS

Figure 4.22 shows the horizontal strain E_{11} at the last load increment of the analysis for retrofitted slab. The bottom fibers at span center of the slab are subjected to large strain.

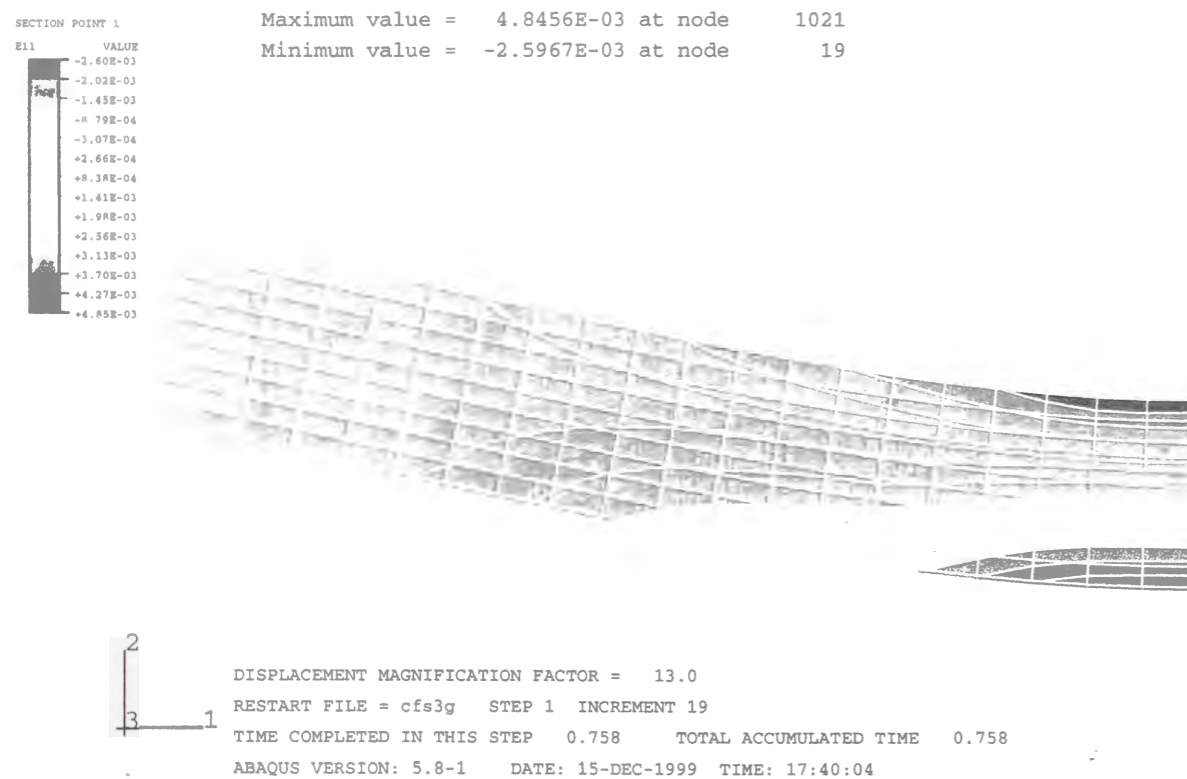


Figure 4.22 Horizontal strain E_{11} at the maximum load for retrofitted slab
(T300 x2layers)

4.5 ONCLUSIONS OF CHAPTER 4

Based on the experimental and analytical results presented herein, the following conclusions can be drawn.

- Failure of the test slab occurred immediately after delamination of CFS from concrete and crushing of concrete in the compression zone followed at the same time. At this time, the strain level developed in CFS was much lower than its rupture strain. Therefore, improvement of bond strength between concrete and CFS is expected farther improvement of the flexural strength of the slab.
- Good anchoring of CFS to the slab surface improved the ductility of the retrofitted slab. This fact should be taken into consideration for the practical application. However, there was almost no difference between normal and perfect anchoring in the load carrying capacity.
- The flexural strength of the retrofitted test slab increases in proportion to the amount of CFS. Retrofit of the test slab with 2 layers of HM300 CFS improved the flexural strength over 2.4 times.
- The section analysis based on the compatibility of deformations and equilibrium of forces, and FE analysis results show good accordance to the experimental results in terms of load-deflection and load-strain response.

Chapter 5

FATIGUE BEHAVIOR OF RC& CARBON FIBER SHEET COMPOSITE SLAB UNDER LARGE REPEATED LOADING

5.1 INTRODUCTION

Fatigue behavior has become an important consideration in the design of bridges, pressure vessels, cranes, and other engineering structures. Reinforced Concrete (RC) structures in civil engineering, such as bridge decks, may be subjected to this fatigue loading. Recently owing to the increasing of traffic and heavy traffic loads, cracking damages to RC bridge slabs have been found in many highway as shown in Figure 5.1~5.2. .

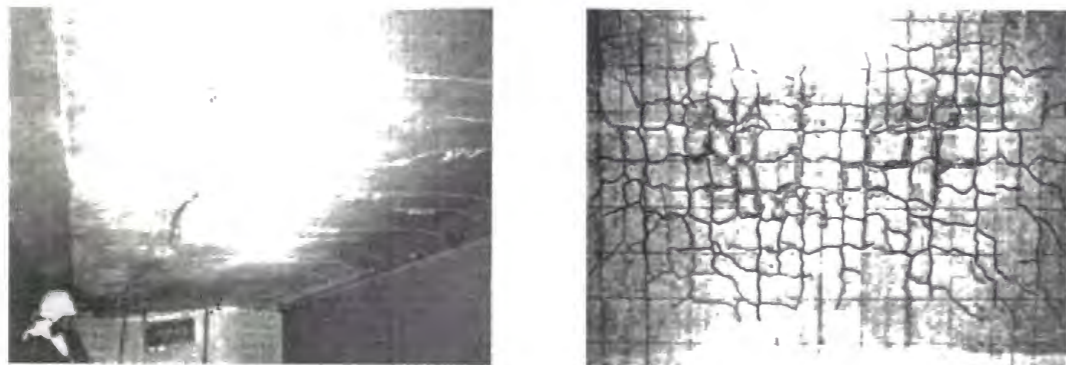


Figure 5.1 Damages of highway bridge slabs (bottom)






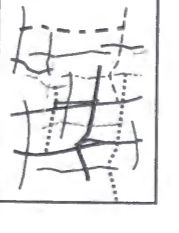

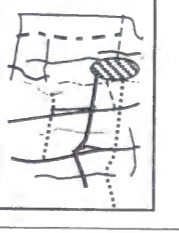

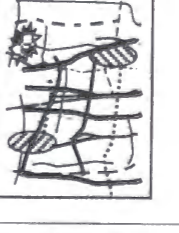

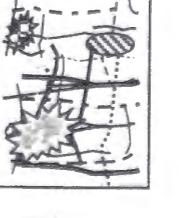
Picture	Figure	Configuration of damage
		Cracking of transverse direction of bridge
		Cracking of longitudinal direction of bridge
		Tortoise armor-shaped cracking
		Penetration of cracks
		Slitting of crack
		Falling down of concrete pieces

Figure 5.2 Damage procedure of bridge slab (From report of Hansin Expressway Co.1991)

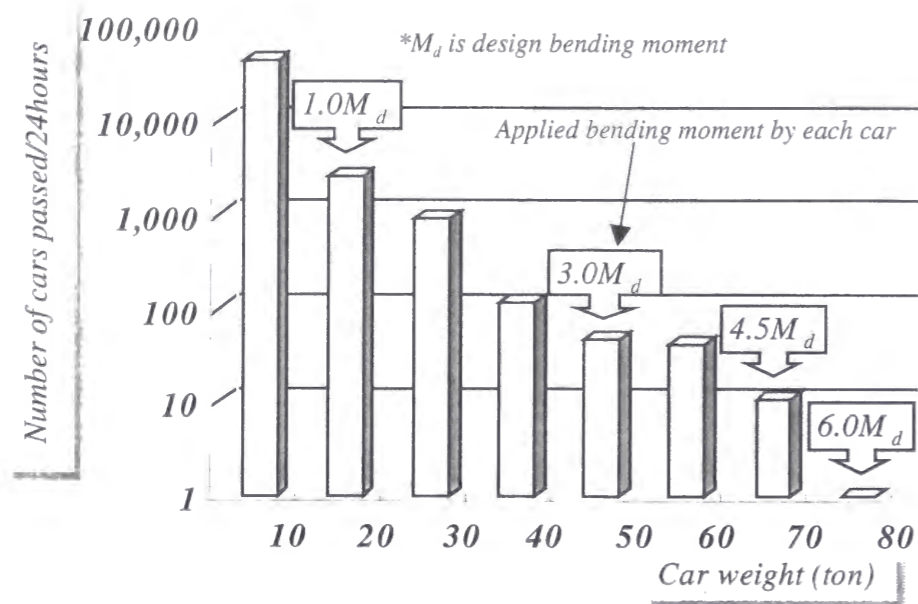


Figure 5.3 Car survey result in a highway

Figure 5.3 shows a survey result of the number of cars and the weight passed at a section of a highway during continuous 24 hours. According to the result, most of the cars passed through the section gave a bending moment less than the design value to the bridge slab. On the other hand, some cars gave a large bending moment up to 4.5 times of the design value. This excess loading is considered to be the main reason of the cracking damage of highway bridge slab.

In order to compensate for these disadvantages, the use of CFS has an advantage over steel plate due to its easy application owing to the lightweight, high tensile strength and good flexibility. Through the recent researches and applications to the practical cases, CFS has been successfully acknowledged as a reinforcing material to make structures more durable and safer. Many researchers have studied the structural behavior of laminated composite RC members on flexure and shear strengthening.

However, the fatigue behavior of RC slab laminated by CFS has not been reported so much. The aim of this chapter is to clarify the fatigue behavior of RC bridge slab laminated by CFS, particularly under very large repeated loading.

5.2 EXPERIMENTAL PROGRAM

5.2.1 TEST SPECIMEN

The test slab is almost identical to an existing slab of a highway in terms of the amount of reinforcement, quality of concrete and thickness of the slab, which is 18cm. Only one directional flexural behavior of the slab is tested. The test slabs are loaded in dry or wet condition. Some of the test slabs are damaged under the repeated load and retrofitted by CFS, then loaded again to see the improvement of the fatigue life.

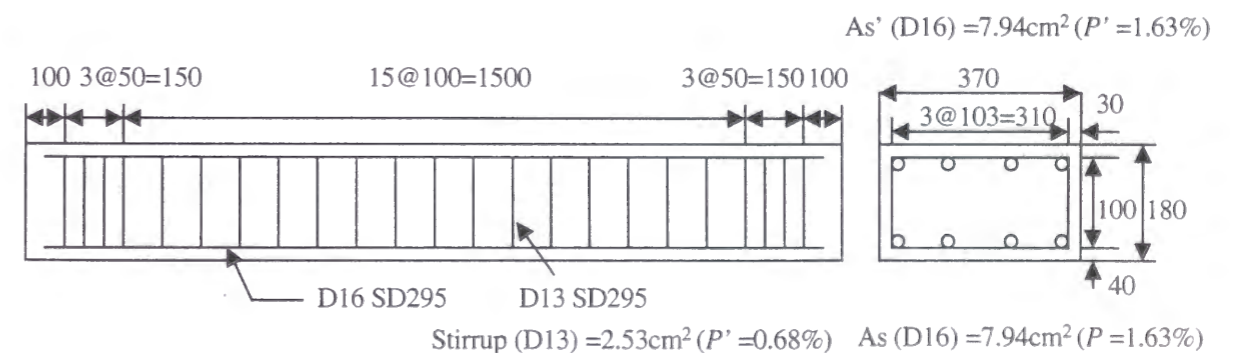


Figure 5.4 Detail of test specimen (mm)

5.2.2 RETROFITTING OF CARBON FIBER SHEETS

According to Figure 5.1, cracks develop both in the parallel and perpendicular direction of a slab. Therefore, CFS should be applied in the both directions to retrofit the slab efficiently. However, only one directional flexural behavior was studied in this research. The CFS was

glued at the bottom of the test slab with normal (NA) or perfect anchoring (PA) as shown in Figure 4.3. Normal type of CFS with 300g/m² (T300), 400g/m² (T400) and high-elastic modulus type of CFS with 300g/m² (HM300) were used for the strengthening.

Table 5.1 Material Properties

Material	Properties					
Concrete	Compressive strength : 39.2 N/mm ²		Elastic modulus : 3.92×10 ⁴ N/mm ²			
Steel	Longitudinal reinforcing : D16		Yield strength : 341 N/mm ²			
Epoxy	Elastic modulus : 2.3×10 ³ N/mm ²		Tensile strength : 55.3 N/mm ²			
CFS	Weight (g/m ²)	Density (g/cm ³)	Thickness (mm)	Tensile strength (N/mm ²)	Elastic modulus (N/mm ²)	Rupture strain (μ)
T 300	300	1.8	0.167	3430	2.53 × 10 ⁵	14900
T 400	400		0.222			
HM 300	300	1.82	0.165	2940	3.92 × 10 ⁵	7500

5.2.3 LOADING SET UP & MEASUREMENT

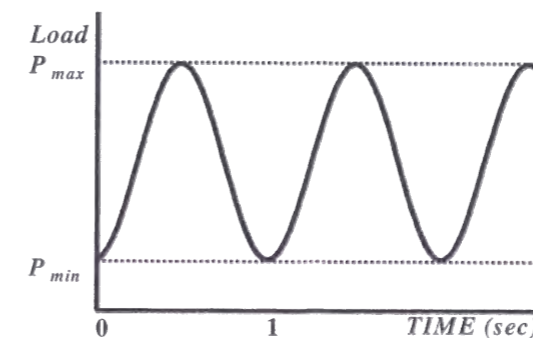
Flexural fatigue test with 6.1 shear-span ratio (a/d) was conducted under four-point flexural cyclic load. All test slabs were simply supported and subjected to two concentrated loads symmetrically placed about the mid-span as shown in Figure 5.5. Repeated load corresponding to 3.0, 4.5 or 6.0M_d, which is the design bending moment was applied to the test slab with 1.0 Hz as shown in Figure 5.6. Measurement of the strain and displacement of the test slab was performed under static load after certain cycles of repeated loading. The magnitude of the statically applied load was limited up to the same magnitude as the present repeated load.



(a) Dry condition

(b) Wet condition

Figure 5.5 Loading Set-up



Repeated load	P _{max} (kN)	P _{min} (kN)
3.0M _d	78.4	4.6
4.5M _d	117.7	4.6
6.0M _d	156.9	4.6

Figure 5.6 Applied Load History

5.3 TEST RESULTS & DISCUSSION

5.3.1 FLEXURAL FATIGUE TEST RESULTS

Table 5.2 shows the static test results obtained from experimental study. Figure 5.7 shows the typical failure pattern. Failure occurred immediately after debonding of CFS from concrete and crushing of concrete in the compression zone followed at the same time. This failure pattern indicates that the bond strength between concrete and CFS is one of the important factors to decide the actual strength of the retrofitted slab.

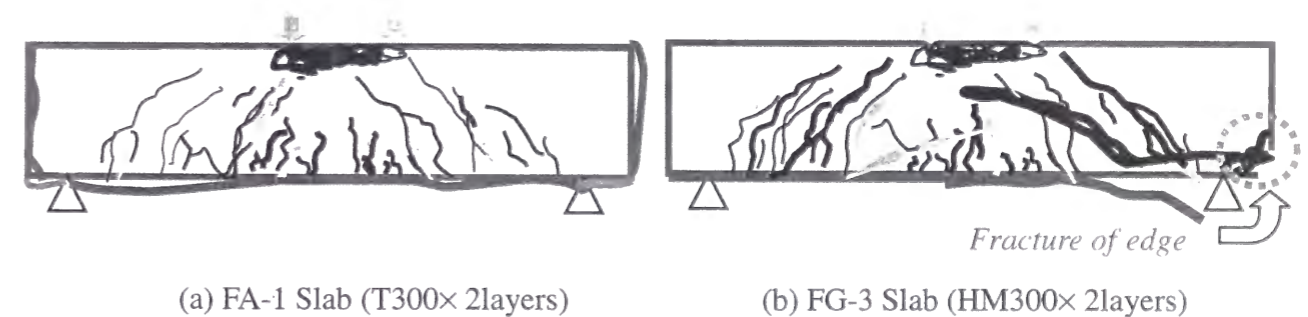
Table 5.2 Fatigue test results

CFS	Anchor type	Test slab	Applied load level	Number of Cycles at failure	Flexural strength	
					Before repeated loading	After repeated loading
No CFS	Control		3.0M _d	n _{max} = 4.6 × 10 ⁵ n _{max} = 3.3 × 10 ⁵	(Dry condition) (Wet condition)	
T300 (300g/m ²) 2 Layers	PA	SA-0			5.94 M _d	
		FA-1	3.0M _d	9.50 × 10 ⁵		
		FA-2	4.5 M _d	6.60 × 10 ⁴		
		FA-3	6.0 M _d	7.63 × 10 ²		
T400 (400g/m ²) 2 Layers	PA	SB-0			6.97 M _d	
		FB-1	3.0M _d	over 5.0 × 10 ⁶		6.49 M _d
		FB-2	4.5M _d	3.03 × 10 ⁵		
		FB-3	6.0M _d	2.10 × 10 ⁴		
T400 (400g/m ²) 2 Layers	NA	SC-0			7.27 M _d	
		FC-1	3.0M _d	over 2.0 × 10 ⁶		7.19 M _d
		FC-2	4.5M _d	4.30 × 10 ⁵		
		FC-3	6.0M _d	2.76 × 10 ⁴		
		FD* ¹ -1	3.0M _d	over 2.0 × 10 ⁶		6.24 M _d
		FE* ² -1	3.0M _d	over 2.0 × 10 ⁶		7.70 M _d
		FF* ³ -1	3.0M _d	over 2.0 × 10 ⁶		5.94 M _d
HM300 (300g/m ²) 2 Layers	NA	SG-0			7.99 M _d	
		FG-1	3.0M _d	over 3.0 × 10 ⁶		7.89 M _d
		FG-2	4.5M _d	over 3.0 × 10 ⁶		7.89 M _d
		FG-3	6.0M _d	1.85 × 10 ⁴		

- M_d = The design flexural moment, which corresponds to 10.9 kN·m for the test slab.
- M_{max} of the control slab without CFS was 36.7 kN·m (= 3.37 M_d)
- *1: FD-1 slab was loaded until n = 2.3 × 10⁵ (50% of n_{max}) cycles before retrofitting by CFS
- *2: FE-1 slab was loaded until n = 4.2 × 10⁵ (90% of n_{max}) cycles before retrofitting by CFS
- *3 : FF-1 slab was loaded in wet condition

The control slabs without CFS retrofitting failed at 4.6 × 10⁵ cycles in dry condition and 3.3 × 10⁵ cycles in wet condition both under 3.0M_d. The FB-1 and FC-1 slabs retrofitted by 2 layers of T400 CFS both under the load of 3.0M_d did not fail at the specified cycles. They were loaded statically until failure. After static test, FB-1 slab maintained 93% of the initial flexural strength even after application of 5.0 million cycles of the 3.0M_d. However, the other test slabs retrofitted by 2 layers of T400 CFS failed under the repeated load of 4.5M_d.

Even badly damaged slab recovered its fatigue strength by the application of CFS. The test slabs FD-1 and FE-1 were loaded up to 50% or 90% of the failure cycles number of control slab. Then, they were retrofitted by 2 layers of T400 and again loaded by 3.0M_d. After the application of 2.0 million cycles, they did not fail by fatigue and possessed enough flexural strength.



(a) FA-1 Slab (T300 × 2 layers)

(b) FG-3 Slab (HM300 × 2 layers)



Figure 5.7 Typical failure by debonding

The test slab FF-1, on the other hand, was retrofitted by 2layers of T400, and then submerged for one month before loaded. Prior to repeated loading, this slab was wound by a vinyl wrapper to prevent evaporation of water and to conserve the wet condition during the test. Due to the application of CFS, this slab did not fail by fatigue and increased its fatigue life from 0.33millions cycles to over 2.0million cycles.

Especially, the high elastic modulus type of CFS exhibited a significant effect to fatigue behavior and restraint of deflection as shown in Figure 5.8. The test slab FG-2 strengthened by 2layers of HM300 CFS still maintained almost the same flexural strength even after the application of 3.0million cycles of $4.5M_d$. Therefore, this amount of CFS is recommended to retrofit of highway bridge slab. Figure 5.9 and 5.10 show load-deflection and load-strain curves under fatigue loading.

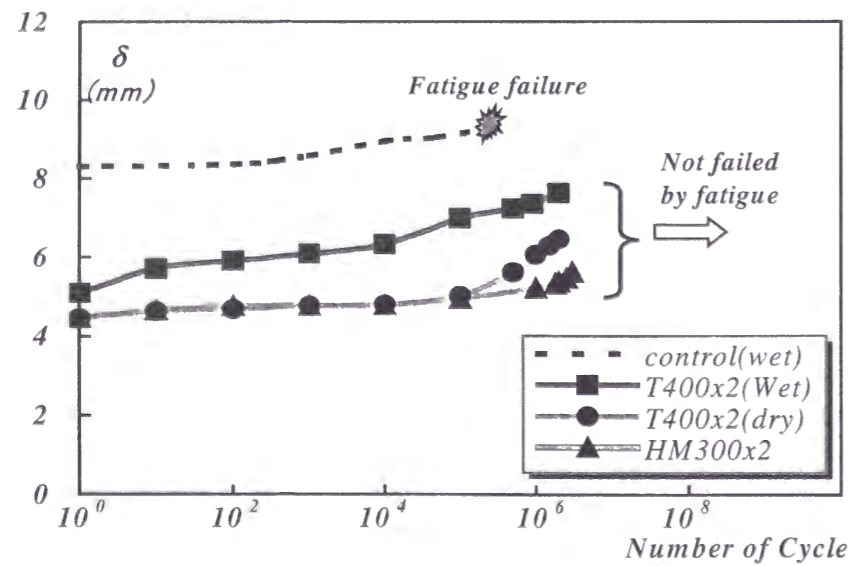


Figure 5.8 Deflection vs number of cycle curves

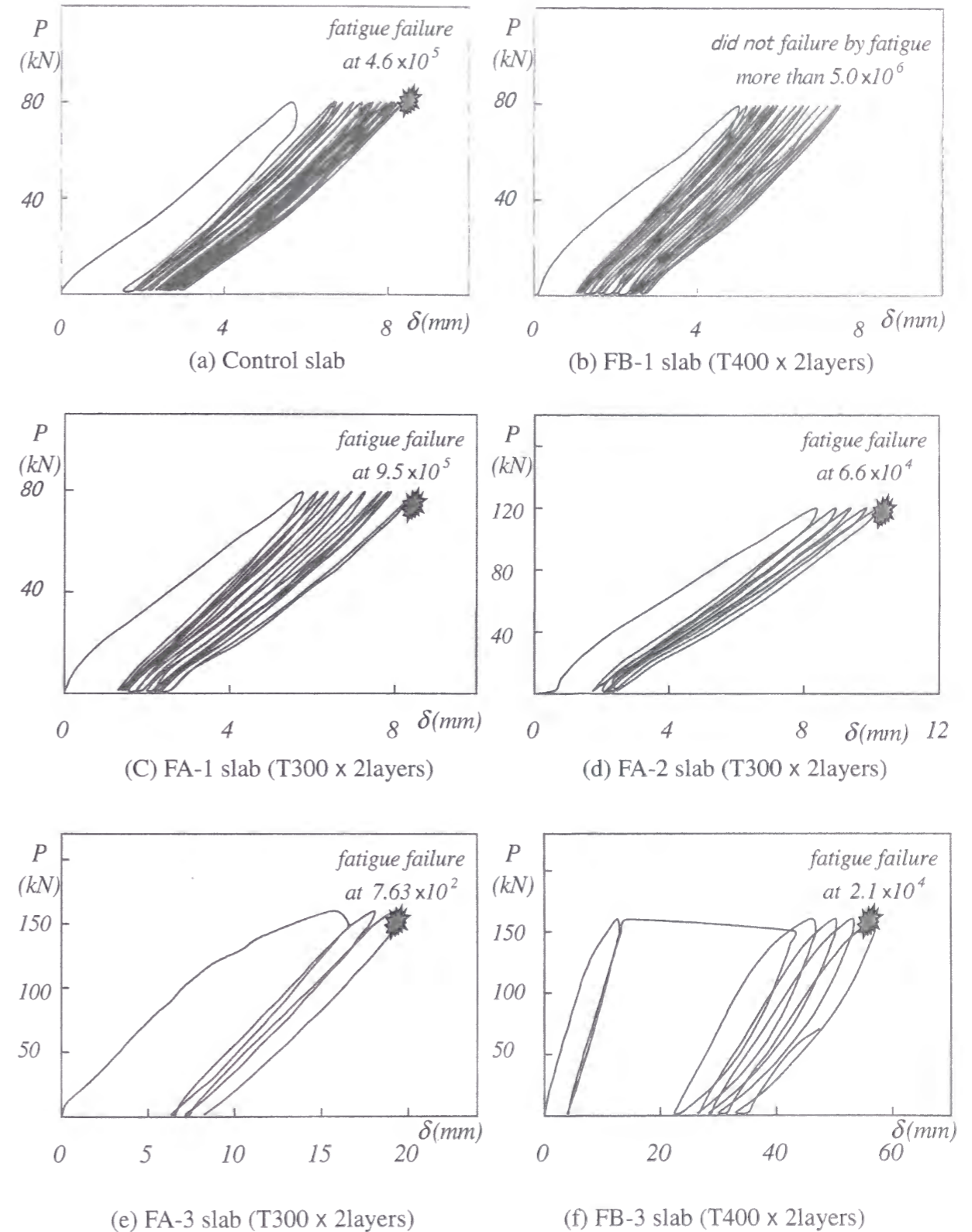


Figure 5.9 Load- deflection curves at the span center

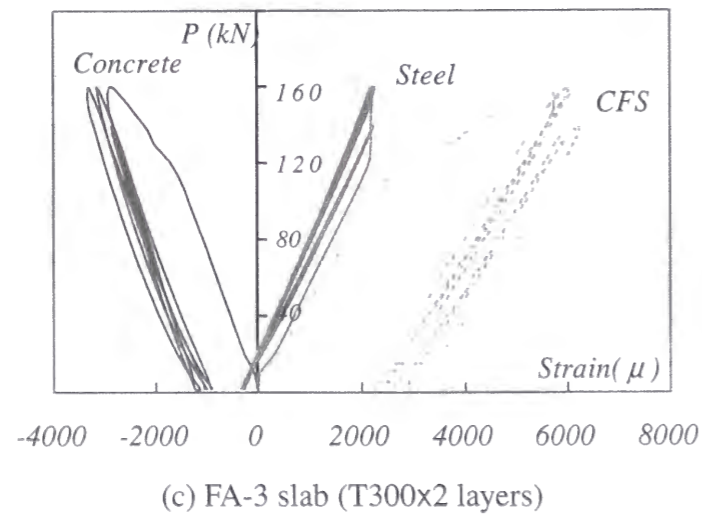
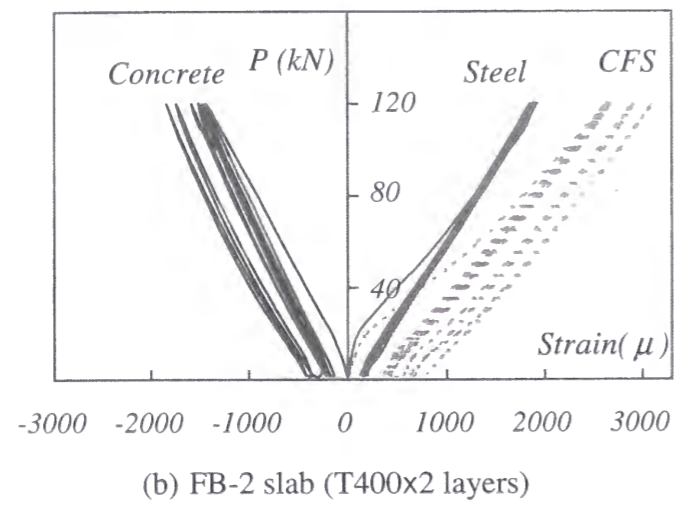
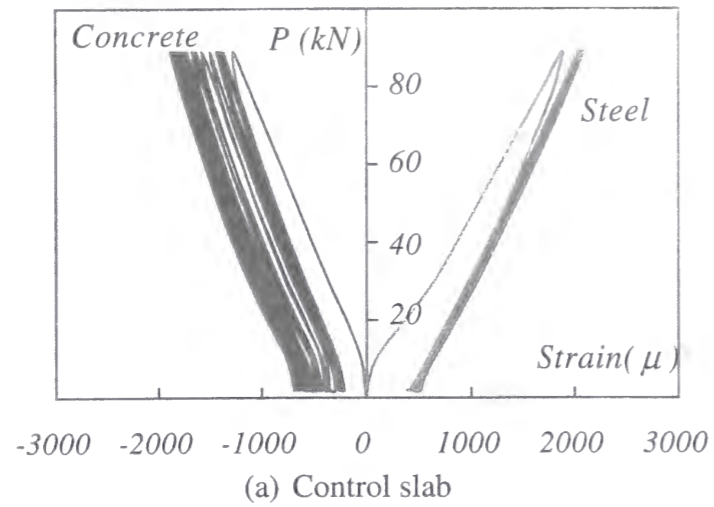


Figure 5.10 Load- strain curves at the span center

Figure 5.11 shows the S-N curves for the test slabs. The slabs retrofitted by 2 layers of T300 CFS failed by fatigue even under the load of $3M_d$. However, the slab retrofitted by 2 layers of T400 CFS did not fail by fatigue under the load of $3.0M_d$, and had more than 10 times longer fatigue life compared to the control slab. In anchoring system, there was almost no difference between PA and NA test slab in fatigue life.

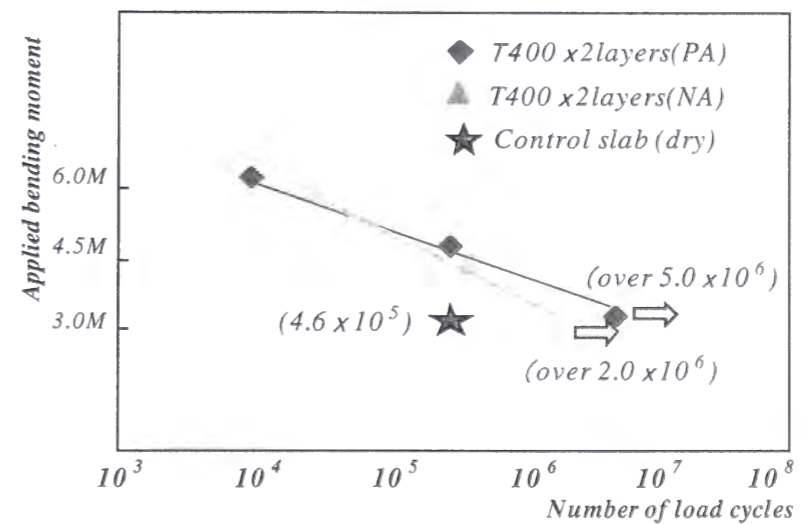
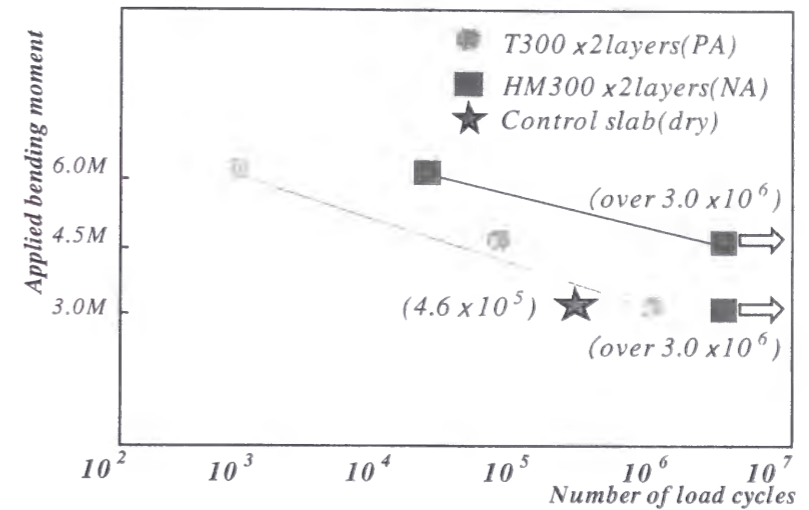


Figure 5.11 S-N curves of retrofitted slab

5.3.2 LOSS OF FLEXURAL STIFFNESS DUE TO FATIGUE

Figure 5.12~13 show the variation of the flexural stiffness due to fatigue. The flexural stiffness of the test slab after each cycle of repeated loading is evaluated as follows:

◆ Before loading $(EI)_0 =$ based on the gross section

◆ After loading
$$EI = \frac{P}{\delta} \left(\frac{aL^2}{16} - \frac{a^3}{12} \right)$$

Where, δ : Deflection at the slab center, L : Length of the span (=1800 mm)

a : Shear span (= 800 mm)

The stiffness of the slab retrofitted by 2layers of HM300 CFS dropped to 62% of the initial value under the application of the static load of $3M_d$. However, the loss of the stiffness under the repeated loading was gradual and even after the 3.0million cycles of $3M_d$ loading, the slab still maintained 76% of the initial stiffness value just after the static loading of $3M_d$.

On the other hand, the test slab FE-1 damaged up to 90% of the failure cycles number of control slab recovered its flexural stiffness up to 50% due to the application of 2layers of T400 CFS. This slab also still maintained 71% of the initial recovered stiffness value after the 2.0million cycles of $3M_d$ loading. Therefore, it is still significant to retrofit a RC bridge slab by CFS even if it is already heavily damaged.

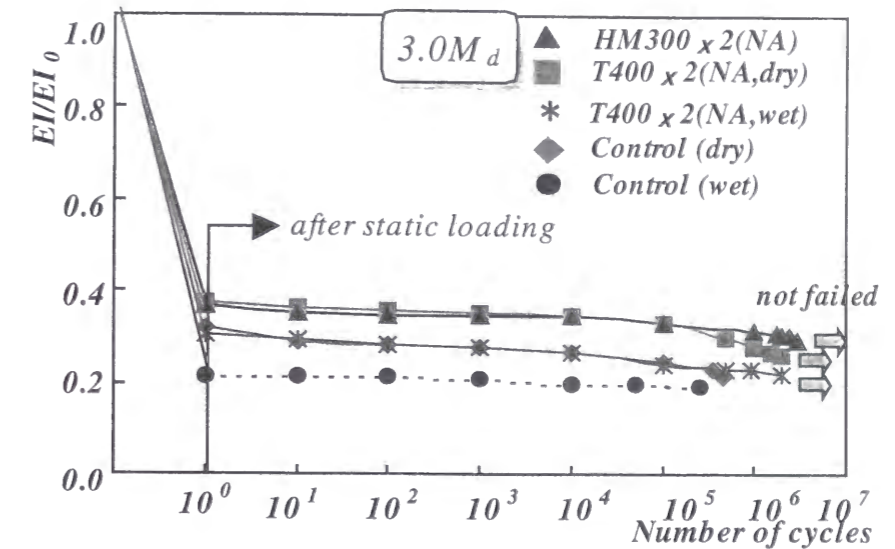


Figure. 5.12 Degradation of stiffness due to fatigue

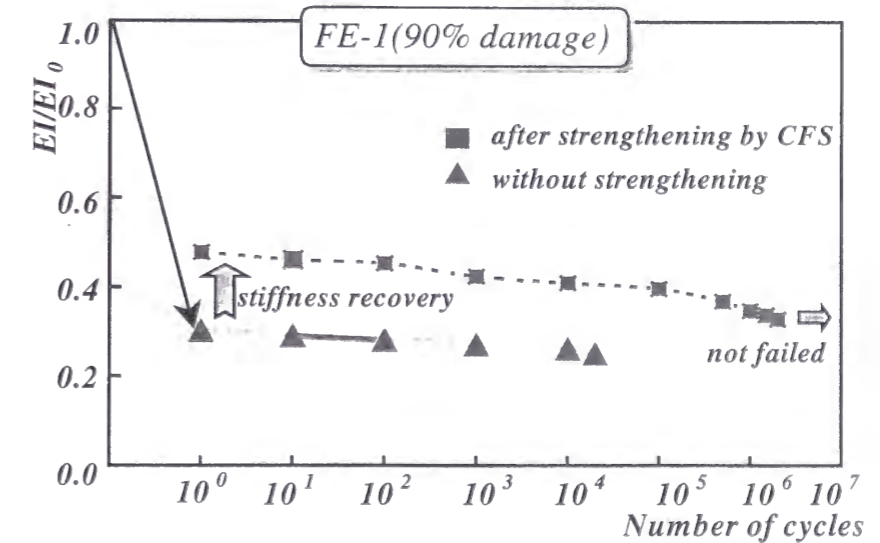


Figure. 5.13 Stiffness recovery due to CFS

5.4 ASSESSMENT OF CUMULATIVE FATIGUE DAMAGE

5.4.1 TOTAL DISSIPATED ENERGY CAPACITY

The energy dissipation characteristic of a laminated RC slab by CFS is investigated. The total dissipated energy capacity E_{total} gained from the total area under the load-deflection curve ($P-\delta$ curve) as shown in Figure 5.14 is defined as follows;

$$E_{total} = E_{inelastic} + E_{elastic}$$

Where, $E_{inelastic}$ is the inelastic energy cumulated before failure

$E_{elastic}$ is the elastic energy released at failure

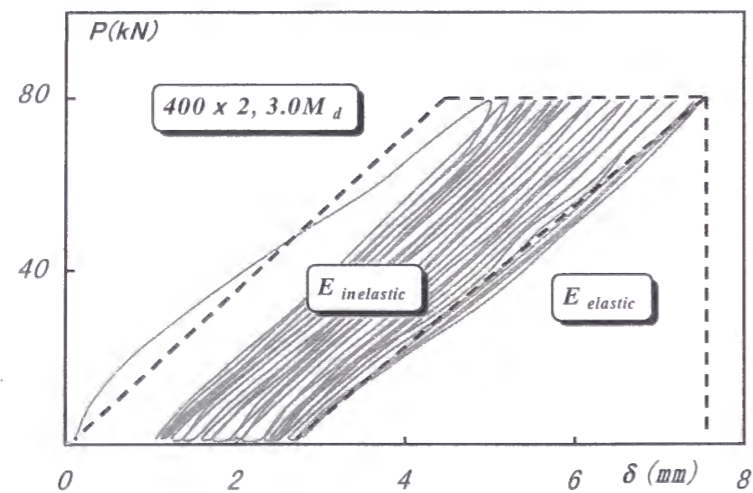


Figure 5.14 Definition of total dissipated energy capacity E_{total}

Figure 5.15 shows the total dissipated energy capacity E_{total} during repeated loading. The effect of CFS on the total dissipated energy capacity is very similar to that on fatigue life. It can be seen that the variation of the total energy is dependent on the CFS. In other words, the total energy dissipation capacity of retrofitted slab under repeated loading is increased with the increase of the amount of CFS.

However, FB and FC slabs retrofitted by 2 layers of T400 CFS with different anchoring systems preserve almost the same energy capacity.

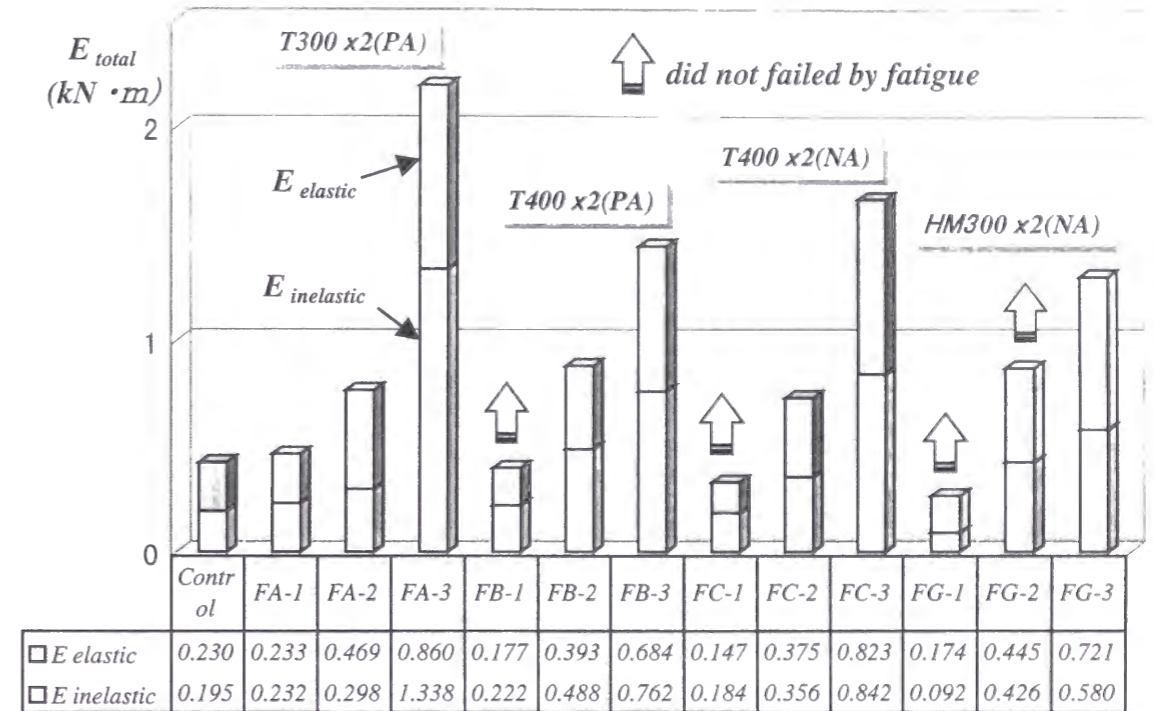


Figure 5.15 Total dissipated energy capacity of test slabs during repeated loading

On the other hand, within the scope of this research, the most significant factor contributing to the total energy capacity is elastic modulus of CFS. For example, FA-1 slab retrofitted with 2 layers of T300 CFS failed at 0.95million cycles with the inelastic cumulative energy of 0.232kN·m.

But, FG-1 slab retrofitted with 2 layers of HM300 CFS possesses about 2.5times less inelastic energy 0.092kN·m even after the application of 3.0million cycles of the same load level. This phenomenon indicates that the high elastic modulus type of CFS gives a much significant effect on delaying the rate of the fatigue damage accumulation.

It may be also supposed that the amount of the elastic energy $E_{elastic}$ released at failure increases due to the increase of the elastic modulus of CFS. But, because of the limited data obtained so far, it is premature to explain clearly. Further experimental investigations are needed to validate the real phenomenon of laminated composite members on dissipated energy capacity.

5.4.2 PROGRESSIVE ACCUMULATION OF DAMAGE

An energy-based damage index $D(E)$ defined as Eq.1 is introduced to evaluate the cumulative fatigue damage.

$$D(E) = \frac{\sum_n^m \Delta E_n}{E_{Total}} \quad 0 \leq D(E) \leq 1$$

Where, ΔE_n : Cumulative energy up to n th cycles due to fatigue (From $P-\delta$ curve)

m : Number of cycle up to failure

E_{Total} : Total energy capacity due to fatigue $(= \frac{E_{total} - E_{initial}}{E_{initial}})$

$E_{total} = E_{elastic} + E_{inelastic}$

$E_{initial}$: Dissipated energy after the initial static loading

Fatigue failure occurs when the value of the cumulative damage index $D(E)$ approaches unity ($=1$). Figure 5.16 indicates the process of cumulative fatigue damage of test slabs retrofitted with T300 CFS. The cumulative damage index $D(E)$ is expressed as a function of the cycle ratio n/N , where n is a certain number of cycle and N is the maximum number of cycle at failure.

A straight line dotted means a linear cumulative damage hypothesis proposed by Palmgren-Miner. In this hypothesis, the failure of structural member will occur when the sum of the n/N_i ratios for the various applied stress ranges equals unity ($=1$) as follows;

$$\sum_{i=1}^n \frac{n_i}{N_i} = \frac{n_1}{N_1} + \frac{n_2}{N_2} + \frac{n_3}{N_3} + \dots = 1$$

Where, n_i = number of cycles of stress range i

N_i = number of cycles to failure of structural member in stress range i

The control slab without CFS was tested under the load of $3.0M_d$. The cumulative energy gradually increases with the increase of the number of load cycles. It can be seen that the value of the damage index $D(E)$ increases with a higher rate during a few initial cyclic loading, and then gradually increases up to failure. Also, the degree of non-linearity in the cumulative damage curves is significant in proportion to the increase of applied load levels.

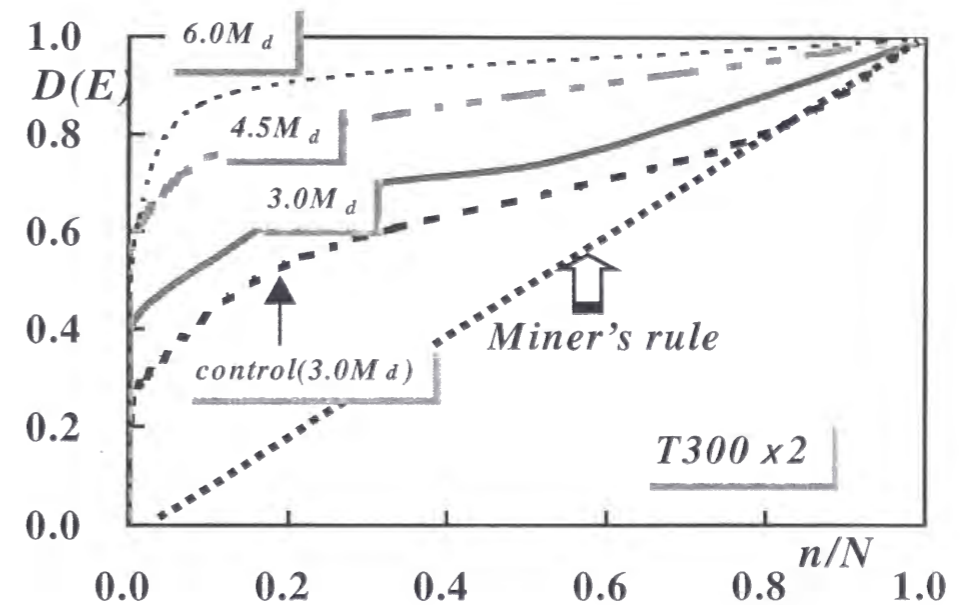


Figure 5.16 Non-linear cumulative fatigue damage curves

After all, the damage accumulation curves for all test slabs deviate from linearity, specifically under large repeated loading. This means that Palmgren-Miner's linear damage accumulation hypothesis is not directly applicable to pursue the damage process of laminated composite slab under large repeated loading.

5.4.3 APPLICATIONS OF INFRARED THERMOGRAPHY

Infrared Thermography (IT) is a well-established tool in the field of NDT (Non-Destructive Testing) and monitoring techniques for investigating deterioration levels of existing structures. The IT method was applied for good understanding of debonding phenomenon of CFS, because debonding failure has been observed in many experimental investigations.

The exfoliation conditions of CFS from the concrete surface can be inspected by collected temperature (actually, amount of infrared rays) radiated from the concrete surface as shown in Figure 5.17~18. From the results, IT method may be applicable to inspect the exfoliation conditions of CFS from the concrete surface.



Figure 5.17 Infrared Thermography Testing

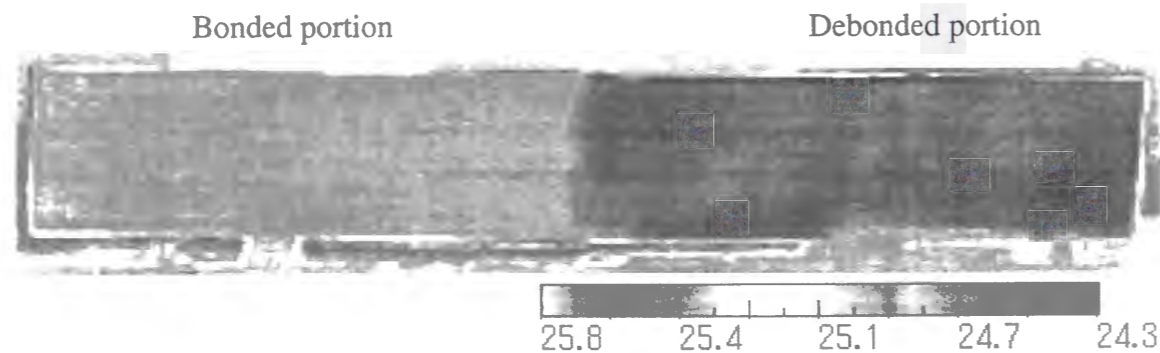


Figure 5.18 Result of Infrared Thermography Testing (FC-3 Test slab)

5.5 RETROFIT DESIGN CONCEPT FOR RC BRIDGE SLAB BY CFS

Retrofit design concept for highway RC bridge slab retrofitted with CFS proposed by Hansin Expressway Co, Japan is briefly introduced in this section. Retrofit design has been developed based on deflection constraint of slab span.

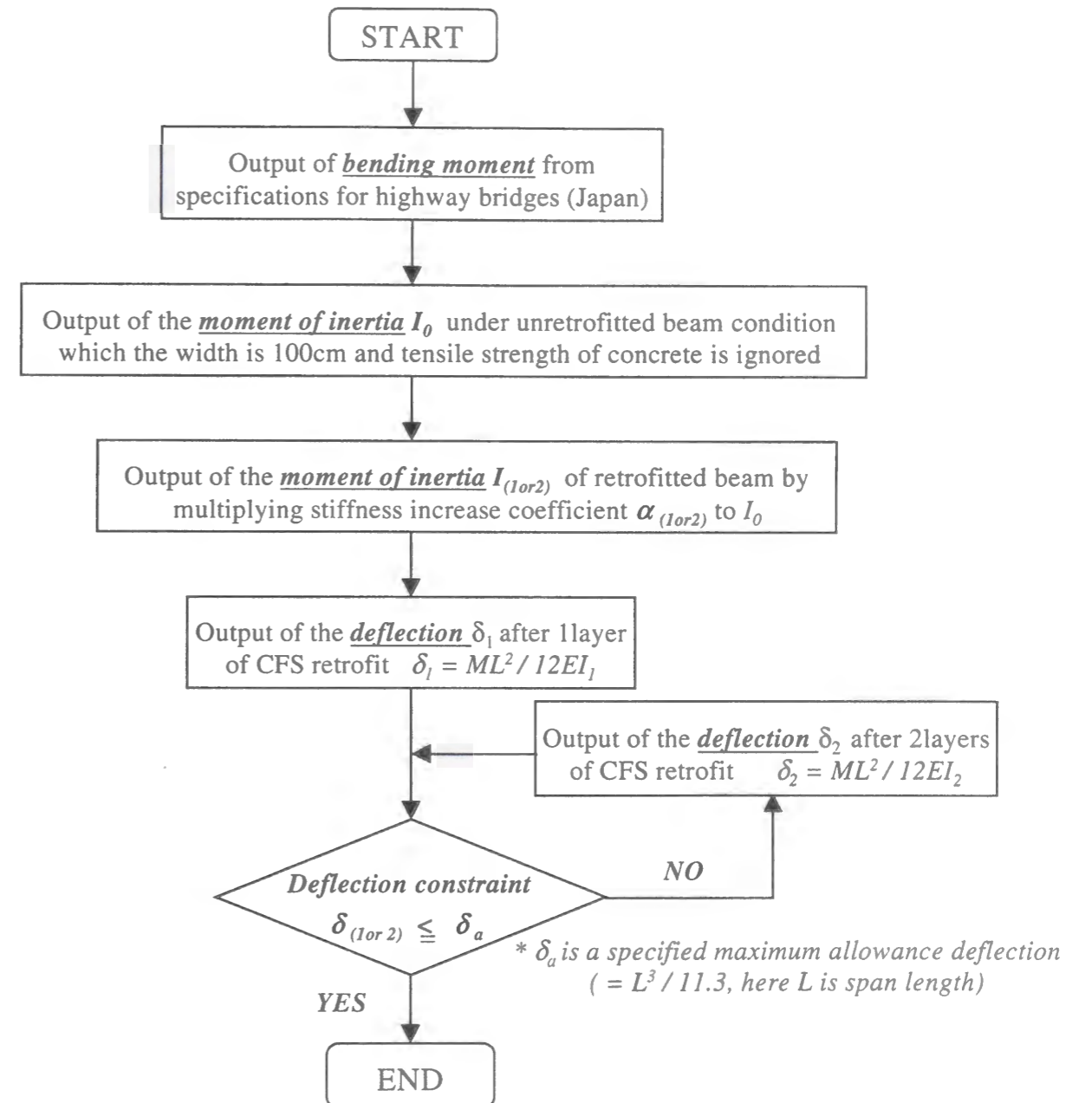


Figure 5.19 Retrofit design flow of RC bridge slab by CFS based on deflection constraint

(From the Committee reports of Hansin Expressway Co, June, 1999)

5.5 CONCLUSIONS OF CHAPTER 5

Based on the experimental results presented herein, the following conclusions can be drawn.

- The fatigue failure of retrofitted slabs mainly occurred by debonding of interface between concrete and CFS. This failure pattern indicates that bond strength between concrete and CFS is one of the key factors to determine the fatigue life of a retrofitted RC slab by CFS.
- The test slab strengthened by 2layers of T400 CFS lasted more than 5millions cycles under 3.0times design load, whereas the control test slab without CFS failed at about 0.46 millions cycles under the same loading.
- The test slab retrofitted with 2layers of high-elastic modulus type of HM300 CFS had kept the same initial flexural strength even after the application of 3.0million cycles of 4.5times design load. Therefore, this amount of application is recommended to retrofit of highway bridge slab.
- Even badly damaged slabs recovered its fatigue strength by the application of CFS. Two test specimens were loaded up to 50% and 90% of the failure cycles number of control slab. Then, they were retrofitted by 2layers of T400. After retrofiting, they were again loaded by 3.0times of the design load until 2.0million cycles. But, they did not fail by fatigue and possessed enough flexural strength even after the application of the cyclic load.
- There was almost no clear difference in fatigue life between Normal and Perfect anchoring.

Chapter 6

FLEXURAL STRENGTH EVALUATION OF A REINFORCED CONCRETE SLAB RETROFITTED WITH CARBON FIBER SHEET

6.1 INTRODUCTION

Through the recent researches and applications to the damaged infrastructures, Carbon Fiber Sheet [CFS] has been successfully played key roles as a feasible reinforcing material due to its light weight, high tensile strength and easy application. However, debonding failure of RC members retrofitted by CFS has been observed in many experiments. This phenomenon indicates that the bond strength between concrete and CFS is considered as one of the important factors to determine the actual strength of retrofitted RC members by CFS.

This chapter reports theoretical investigation for evaluating the flexural strength of RC bridge slab strengthened with CFS. The estimation of the ultimate strength of a slab is

tried under the assumption that the failure occurs when the shear stress mobilized at the interface between the concrete bottom and the glued CFS reaches the bond strength. The shear stress is evaluated theoretically and the bond strength is obtained by a laboratory test. The ultimate flexural strength of the test slabs is obtained by the bending test. The test slab is almost identical to the real highway RC bridge slab in terms of concrete quality, the amount of reinforcement and the thickness of the slab.

6.2 PROPOSED ANALYTICAL METHOD BASED ON BOND STRENGTH

6.2.1 STRAIN, STRESS AND CURVATURE IN COMPOSITE SECTION

Figure 6.1 shows the cross section of a composite member composed of different materials. For the analysis of stresses subjected to axial forces or moment on the composite section, transformed section analysis can be used. For example, the actual area of layer i can be replaced by a transformed area as follows;

$$A_i = n_i A_i$$

Where, n_i is the ratio of elastic modulus ($= E_i/E_0$)

E_i is the elastic modulus of i -th layer

E_0 is the elastic modulus of reference material of the composite cross section

The position of centroid of the transformed section can be calculated as

$$x_0 = \frac{\sum_{i=1}^m n_i d_i A_i}{\sum_{i=1}^m n_i A_i}$$

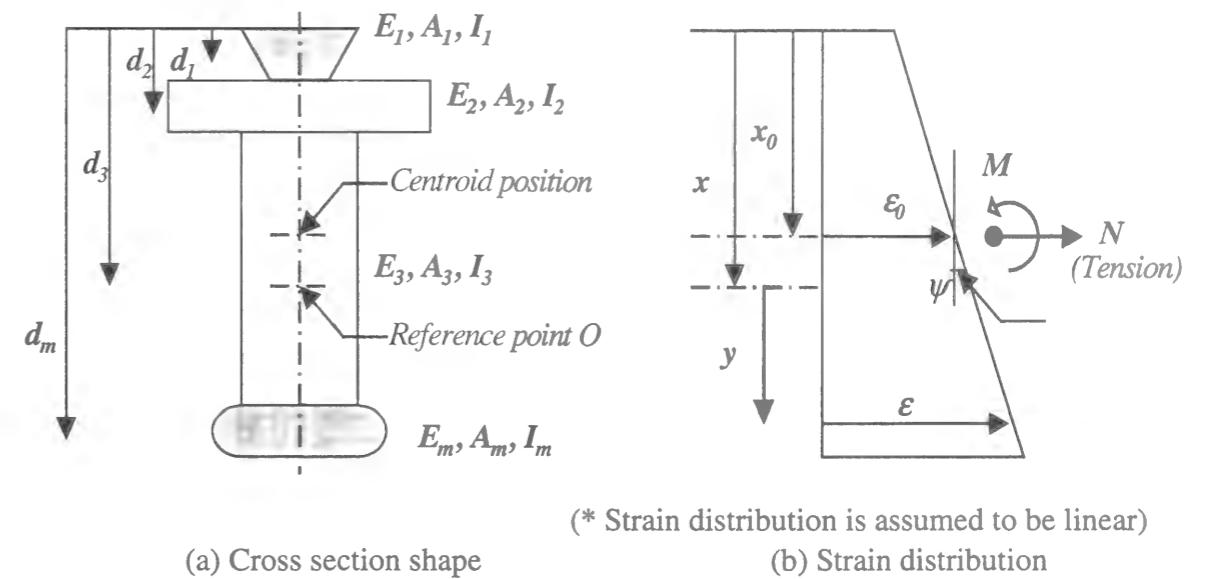


Figure 6.1 Composite section composed of different materials

If the cross section is subjected to a axial force N at any point of cross section, this force is equivalent to a system composed of axial force N and bending moment M at the arbitrarily chosen reference point O , as shown in Figure 6.1(a).

If a plane cross section is assumed to remain plane after deformation, the strain of any fiber ϵ can be expressed as follows,

$$\epsilon = \epsilon_0 + \psi y$$

Where, ϵ_0 is the strain at the reference point O and ψ is the curvature
 y is the distance of certain point from the reference point

y is considered as positive when the point is below the reference point. When the fiber is i -th layer of the composite section, the stress at the fiber is

$$\sigma = E_i (\epsilon_0 + \psi y)$$

The axial force N and bending moment M at the reference point O can be calculated as follows;

$$N = \int \sigma dA = \varepsilon_0 \sum_{i=1}^m E_i \int dA + \psi \sum_{i=1}^m E_i \int y dA$$

$$M = \int \sigma y dA = \varepsilon_0 \sum_{i=1}^m E_i \int y dA + \psi \sum_{i=1}^m E_i \int y^2 dA$$

If substitute for $E_i = n_i E_0$, above equations can be rewritten as

$$N = E_0(A\varepsilon_0 + B\psi)$$

$$M = E_0(B\varepsilon_0 + I\psi)$$

Here,

$$A = \sum_{i=1}^m n_i \int dA = \sum_{i=1}^m n_i A_i = \sum_{i=1}^m \left(\frac{E_i}{E_0} A_i\right)$$

$$B = \sum_{i=1}^m n_i \int y dA = \sum_{i=1}^m n_i B_i = \sum_{i=1}^m \left(\frac{E_i}{E_0} B_i\right)$$

$$I = \sum_{i=1}^m n_i \int y^2 dA = \sum_{i=1}^m n_i I_i = \sum_{i=1}^m \left(\frac{E_i}{E_0} I_i\right) = \sum_{i=1}^m n_i \{I_i + (x - d_i)^2 A_i\}$$

Where A , B and I are the total transformed cross section area and its first and second moment about an axis through point O .

Also, A_i , B_i and I_i are the area of the i -th layer and its first and second moment about an axis through point O .

If change to the matrix form

$$\begin{Bmatrix} N \\ M \end{Bmatrix} = E_0 \begin{bmatrix} A & B \\ B & I \end{bmatrix} \begin{Bmatrix} \varepsilon_0 \\ \psi \end{Bmatrix}$$

$$\begin{Bmatrix} \varepsilon_0 \\ \psi \end{Bmatrix} = \frac{1}{E_0} \begin{bmatrix} A & B \\ B & I \end{bmatrix}^{-1} \begin{Bmatrix} N \\ M \end{Bmatrix}$$

The above equation can be used to find N and M , when ε_0 and ψ are known, or to find ε_0 and ψ , when N and M are known.

$$\begin{bmatrix} A & B \\ B & I \end{bmatrix}^{-1} = \frac{1}{(AI - B^2)} \begin{bmatrix} I & -B \\ -B & A \end{bmatrix}$$

$$\begin{Bmatrix} \varepsilon_0 \\ \psi \end{Bmatrix} = \frac{1}{E_0(AI - B^2)} \begin{bmatrix} I & -B \\ -B & A \end{bmatrix} \begin{Bmatrix} N \\ M \end{Bmatrix}$$

When the reference point O is chosen at the centroid of the transformed section, the first moment of area B about an axis through point O becomes zero ($x = x_0$).

$$\begin{Bmatrix} \varepsilon_0 \\ \psi \end{Bmatrix} = \frac{1}{E_0} \begin{Bmatrix} N/A \\ M/I \end{Bmatrix}$$

Therefore, the stress of i -th layer of the composite section is

$$\sigma_i = E_i (\varepsilon_0 + \psi y) = n_i (N/A + M \cdot y/I)$$

If axial force $N = 0$,

$$\sigma_i = n_i (M \cdot y/I)$$

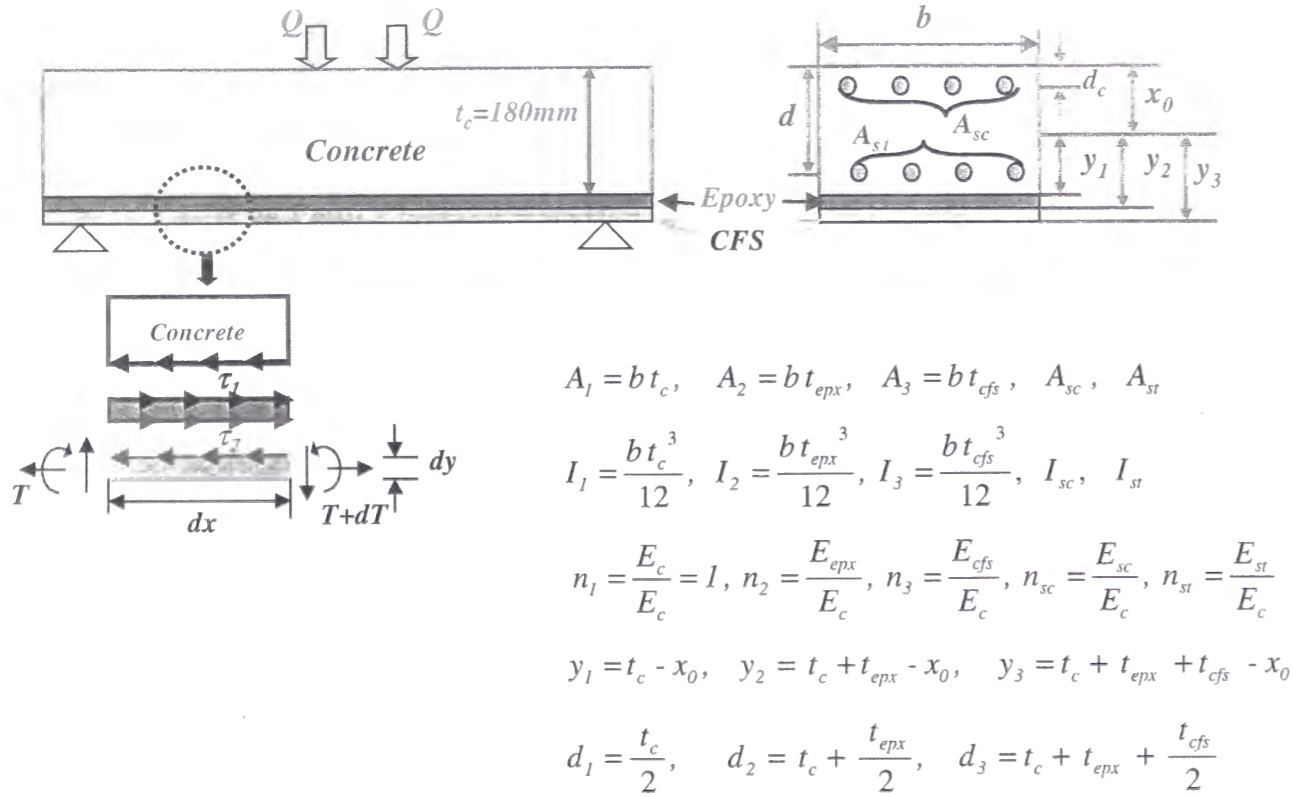
6.2.2 ESTIMATION OF THE ULTIMATE FLEXURAL STRENGTH

A new analytical investigation for evaluating ultimate flexural strength of laminated RC slab by CFS is introduced. The estimation of the ultimate flexural strength of a slab was tried under the assumption that the failure occurs when the shear stress between the concrete bottom and the glued CFS reaches the bond strength. The shear stress will be evaluated theoretically in this Chapter and the bond strength was obtained by a laboratory test as shown in Chapter 3. The ultimate flexural strength of the test slabs was obtained by

the bending test as shown in Chapter 4.

DERIVATION OF SHEAR STRESS AND FAILURE LOAD

Debonding of CFS from concrete is actually delamination of epoxy layer from the concrete surface. The section of the test slab is divided into RC slab, epoxy resin and CFS as shown in Figure 6.2.



Where, A_i is the section area of each material (A_{sc} and A_{st} are the section area of the compressive and tensile steel), I_i is the moment of inertia of each material, x_0 is the centroid position of the composite section measured from the top of the slab, n_i is the elastic modulus ratio of each material to the concrete, d_c is the cover of the re-bar in the compression side.

Figure 6.2 Analysis of composite slab

The centroid position of the transformed composite section measured from the top of the slab is

$$x_0 = \frac{n_1 A_1 d_1 + n_2 A_2 d_2 + n_3 A_3 d_3 + n_{sc} A_{sc} d_c + n_{st} A_{st} d}{n_1 A_1 + n_2 A_2 + n_3 A_3 + n_{sc} A_{sc} + n_{st} A_{st}}$$

The moment of inertia of the composite section I_0 is

$$I_0 = \sum_{i=1}^3 n_i \{I_i + (x_0 - d_i)^2 A_i\} + [n_{sc} \{I_{sc} + (x_0 - d_c)^2 A_{sc}\}] + [n_{st} \{I_{st} + (x_0 - d)^2 A_{st}\}]$$

The shear stress τ_1 and τ_2 mobilized between concrete and epoxy layer and between epoxy layer and CFS can be derived by considering the equilibrium conditions of an infinitesimal part dx as shown in Figure 6.2.

First, the tensile stress in the CFS is

$$\sigma_{cfs} = n_3 (N/A + M/I \cdot y)$$

If axial force $N = 0$, the incremental stress of CFS in the distance dx is

$$d\sigma_{cfs} = n_3 \left(\frac{y}{I} \cdot dM\right)$$

$$d\sigma_{cfs}/dx = n_3 \left(\frac{dM}{dx} \cdot \frac{y}{I}\right) = n_3 \left(\frac{Q}{I} \cdot y\right)$$

$$d\sigma_{cfs} = n_3 \left(\frac{Q}{I} \cdot y\right) dx$$

Therefore, the incremental tension force dT in the CFS is

$$dT = \sigma_{cfs} \cdot dA = n_3 \int_{y_2}^{y_3} \left(\frac{Q}{I} \cdot y \cdot dx\right) \cdot dA$$

On the other hand, from the equilibrium of horizontal force

$$dT = \tau_2 \cdot b \cdot dx$$

$$n_3 \int_{y_2}^{y_3} \left(\frac{Q}{I} \cdot y \right) dx \cdot dA = \tau_2 \cdot b \cdot dx$$

Therefore, the shear stress τ_2 between epoxy layer and CFS can be defined as follows

$$\tau_2 = \frac{Q}{Ib} \left[n_3 \int_{y_2}^{y_3} y dA \right] = \frac{Q}{I} \left[n_3 \int_{y_2}^{y_3} y dy \right] = \frac{n_3 Q}{2I} [y_3^2 - y_2^2]$$

and, the shear stress τ_1 between concrete and epoxy layer is

$$\tau_1 = \frac{Q}{Ib} \left[n_2 \int_{y_1}^{y_2} y dA + n_3 \int_{y_2}^{y_3} y dA \right]$$

$$= \frac{Q}{I} \left[n_2 \int_{y_1}^{y_2} y dy + n_3 \int_{y_2}^{y_3} y dy \right] = \frac{n_2 Q}{2I} [y_2^2 - y_1^2] + \tau_2$$

Where, Q is the shear force acting to the section,

n_2 and n_3 are the elastic modulus ratio of epoxy resin and CFS to the concrete, respectively.

Assuming that failure of the slab occurs when $\tau_1 = f_b$ (=bond strength between concrete and CFS obtained by a laboratory test), the flexural strength of the slab in the above equation becomes

$$Q = 2 f_b I / k$$

Where, $k = n_2 \{ y_2^2 - y_1^2 \} + n_3 \{ y_3^2 - y_2^2 \}$

Neglecting t_{epx} and t_{cfs} comparing to $(t_c - x_0)$,

$$(y_2^2 - y_1^2) = (y_2 + y_1)(y_2 - y_1) = (2t_c - 2x_0 + t_{epx}) \cdot t_{epx} \approx 2(t_c - x_0) \cdot t_{epx}$$

$$(y_3^2 - y_2^2) = (2t_c - 2x_0 + t_{epx} + t_{cfs}) \cdot t_{cfs} \approx 2(t_c - x_0) \cdot t_{cfs}$$

and also neglecting $E_{epx} \cdot t_{epx}$ comparing to $E_{cfs} \cdot t_{cfs}$

$$k = \frac{2(t_c - x_0)}{E_c} \{ E_{epx} \cdot t_{epx} + E_{cfs} \cdot t_{cfs} \} \approx 2(t_c - x_0) \frac{E_{cfs}}{E_c} \cdot t_{cfs}$$

Then

$$Q = 2 f_b E_c I / (t_c - x_0) E_{cfs} \cdot t_{cfs}$$

Therefore, flexural failure load is

$$P = 2Q = 4 f_b E_c I / (t_c - x_0) E_{cfs} \cdot t_{cfs}$$

Here, $I = \frac{1}{3} b x_0^3 + n_{st} A_{st} (d - x_0)^2 + n_{sc} A_{sc} (x_0 - d_c)^2 + n_2 A_{epx} (t_c - x_0 + \frac{1}{2} t_{epx})^2 + n_3 A_{cfs} (t_c - x_0 + t_{epx} + \frac{1}{2} t_{cfs})^2$

Neglecting t_{epx} and t_{cfs} comparing to $(t_c - x_0)$ as before

$$I = \frac{1}{3} b x_0^3 + n_s A_{st} (d - x_0)^2 + n_s A_{sc} (x_0 - d_c)^2 + (n_2 A_{epx} + n_3 A_{cfs}) (t_c - x_0)^2$$

Where, n_{sc} and n_{st} are the elastic modulus ratio of compression steel and tension steel to concrete

d_c is the cover of the steel in the compression side

A_{epx} and A_{cfs} are the section area of the epoxy layer and CFS

EVALUATION OF THE ELASTIC MODULUS OF CONCRETE BY BACK ANALYSIS

I and x_0 are calculated on the assumption that the concrete in tension zone and yielded rebar do not contribute to the gross section. It is however difficult to choose the approximate value for the elastic modulus of the concrete since the elastic modulus is dependent on the strain level which varies with load level and also varies from the place to place in the concrete slab.

The over-all elastic modulus of concrete at the near failure of the test slab is evaluated by comparing the flexural rigidity at the initial state $E_{co}I_o$ and at the final state E_cI both evaluated from the deflection at the span center. Where, E_{co} is the initial tangent of the concrete and I_o is the moment of inertia of the composite slab based on the gross section. E_c is called as the over-all elastic modulus of concrete in this research. Under the above assumptions, E_c does not differ from E_{co} so much as shown in Table 6.1. Therefore, the elastic modulus may be taken as a constant value in this analysis.

Table 6.1 Experimental test results of slab specimens

CFS 2 layers	Test slab	Anchor -ing	E_{co} (N/mm ²) × 10 ⁴	E_c (N/mm ²) × 10 ⁴	I_o (cm ⁴)	I (cm ⁴)	x_0 (cm)	P_{exp} (KN)
	SA-5	PA	3.10	2.74	20710	3130	3.52	161.7
T300	SA-6	NA	2.95	2.53	20860	3230	3.57	165.6
	SA-7	NA	2.90	2.78	20920	2950	3.44	157.8
	SB-2	PA	3.01	2.84	21090	3820	3.76	189.1
T400	SB-3	PA	3.13	2.74	20960	3610	3.67	190.1
	SB-4	NA	3.30	3.08	20790	3940	3.80	198.0

EVALUATION OF BOND STRENGTH f_B

On the other hand, bond strength f_B between concrete and CFS (actually epoxy layer) was

conducted by a laboratory test and evaluated by two methods as shown in Chapter 3. Only two specimens were tested for each case and the gap of these two data is large.

Table 6.2 Bond strength f_B (N/mm²)

CFS 2 layers	f_B by the Method 1 [$f_B = P_{max} / 2A$]			f_B by the Method 2 [$f_B = \int_0^l E_{cfs} \cdot t_{cfs} \left(\frac{d\varepsilon}{dx} \right) dx / l$]		
	Specimen No.1	Specimen No.2	Average bond strength	Specimen No.1	Specimen No.2	Average bond strength
T300	1.69	1.23	1.46	1.62	1.14	1.38
T400	2.16	1.89	2.03	1.63	1.38	1.51

6.2.3 COMPARISON OF ANALYTICAL AND EXPERIMENTAL RESULTS

The theoretically obtained ultimate flexural strength is compared with the test result. Table 6.3 shows the comparison of the calculated strength with the corresponding experimental result. The corresponding average bond strength is used in the evaluation of the flexural strength. In this table, the result of conventional RC calculation based on perfect bond between concrete and CFS is also included.

Table 6.3 Comparison of the calculated and experimental results on flexural strength

CFS 2 layers	Test slab	P_{cal} / P_{exp} (f_B by the Method 1)			P_{cal} / P_{exp} (f_B by the Method 2)			P_{cal} / P_{exp} by RC Calculation
		f_B -No.1	f_B -No.2	f_B -ave	f_B -No.1	f_B -No.2	f_B -ave	
	SA-5	1.41	1.03	1.22	1.35	0.95	1.15	1.47
T300	SA-6	1.38	1.0	1.19	1.32	0.93	1.13	1.43
	SA-7	1.46	1.06	1.26	1.40	0.98	1.19	1.50
	SB-2	1.49	1.30	1.40	1.12	0.95	1.04	1.50
T400	SB-3	1.49	1.30	1.40	1.12	0.95	1.04	1.49
	SB-4	1.41	1.24	1.32	1.07	0.90	0.99	1.43

It is found that this new method gives a relatively good estimate of the ultimate flexural strength of the composite slab compared to the conventional RC calculation where the entire section of CFS is considered to be effective. The gap between the calculated value P_{cal} and the corresponding experimental value P_{exp} is considered to arise mainly from the unsatisfactory evaluation of the bond strength f_b .

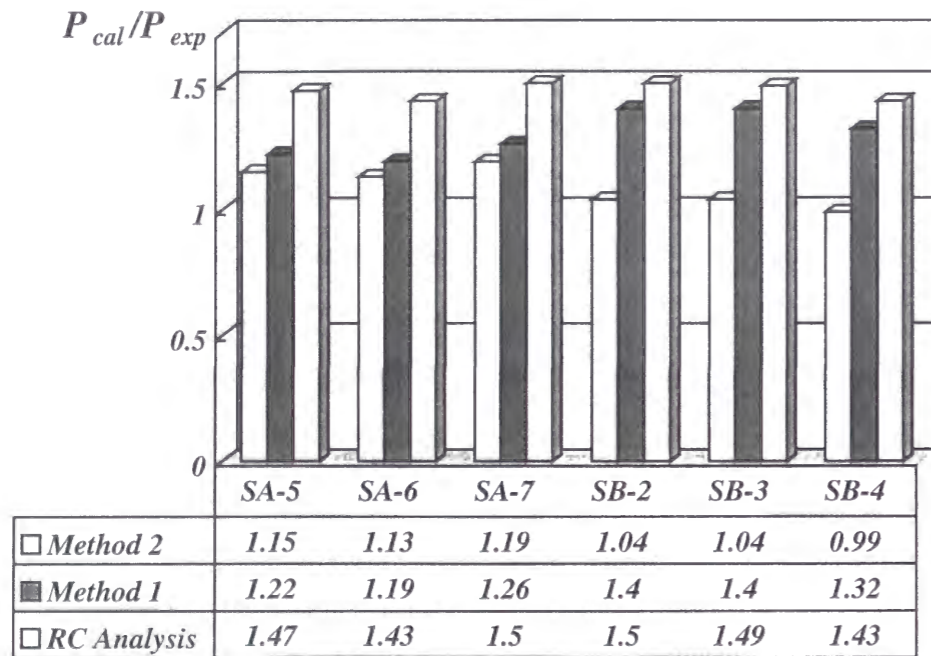


Figure 6.3 Comparison of the calculated and experimental results

6.2.4 PARAMETRIC STUDY

In order to investigate the effects of design variables such as, thickness of the CFS, and the elastic modulus of CFS on flexural strength of a RC slab retrofitted with CFS, a parametric study is performed. In this new analytical method, the flexural strength of a laminated RC slab by CFS is influenced by the combination of two terms, one is f_b term and the other is I/k term, as follows;

$$Q = 2 f_b \cdot \frac{I}{k} \quad \text{here, } k \approx 2(t_c - x_0) \frac{E_{cfs}}{E_c} \cdot t_{cfs}$$

Where, f_b is bond strength between concrete and CFS obtained by a laboratory test

I and x_0 are the moment of inertia and the neutral axis calculated on the assumption that the concrete in tension zone and yielded re-bar do not contribute to the gross section

t_c, t_{cfs} and the E_c, E_{cfs} are the thickness and the elastic modulus of concrete and CFS

EFFECT OF THICKNESS OF CFS

Table 6.4 shows the parametric analysis results on the effect of CFS thickness. The flexural strength of a laminated RC slab by CFS is increased with the increase of thickness of CFS.

Table 6.4 Parametric analysis results on the effect of CFS thickness

CFS (×layer)	t_{cfs} (cm)	t_c (cm)	E_{cfs} (N/mm ²)	E_{co} (N/mm ²)	I_0 (cm ⁴)	I (cm ⁴)	x_0 (cm)	k (cm ²)	I/k (cm ²)
T300×1	0.0167				20360	1680	2.93	4.2	396
T400×1	0.0223				20510	2070	3.08	5.6	369
T300×2	0.0334				20790	2830	3.38	8.2	344
T400×2	0.0446	18	2.50×10^5	2.94×10^4	21080	3560	3.65	10.8	330
T300×4	0.0668				21660	4940	4.13	15.6	316
T400×4	0.0891				22240	6240	4.55	20.2	308

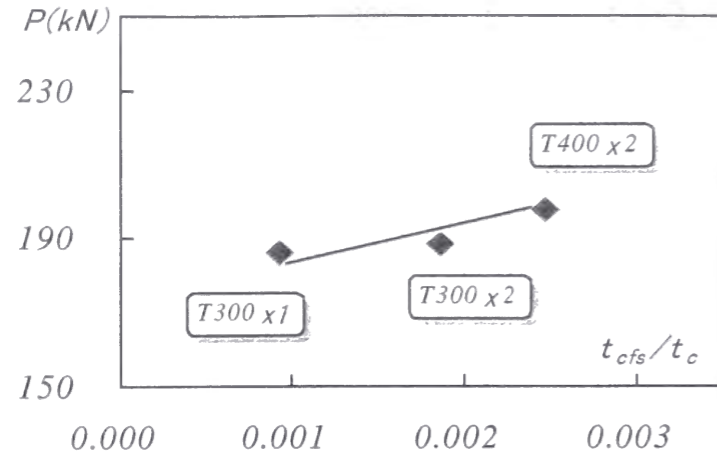


Figure 6.4 Effect of thickness of CFS to flexural strength

EFFECT OF ELASTIC MODULUS OF CFS

The laminated RC slab retrofitted by high elastic modulus of CFS shows a better load carrying capacity than high strength of CFS.

Table 6.5 Parametric study results on the effect of elastic modulus of CFS

CFS (2layers)	t_{cfs} (cm)	t_c (cm)	E_{cfs} (N/mm ²)	E_{co} (N/mm ²)	I_0 (cm ⁴)	I (cm ⁴)	x_0 (cm)	k (cm ²)	I/k (cm ²)
T300	0.0334	18	2.50×10^5	2.94×10^4	20790	2830	3.38	8.2	344
HM300	0.0330		3.92×10^5		21270	4040	3.82	12.8	324

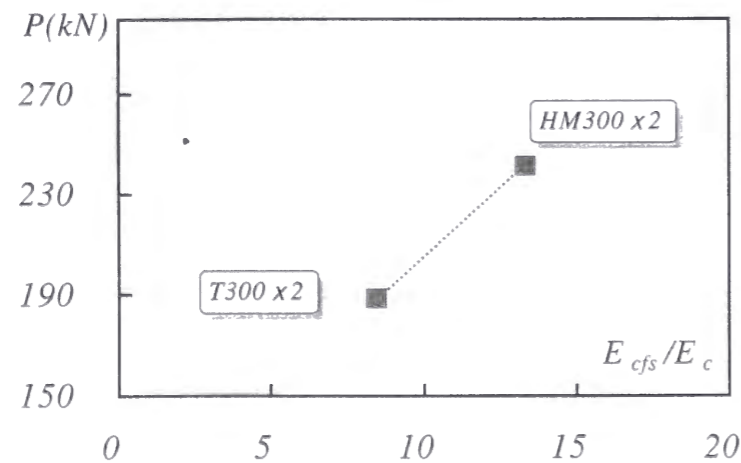


Figure 6.5 Effect of elastic modulus of CFS to flexural strength

EFFECT OF ELASTIC MODULUS OF CONCRETE

The flexural strength of a laminated RC slab by CFS increases with the increase in elastic modulus of concrete.

Table 6.6 Parametric study results on the effect of elastic modulus of concrete slab

CFS (2layers)	t_{cfs} (cm)	t_c (cm)	E_{cfs} (N/mm ²)	E_{co} (N/mm ²)	I_0 (cm ⁴)	I (cm ⁴)	x_0 (cm)	k (cm ²)	I/k (cm ²)
				2.94×10^4	20790	2830	3.38	8.2	344
T300	0.0334	18	2.50×10^5	3.94×10^4	20010	2220	3.04	6.3	351
				4.94×10^4	19540	1830	2.78	5.1	356

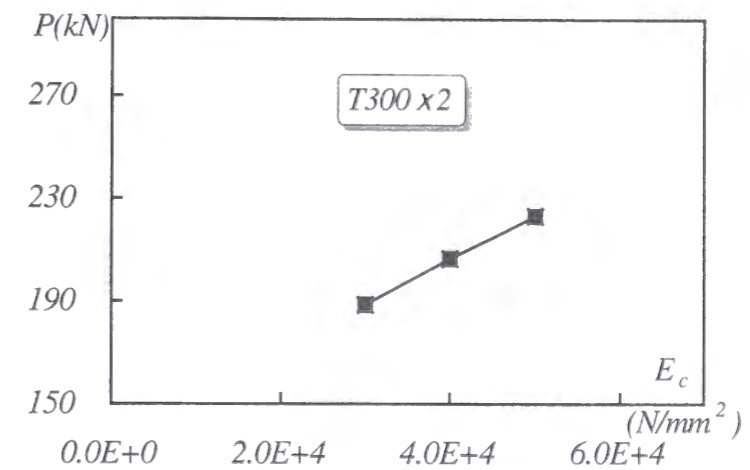


Figure 6.6 Effect of elastic modulus of concrete to flexural strength

6.2.5 ITERATIVE ANALYSIS METHOD

In order to simulate the load-displacement relation of a laminated RC slab, iterative analysis was conducted. This method is also constructed based on the same concept as already mentioned before section. This method does not ignore concrete tensile strength even cracks happened, that is concrete can exhibit its tensile strength in the tension zone of composite slab. The iteration technique can be summarized as following flow chart.

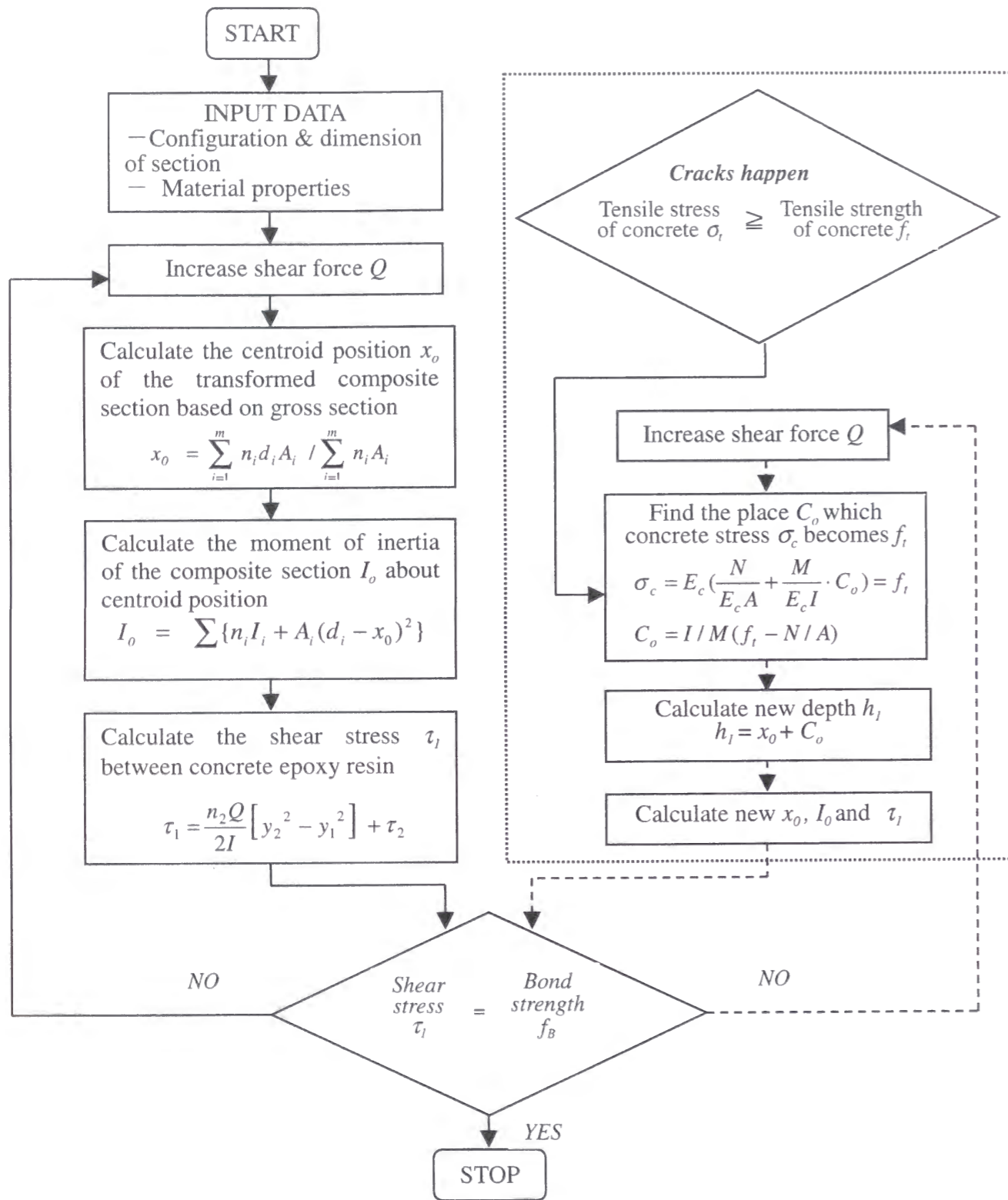


Figure 6.7 Procedure of iterative analysis

Table 6.7 Iterative analysis results (Tensile strength of concrete $f_t=3.25\text{N/mm}^2$)

Load P (kN)	Neural axis x_o (cm)	C_o (cm)	New h (cm)	E_c (N/mm ²)	E_b (N/mm ²)	I (cm ⁴)	τ_1 (N/mm ²)	τ_2 (N/mm ²)	δ (mm)
10	9.13	8.87	18.0	3.0×10^4	2.8×10^3	20780	0.0063	0.0059	0.19
20	9.01	8.31	17.32			19950	0.0123	0.0119	0.40
30	8.83	6.25	15.08			18760	0.022	0.021	0.62
40	7.90	3.41	11.32			13650	0.044	0.042	1.14
50	6.48	2.73	9.22			8540	0.109	0.105	2.27
60	5.82	1.20	7.02			7200	0.176	0.165	3.23
80	5.31	0.83	6.14			6640	0.255	0.248	4.67
100	5.18	0.66	5.84			6580	0.354	0.344	5.89
120	5.15	0.55	5.69			6570	0.396	0.386	7.08
130	4.68	0.41	5.10			5380	0.646	0.630	9.38
140	4.29	0.32	4.62			4550	0.892	0.870	11.94
150	3.86	0.24	4.10			3650	1.290	1.260	15.94

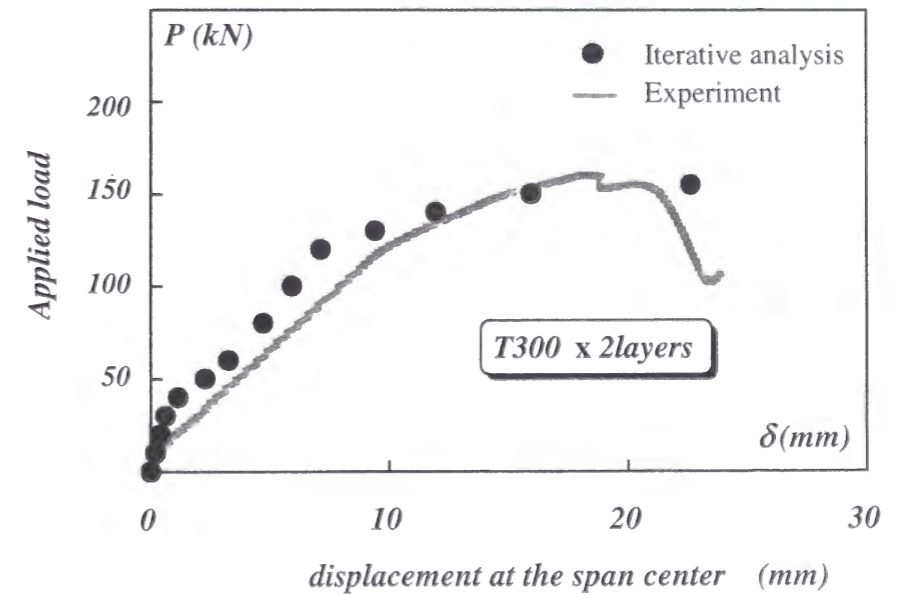


Figure 6.8 Comparison of Load-displacement curve

6.3 CONCLUSIONS OF CHAPTER 6

A proposed analytical method based on bond strength between concrete and CFS to evaluate the flexural strength of RC slab strengthened with CFS was discussed. The following conclusions can be drawn;

- The proposed method looks feasible to estimate flexural strength of composite RC slab retrofitted with CFS. It is found in this study, however that the evaluation of the bond strength is the key and that the evaluation of the moment of inertia of the composite section in which concrete being cracked and the rebar being yielded is also the key.
- A parametric study was performed to investigate the retrofitting effects of CFS on flexural strength of a retrofitted RC slab. From the results, the high elastic modulus of CFS shows a significant effect to improve the flexural strength of a retrofitted RC slab than other variables.

Chapter 7

SUMMARY AND CONCLUSIONS

SUMMARY OF EACH CHAPTER

◆ *Chapter 2*

Review of previous researches for structural behavior of strengthened RC members by FRP materials is introduced. This chapter also contains a brief review of seismic retrofitting techniques and experimental results of viaduct column and beam-column connections retrofitted with CFS.

◆ *Chapter 3*

Experimental and analytical investigations on interfacial bond behavior between concrete and CFS are discussed. Bond strength between concrete surface and CFS (actually epoxy layer) is evaluated by laboratory test. A Finite Element (FE) analysis is also developed to simulate the strain distributions along the bonded length of CFS.

Conclusions

- (1) The failure of bond test specimens mainly occurs by sudden delamination of CFS from the concrete surface before reaches its rupture strain.
- (2) The maximum pull load increases as the thickness of bonded CFS increases. Also, test specimens bonded by high elastic modulus of CFS show better load capacity.
- (3) Finite Element [FE] analysis is conducted to simulate the strain distributions along the bonded length of CFS. The FE analysis shows good accordance to the experimental results, and also within the scope of this bond test, 100mm length is considered as an effective bond length of CFS.

◆ **Chapter 4**

Improvement of flexural strength of laminated RC bridge slab by CFS is discussed. An experimental investigation was conducted with test slabs under static load. Section analysis based on the compatibility of deformations and equilibrium of forces and 2-D (Two-dimensional) FE analysis are developed to predict the structural behavior of strengthened RC slab.

Conclusions

- (1) Failure of the test slab occurred immediately after debonding of CFS from concrete and crushing of concrete in the compression zone followed at the same time.
- (2) The strain level developed in CFS at the failure was much lower than the ruptured strain. Therefore, improvement of bond strength between concrete

and CFS is expected farther improvement of the flexural strength of concrete slab.

- (3) Good anchoring of CFS to the slab surface improved the ductility of the retrofitted slab. This fact should be taken into consideration for the practical application.
- (4) The flexural strength of the retrofitted test slab increases in proportion to the amount of CFS. Retrofit of the test slab with 2 layers of HM300 CFS improved the flexural strength over 2.4 times.
- (5) The section analysis based on the compatibility of deformations and equilibrium of forces, and FE analysis results show good accordance to the experimental results

◆ **Chapter 5**

Experimental study of flexural fatigue behavior of RC slab retrofitted with CFS, particularly under very large repeated loading is discussed. The test slab is almost identical to an existing slab of a highway in terms of the amount of reinforcement, quality of concrete and thickness of the slab, which is 18cm. Only one directional flexural behavior of the slab was tested.

Repeated loads corresponding to 3.0, 4.5 or 6.0 times of the design bending moment were applied to the test slab until failure. Normal type of CFS with 300g/m^2 (T300), 400g/m^2 (T400) and high-elastic modulus type of CFS with 300g/m^2 (HM300) were used for the strengthening.

The test slabs were loaded in dry or wet condition. Some of the test slabs were

damaged under the repeated load and retrofitted by CFS, then loaded again to see the improvement of the fatigue life. An energy-based damage index is discussed to estimate the cumulative fatigue damage of retrofitted RC slab.

Finally, Infrared Thermography, one of the monitoring techniques in the NDT (Non-Destructive Testing) field, and retrofit design concept for existing RC bridge slab are also introduced.

Conclusions

- (1) The fatigue failure of retrofitted slabs mainly occurred by debonding of interface between concrete and CFS. This failure pattern indicates that bond strength between concrete and CFS is one of the key factors to decide the fatigue life of a retrofitted RC slab by CFS.
- (2) The test slab strengthened by 2 layers of T400 CFS lasted more than 5millions cycles of the 3.0times design load, whereas the test slab without CFS failed at about 0.46 millions cycles under the same loading.
- (3) The test slab retrofitted with 2layers of high-elastic modulus type of HM300 CFS had kept the same initial flexural strength even after the application of 3.0million cycles of 4.5times design load. Therefore, this amount of application is recommended to retrofit of highway bridge slab.
- (4) Even badly damaged slabs recovered its fatigue strength by the application of CFS. The control test slab loaded up to 90% of the fatigue life cycles at the load level of 3.0times design load endured to additional 2.0million cycles of 3.0times design load by CFS retrofitting. Therefore, it is still significant to retrofit a RC bridge slab by CFS even if it is already heavily damaged.

- (5) Fatigue life of the wet slab under 3.0times of the design load increased from 0.33millions cycles to over 2.0million cycles by the application of 2 layers of T400 CFS.
- (6) There was almost no clear difference in fatigue life between Normal and Perfect anchoring.

◆ Chapter 6

A proposed analytical method based on bond strength between concrete and CFS to evaluate the flexural strength of RC bridge slab strengthened with CFS is discussed.

The evaluation of the ultimate flexural strength of a slab is tried under the assumption that the failure occurs when the shear stress mobilized at the interface between the concrete bottom and the glued CFS reaches the bond strength. The shear stress is evaluated theoretically and the bond strength is obtained by a laboratory test.

Conclusions

- (1) The proposed method to evaluate the flexural strength of a RC member strengthened by CFS is expected to give a good estimate of the ultimate strength. It is found in this study, however that the evaluation of the bond strength between concrete and CFS is the key and that the evaluation of the moment of inertia of the composite section in which concrete being cracked and the re-bar being yielded is also the key. The accuracy of the thickness and the elastic modulus of CFS are also influential.

CONCLUSIONS & RECOMMENDATION OF FUTURE STUDY

The mechanical behavior of RC slab retrofitted with Carbon Fiber Sheet (CFS) under static and fatigue loading was investigated. From the whole results of this thesis, the following conclusions can be drawn.

- ◆ Retrofit of the test slab with 2 layers of CFS improved the flexural strength up to 2.4times.
- ◆ The retrofitted RC slab with 2 layers of CFS prolonged its fatigue life up to 5 times in wet condition, and 10 times in dry condition under 3.0times of the design load.
- ◆ It will be possible to estimate the flexural strength of a RC slab retrofitted with CFS by the proposed analytical method based on bond strength between concrete and CFS with accuracy.
- ◆ Further research concerning the new failure modes such as delamination of CFS, evaluation of bond strength and retrofit design methodologies must be studied to clarify the mechanical behavior of laminated composite member and to assure safe practical application in construction site.

- ◆ Also, studies in nondestructive evaluation methodologies such as Infrared Thermography must be performed simultaneously to confirm deterioration and exfoliation circumstances of retrofitted structures by fiber materials, effectively.

※ Carbon Fiber Sheet can be applied to the RC bridge slab as a feasible retrofitting material.

Mean

REFERENCE

1. ABAQUS/Standard User's Manual, *Version 5.8* (1998) Hibbit, Karlsson & Sorensen Inc., Providence, R.I.
2. Aboutaha, R.S., Engelhardt, M.D., Jirsa, J.O., and Kreger, M.E. (1999) "Experimental Investigation of Seismic Repair of Lap Splice Failure in Damaged Concrete Columns," *ACI Structural Journal*, Vol.96, No.2, Mar-Apr, pp.297-306.
3. Adin, M.A., et al. (1993) "Cyclic Behavior of Epoxy-Repaired Reinforced Concrete Beam-Column Joints," *ACI Structural Journal*, Vol. 90, Mar-Apr, pp.170-179.
4. Ahmad, S.H., and Irshaid (1991) "Behavior of concrete spirally confined by fiberglass filaments," *Magazine of Concrete research*, 1991,43, No.156, pp.143-148.
5. Al-Sulaimani, G.J., and B.N. Ghaleb (1994). "Shear Repair for Reinforced Concrete by Fiberglass Plate Bonding," *ACI Structural Journal*, Vol.91, No.3, pp.458-464.
6. An W., Saadatmanesh, H., and Ehsani, M.R. (1991) "RC Beams Strengthened with GFRP Plates. II: Analysis and Parametric study," *ASCE, Journal of Structural Engineering*, Vol.117, No.11, pp.3434-3455.
7. Arduini, M., Tommaso, A.D., and Nanni, A. (1997a) "Brittle Failure in FRP Plate and Sheet Bonded Beams," *ACI Structural Journal*, July, pp.363-370.
8. Arduini, M., Tommaso, A.D., and Nanni, A. (1997b) "Parametric Study of Beams with Externally Bonded FRP Reinforcement," *ACI Structural Journal*, July, pp. 493-501.
9. Arduini, M., et al (1997)"Behavior of Pre-cracked RC Beams Strengthened with Carbon Fiber Sheets," *ASCE, Journal of Composites for Construction*, Vol.1, No.2, May, pp.63-70.
10. Bakis, C.E., et al. (1999) "An Optical Investigation of Damage and Load Transfer Mechanisms in Concrete with External FRP Sheet Reinforcement," *Proc. of the 8th International conference and Exhibition, Structural Faults & Repair-99*, CD-ROM.
11. Baluch, M.H., Ziraba, Y.N., Azad, A.K., Sharif, A.M, Al-Sulaimani, G.J., and Basunbul, I.A. (1995) "Shear Strength of Plated RC Beams," *Magazine of Concrete Research*, Vol.47, No.173, Dec, pp.369-374.
12. Barnes, R.A., and Mays. G. C (1999) "Fatigue Performance of Concrete Beams Strengthened with CFRP Plates," *ASCE, Journal of Composites for Construction*, Vol.3, No.2, May, pp.63-72.
13. Brosens, K., et al. (1997) "Anchoring Stress Between Concrete and Carbon Fiber Reinforced Laminates" *Non-Metallic (FRP) Reinforcement for Concrete Structures, Proceedings of the 3rd international Symposium*, Sapporo, Vol. 1, pp.271-278.
14. Buyukozturk, O., and Hearing, B. (1998) "Failure Behavior of Precracked Concrete Beams Retrofitted with FRP," *ASCE, Journal of Composites for Construction*, Vol.2, No.3, pp.138-144.
15. Buyukozturk, O., Hearing, B., and Gunes, O. (1999) "FRP Strengthening & Repair: WHERE DO WE GO FROM HERE?," *Proc. of the 8th International conference and Exhibition, Structural Faults & Repair-99*, London, CD-ROM.
16. Chaallal, O., Nollet, M. J., and Perraton, D. (1998) "Shear Strengthening of RC Beams by Externally Bonded Side CFRP Strips," *Journal of Composites for Construction*, Vol.2, No.2, pp.111-114.
17. Chai, Y.H., Priestley, M.J.N., and Seible, F. (1991) "Seismic Retrofit of Circular Bridge Columns for Enhanced Flexural Performance," *ACI Structural Journal*, Vol.88, No.5, pp.572-584.
18. Chajes, M.J., Thomson, T.A., Jr., Januszka, T.F and W.W. Finch. (1994) "Flexural Strengthening of Concrete Beams Using Externally Bonded Composite Materials," *Construct. Build. Mater*, 8, No.3, pp.191-201.
19. Chajes, M.J., Januszka, T.F., Mertz, D.R., Thomson, T.A., and Finch, W.W. (1995)

- “Shear Strengthening of Reinforced Concrete Beams Using Externally Applied Composite Fabrics,” *ACI Structural Journal*, Vol. 92, No.3, May-June, pp.295-303.
20. Chajes, M. J. and et al. “Bond and Force Transfer of Composite Material Plate Bonded to Concrete,” *ACI Structural Journal*, Vol.93, No.2, 1996, pp.208-217.
 21. Chai, Y.H., et al. (1991) “Seismic Retrofit of Circular Bridge Columns for Enhanced Flexural Performance,” *ACI Structural Journal*, Vol. 88, No.5, Sep-Oct, pp.572-584.
 22. Chung, Y.S., and Hwang, E.S. (1999) “Experimental Seismic Performance of Circular Hollow R.C Bridge Piers before and after Retrofitting” *Proc. of the 8th International conference and Exhibition, Structural Faults & Repair-99*, London, CD-ROM.
 23. David, E., Djelal, C., Ragneau, E., and Buyle-Bodin, F. (1999) “Use of FRP to Strengthen and Repair RC Beams,” *Proc. of the 8th International conference and Exhibition, Structural Faults & Repair-99*, London, CD-ROM.
 24. Demers, M. and Neal, K.W. (1994) “Strengthening of Concrete Columns with Unidirectional Composite Sheets,” *Proc. of the 4th International Conference on Short and Medium Span Bridges*, Halifax, Nova Scotia, Canada, Aug, pp.895-905.
 25. Demers, M., Hebert, D., Labossiere, P.W (1996) “The Strengthening of Structural Concrete with an Aramid Woven Fiber/Epoxy Resin Composite,” *Proc. Advanced Composite Materials in Bridges and Structures II*, Montreal, Aug, 435-442.
 26. Deskovic, N., Triantafillou, T.C., and Meier, U. (1995) “Innovative Design of FRP Combined with Concrete: Short-Term Behavior,” *ASCE, Journal of Structural Engineering*, Vol.127, No.7, pp.1069-1078.
 27. Deskovic, N., Meier, U., and Triantafillou, T.C. (1995) “Innovative Design of FRP Combined with Concrete: Long-Term Behavior,” *ASCE, Journal of Structural Engineering*, Vol.127, No.7, pp.1079-1089.
 28. Deuring, M., (1990) “Post Strengthening of Concrete Structures with Prestressed Advanced Composite,” Published by the EMPA in German as Research, No. 224.
 29. Dolan, B.E., Hamilton, H.R., Dolan, C.W. (1998) “Strengthening with Bonded FRP Laminate,” *Concrete International*, June, pp.51-55.

30. Editorial Committee for the Report on the Hansin-Awaji Earthquake Disaster. (1997) “Report on the Hansin-Awaji Earthquake disaster, Investigation of causes of Damage to Civil Engineering Structures,”
31. EL-Hacha, R, Green, M (1999) “CFRP Wrapped Concrete Cylinders in Severe Environmental Conditions,” *Proc. of the 8th International conference and Exhibition, Structural Faults & Repair-99*, London, CD-ROM.
32. Emmons, P.H., Vaysburd, A.M., and Thomas, J. (1998) “Strengthening Concrete Structures, Part I,” *Concrete International*, Mar, pp.53-58.
33. Emmons, P.H., Vaysburd, A.M., and Thomas, J. (1998) “Strengthening Concrete Structures, Part II,” *Concrete International*, Apr, pp.56-59.
34. Erki, M.A, and Heffernan, P.J. (1995) “Reinforced Concrete slabs Externally Strengthened with Fibre-Reinforced Plastic Materials,” *Non-metallic (FRP) Reinforcement for Concrete Structures*. Edited by L. Taerwe, pp.509-516.
35. Fanning, P., and Kelly, O. (1999) “Shear Strengthening of Reinforced Concrete Beams: An Experimental Study Using CFRP Plates,” *Proc. of the 8th International conference and Exhibition, Structural Faults & Repair-99*, CD-ROM.
36. Fardis, M.N., and Khalili, H. (1981) “Concrete Encased in Fiberglass-Reinforced Plastic,” *ACI Structural Journal*, Nov-Dec, pp.440-446.
37. Fardis, M.N., and Khalili, H. (1982) “FRP Encased Concrete as Structural Material,” *Magazine of Concrete Research*, Vol.34, No.121, pp.191-202.
38. Faza, S.S., and GangaRao, H.V.S. (1994) “Fiber Composite Wrap for Rehabilitation of Concrete Structures”, *Proc. of the 3rd Materials Engineering Conference, Infrastructure*, ASCE Publications, California, Nov, pp.1135-1139.
39. Foley, C. M., and Buckhouse, E. R. (1999) “Method to Increase Capacity and Stiffness of Reinforced Concrete Beams” *ASCE, Pract. Periodical on Struct. Des. and Constr.*, Vol.4, No.1, Feb, pp.36-42.
40. GangaRao, H.V.S., et al. (1998) “Bending Behavior of Concrete Beams Wrapped with Carbon Fabric,” *ASCE, Journal of Structural Engineering*, Vol.124, No.1, pp.3-10.
41. Garden, H.N., Hollaway, L.C., and Thorne, A.M. (1997) “A Preliminary Evaluation

- of Carbon Fibre Reinforced Polymer Plates for Strengthening Reinforced Concrete Members,” *Proc. Instn Civ Engrs Structs & Bldge*, 123, May, pp.127-142.
42. Gergely, I., Pantelides, C.P., Nuismer, R.J., and Reaveley, L.D. (1998) “Bridge Pier Retrofit using Fiber Reinforced Plastic Composites,” *ASCE, Journal of Composites for Construction*, Vol.2, No.4, Nov, pp.165-174.
 43. Grace, N.F., and Abdel-Sayed, G. (1999) “Use of CFRP/CFCC Strands in Prestressed Concrete Bridges,” *Proc. of the 8th International conference and Exhibition, Structural Faults & Repair-99*, London, CD-ROM.
 44. Hamoush, S.A., et al. (1990) “Debonding of Steel Plate-Strengthened Concrete Beams,” *ASCE, Journal of Structural Engineering*, Vol.116, No.2, Feb, pp. 356-371.
 45. Han, M.Y., Lee, K.M., and Sim, J.S. (1999) “Structural Behavior of RC Beam Strengthened With Notched Steel Plate,” *Proc. of the 8th International conference and Exhibition, Structural Faults & Repair-99*, London, CD-ROM.
 46. Harmon, T.G., et al. (1998) “Confined Concrete Subjected to Uniaxial Monotonic Loading,” *ASCE, Journal of Engineering Mechanics*, Vol.124, No.12, pp.1303-1309.
 47. Harries, K., Kestner, J., Pessiki, S., Sause, S., and Ricles, J. (1998) “Axial Behavior of Reinforced Concrete Columns Retrofit with FRPC Jackets,” *Proc. 2nd Int. Conf. on Composites in Infrastructure*, Tucson, Arizona, 411-425.
 48. Hemanth, K., and Gangarao, V.S., (1998) “FRP Reinforcement in Bridge Deck,” *Concrete International*, June, pp.47-50.
 49. Horiguchi, T. and Saeki, N. (1997) “Effect of Test Methods and Quality of Concrete on Bond Strength of CFRP Sheet,” *Proc. of the 3rd International Conference on Non-Metallic (FRP) Reinforcement for Concrete Structures*, Vol.1, pp. 265-270.
 50. Howie, I. and Karbhari, V.M. (1994) “Effect of Materials Architecture on Strengthening Efficiency of Composite Wraps for Deteriorating Columns in the North-East”, *Proc. of the 3rd Materials Engineering Conference, Infrastructure*, ASCE Publications, California, Nov, pp.199-206.
 51. Hoshijima, Y., Otaguro, H., Sakai, H., and Matui, S. (1998) “Experimental Study

- on Effect of Strengthening to the Damage Road Bridge Deck Slabs by Carbon Fiber Sheets,” *Bridge and Foundation Engineering*, Sep, pp.23-28. (In Japanese)
52. Hosotani, M., and Kawashima, K. (1999) “Stress-Strain Model for Concrete Cylinders Confined by both Carbon Fiber Sheets and Hoop Reinforcement,” *Proc. of JSCE*, No.620, Vol.43, pp.25-42. (In Japanese)
 53. Ichimasu, H et al. (1993) “RC Slabs Strengthened by Bonded Carbon FRP Plates: Part2 application,” *Fiber Reinforced Plastic Reinforcement for Concrete structures (SP-138)*, ACI, Detroit, pp.967-970.
 54. Iemura, H. (1999) “Performance based Design against Extreme Earthquake Ground Motion from Conventional Ductility Demand to Advanced Structural Control Design,” *Proc. of JSCE*, Vol.43, No.623, pp.1-8. (In Japanese)
 55. Inoue, S., et al. (1996) “Deformation characteristics, static and fatigue strengths of reinforced concrete beams strengthened with carbon fiber reinforced plastic plate,” *Transactions of the Japan Concrete Institute*, Vol.18, pp.143-150.
 56. Izuno, K., et al. (1998) “Bond Behavior of Aramid and Carbon Fiber Sheet,” *Concrete Research and Technology*, Vol.9, No.2, July, pp.1-7. (In Japanese)
 57. Jones, R., Swamy, R.N., and Sharif, A. (1988) “Plate Separation and Anchorage of Reinforced Concrete Beams Strengthened by Epoxy-Bonded Steel Plates,” *The Structural Engineer*, Vol.66, No.5, pp.85-94.
 58. Kaiser H. (1989) “Strengthening of Reinforced Concrete with Epoxy-Bonded Carbon Fibre Plastics,” Thesis submitted to ETH, Switzerland, in partial fulfilment of the requirements for the degree of Doctor of Philosophy, 1989, (In German)
 59. Karbhari, V.M and Gao, Y. (1997) “Composite Jacketed Concrete under Uniaxial Compression Verification of Simple Design Equations,” *ASCE, Journal of Materials in Civil Engineering*, Vol.9, No.4, Nov, pp.185-193.
 60. Kendall, D. (1999) “The Selection of Reinforcing Fibers For Strengthening Concrete And Steel Structures Using Reinforced Plastics,” *Proc. of the 8th International conference and Exhibition, Structural Faults & Repair-99*, CD-ROM.
 61. Khalifa, A., Gold, W.J., Nanni, A., and M.I., A.A. (1998) “Contribution of Externally Bonded FRP to Shear Capacity of RC Flexural Members,” *ASCE*,

62. Kobatake, Y., et al. (1993) "A Retrofitting Method for Reinforced Concrete Structures using Carbon Fiber," *Fiber-Reinforced-Plastic (FRP) Reinforcement for Concrete Structures*, pp.435-450.
63. Kshirsagar, S., et al. (1998) "Durability of Fiber-Reinforced Composite Wrapping for the Rehabilitation of Concrete Piers," *Proc. of the First International on Durability of Fibre Reinforced Polymer (FRP) Composites for Construction*, Canada, pp.117-128.
64. Lawrance, G.M., and Jacks, D.H.(1990) *Repair techniques for plastic hinge zones in bridge piers*, Central Laboratories Report 90-B5410. Lower Hutt, New Zealand.
65. Lee, H.S., Tomosawa, F., Noguchi, T., and Kage, T. (1996) "Finite Element Analysis Effect of CFRP Sheet on the Flexural Performance of RC Beams," *Proc. Japan Concrete Inst. (JCI)*, Japan, Vol.1, pp.1065-1070. (In Japanese)
66. Maeda, T., Asano, Y., Sato, Y., Ueda, T., and Kakuta, Y. (1997) "A Study on Bond Mechanism of Carbon Fiber Sheet," *Proc. of the 3rd International Conference on Non-Metallic (FRP) Reinforcement for Concrete Structures*, Oct, pp.279-286.
67. Malek A, M., and Saadatmanesh H. (1996) "Physical and Mechanical Properties of Typical Fibers and Resins," *Proc. 1st Int. Conf. on Compo. in Infrastr. ICCI 96*.
68. Malek A, M., Saadatmanesh H. and Ehsani M.R. (1998) "Prediction of Failure Load of R/C Beams Strengthened with FRP Plate due to Stress Concentration at the Plate End," *ACI Structural Journal*, Vol. 95, No.2, Mar-Apr, pp.142-152.
69. Malek A, M., and Saadatmanesh H. (1998) "Analytical Study of Reinforced Concrete Beams Strengthened with Web-Bonded Fiber Reinforced Plastic Plates or Fabrics," *ACI Structural Journal*, Vol.95, No.3, May-June, pp.343-352.
70. Mallett, G.P. (1994) "State-of-the-Art Review; Repair of Concrete Bridges," Published by Thomas Telford Services Ltd, London.
71. Matsui et al. (1997) "Experimental Study on Strengthening Effect of High-Modulus Carbon Fiber Sheet on Damaged Concrete Deck Slab," *Proceedings of the 7th KAIST-NTU-KU Tri-Lateral Seminar on Civil Engineering*, Kyoto, Japan, pp.239-244.
72. Matuo, M., et al. (1997) "Flexural Fatigue Behavior of Prestressed Concrete Beams with Non-Metallic Fiber Tendon under Water," *Proc.of the 3rd International Conference on Non-Metallic Reinforcement for Concrete Structures*, Japan, pp.775-782.
73. Meier, U. (1982) "Carbon Fiber Reinforced Polymers: Modern Materials in Bridge Engineering," *Structural Engineering International*, No.2, pp.7-12.
74. Meier, U. (1987) "Bridge Repair with High Performance Composites Material," *Material and Technique*, 4, pp.125-128.
75. Meier, U. (1993) "CFRP Bonded Sheets," *Fiber-Reinforced-Plastic (FRP) Reinforcement for Concrete Structures: Properties and Applications*, A.Nanni (Editor) Elsevier Science publishers B.V. pp.423-434.
76. Michaluk, C.R., Rizkalla,S.H et al. (1998) "Flexural Behavior of One-way Concrete Slabs Reinforced by fiber Reinforced plastic Reinforcements," *ACI Structural Journal*, Vol.95, No.3, May-June, pp.353-365.
77. Mirmiran, A., et al. (1997) "Behavior of Concrete Columns Confined by Fiber Composites," *ASCE, Journal of Structural Engineering*, Vol.123, No.5, pp.583-590.
78. Mirmiran, A., et al. (1998) "Effect of Column Parameters on FRP-Confined Concrete," *ASCE, Journal of Composites for Construction*, Vol.2, No.4, Nov, pp.175-185.
79. Miyauchi, K., et al. (1997) "Estimation of Strengthening Effects with Carbon Fibre Sheet for Concrete Column," *Proc. of the 3rd International Symposium on Non-Metallic (FRP) Reinforcement for Concrete Structures*, Japan, Oct, Vol. 1, pp.217-224.
80. Mosallam, A.S. (1999) "Structural Capacity Upgrade of Reinforced Concrete Beam-Column Connections," *Proc. of the 8th International conference and Exhibition, Structural Faults & Repair-99*, London, CD-ROM.
81. Mukhopadhyaya, P., Swamy, R.N. and Lynsdale, C. (1998) "Optimizing Structural Response of Beams Strengthened with GFRP" *ASCE, Journal of Composites for Construction*, Vol.2, No.2, pp.87-95.

82. Mutsuyoshi, H., Aravinthan, T., and Hikimura, T. (1998) "Retrofitting of Reinforced Concrete Beams with External Tendons and Plates," *Proc. 2nd International Conference on Concrete under Severe Conditions, CONSEC'98*, Norway, pp.1176-1184.
83. Najjar, S., Pilakoutas, K., and Waldron, P. (1997) "Finite Element Analysis of GFRP Reinforced Concrete Beams," *Proc. 3rd International Symposium on Non-Metallic (FRP) Reinforcement for Concrete Structures*, Japan, Vol.2, pp.511-518.
84. Nakamura, M., Sakai, H., Yagi, K., and Tanaka, T. (1996) "Experimental Studies on the Flexural Reinforcing Effect of Carbon Fiber Sheet Bonded to Reinforced Concrete Beam," *Proc. 1st Int. Conf. on Compo. in Infrastr. ICCI 96*, pp.760 -773.
85. Nakatuka, T., Komure, K., Tagaki, K. (1998) "Stress-Strain Characteristics of Confined Concrete with Carbon Fiber Sheet," *Concrete Research and Technology*, Vol.9, No.2, July, pp.65-78. (In Japanese)
86. Nanni, A. (1993) "Flexural Behavior and Design of RC Members using FRP Reinforcement," *ASCE, Journal of Structural Engineering*, Vol.119, No.11, Nov.
87. Nanni, A. (1995) "Concrete Repair with Externally Bonded FRP Reinforcement: Examples from Japan," *Concrete International*, June, pp.23
88. Nanni, A., and Bradford, N.M. (1995) "FRP Jacketed Concrete Under Uniaxial Compression," *Const. and Build. Mat*, Vol.9, No.2, pp.115-124.
89. Nanni, A. (1997) "Carbon FRP Strengthening: New Technology Becomes Mainstream," *Concrete International: Design and Construction*, Vol. 19, pp.19-23.
90. Norris, T., et al (1997) "Shear and Flexural Strengthening of RC Beams with Carbon Fibre Sheets," *ASCE, Journal of Structural Engineering*, July, pp.903-911.
91. Oehlers, D.J. (1992) "Reinforced Concrete Beams with Plates Glued to Their Soffits," *ASCE, Journal of Structural Engineering*, Vol.118, No. 8, pp.2023-2038.
92. Oehlers, D.J., et al. (1990) "Premature Failure of Externally Plated Reinforced Concrete Beams," *ASCE, Journal of Structural Engineering*, Vol.116, No.4, Apr, pp.978-995.
93. Ogata, N., et al. (1994) "Strengthening Existing Bridge Piers by Using Carbon Fiber against Earthquake," *Report of Japan Expressway Co.* Vol.31, pp.55-63.
94. Okano, M., Ohuchi, H., Moriyama, T., and Matumoto, N. (1997) "Shear Strengthening of Railway viaduct Column by Carbon Fiber Sheet," *Proc. of Japan Concrete Institute*, Vol.19, No.2, pp.243-248. (In Japanese)
95. Ono, K. (1995) "Seismic Analysis of Bridge Piers Damaged by the Great Hansin Earthquake," *Proc. of the 5th KAIST-NTU-KU Tri-Lateral Seminar on Civil Engineering*, Korea.
96. Ono, K., Mashima, M, and Kitamura, H. (1998) "Record of RC Bridge Piers Damaged during the Great Hansin-Awaji earthquake and the Analysis," *Proc. 2nd International Conference on Concrete under Severe Conditions, CONSEC'98*, Norway, pp.817-824.
97. Ono, K. (1996) "Earthquake and Lifetime," *J. Soc. Mat. Sci., Japan*, Vol.45, No.10, pp.1164-165. (In Japanese)
98. Ono, K. (1996) "Damage of Bridge Pier and Simulation," *Concrete Engineering*, Japan, Vol.34, No.11, pp.53-55. (In Japanese)
99. Ono, K., Matumura, M., Sakanishi, S., and Miyata, K. (1997) "Strength Improvement of RC Bridge Piers By Carbon Fiber Sheet," *Proc. 3rd International Symposium on Non-Metallic (FRP) Reinforcement for Concrete Structures*, Japan Vol.1, pp.563-570.
100. Ono, K., Morita. (1998) "Retrofitting of RC beam-column connections with Carbon Fiber Sheet," *Proc. 53th JSCE Annual Conference*, Japan.
101. Osada, K., Ohno, S., Yamaguchi, T., and Ikeda, S. (1997) "Seismic Behavior of Reinforced Concrete Piers Strengthened with Carbon Fiber Sheets," *Concrete Research and Technology*, Vol.8, No.1, Jan, pp.189-203 (In Japanese).
102. Park, R., and Paulay, T. (1975) *Reinforced Concrete Structures*, John Wiley & Sons.
103. Picher, F., et al. (1996) "Confinement of Concrete Cylinders with CFRP", *Fiber Composites in Infrastructure, ICCI '96*, University of Arizona, Tucson, Arizona, pp.829-841.
104. Plevris, N. and Triantafillou, T.C. (1992) "Time Dependent Behavior of RC members Strengthened with FRP Laminates," *ASCE, Journal of Structural*

- Engineering*, Vol.120, No.3, pp.1017-1042.
105. Plevris, N., et al. (1995) "Reliability of RC Members Strengthened with CFRP Laminates," *ASCE, Journal of Structural Engineering*, Vol.121, No.7, pp.1037-1044.
106. Priestley, M.J.N., et al. (1994) "Steel Jacket Retrofitting of Reinforced Concrete Bridge Columns for Enhanced Shear Strength –Part1: Theoretical Considerations and Test Design," *ACI structural Journal*, Vol. 91, No.4, July-Aug, pp.394-405.
107. Priestley, M.J.N., Seible, F., et al. (1994) "Steel Jacket Retrofitting of Reinforced Concrete Bridge Columns for Enhanced Shear Strength –Part2: Test results and Comparison with theory," *ACI structural Journal*, Vol.91, No.5, Sep-Oct, pp.537-551.
108. Priestley, M.J.N., Seible, F., and Calvi, G.M. (1996) "Seismic Design and Retrofit of Bridges," *JOHN WILEY & SONS, Inc*
109. Quantrill R. J., Hollaway L. C. and Thirne A.M. (1996) "Experimental and Analytical Investigation of FRP Strengthened Beam Response: Part I ," *Magazine of Concrete Research*, Vol. 48, No.177, pp.331-342.
110. Quantrill R. J., Hollaway L. C. and Thirne A.M. (1996) "Predictions of the Maximum Plate End Stresses of FRP Strengthened Beams: Part II ," *Magazine of Concrete Research*, Vol.48, No.177, pp.343-351.
111. Richard, A.B., and Geoffrey, C.M. (1999) "Fatigue Performance of Concrete Beams Strengthened with CFRP Plates," *ASCE, Journal of Composites for Construction*, Vol.3, No.2, May, pp.63-72.
112. Richart et al. (1928) "A study of failure of concrete under combined compressive stresses," *Bulletin 190*, Univ. of Illinois, Champaign.
113. Ritchie, P.A., et al. (1991) "External Reinforcement of Concrete Beams using Fiber Reinforced Plastics," *ACI Structural Journal*, Vol.88, No.4, pp.490-500.
114. Robert, T. M. (1989) "Approximate Analysis of Shear and Normal stress Concentrations in the adhesive layer of Plated RC Beams" *Magazine of Concrete Research*, Vol. 48, No.12/20, pp.229-233.
115. Rodriguez. M., et al. (1994) "Seismic Load Tests on Reinforced Concrete Columns

- Strengthened by Jacketing," *ACI Structural Journal*, Vol.91, No.2, pp.150-159.
116. Ross, C.A., Jerome, D. M., Tedesco, J.W and Hughes, M.L. (1999) "Strengthening of Reinforced Concrete Beams with Externally Bonded Composite Laminates," *ACI Structural Journal*, Vol.96, No.2, Mar-Apr, pp.490-500.
117. Rostasy, F.S., and Neubauer, U. (1997) "Bond Behavior of CFRP-Laminates for the Strengthening of Concrete Members," *Proc. of the IABSE Conference Composite Construction-Conventional and Innovative*, Austria, Sep, pp.717-722.
118. Saadatmanesh, H., and Ehsani, M. R. (1990) "Fiber Composite Plates Can Strengthen Beams," *Concrete International*, Vol.12, No.3, Mar, pp.65-71.
119. Saadatmanesh, H., and Ehsani, M.R. (1991) "RC Beams Strengthened with GFRP Plates. I : Experimental study," *ASCE, Journal of Structural Engineering*, Vol.117, No.11, pp.417-3433.
120. Saadatmanesh, H. (1994) "Fiber Composites for New and Existing Structures," *ACI Structural Journal*, Vol. 91, No.3, May-June.
121. Saadatmanesh, H., Ehsani, M. R., and Li, M.W. (1994) "Strength and Ductility of Concrete Columns Externally Reinforced with Fiber Composite Straps," *ACI Structural Journal*, Vol.91, No.4, Jul-Aug.
122. Saadatmanesh, H., et al. (1994) "Seismic Strengthening of Circular Bridge Pier Models with Fiber Composites," *ACI Structural Journal*, Vol.93, No.6, Nov-Dec.
123. Saadatmanesh, H., Ehsani, M. R., and Jin, L. (1997) "Repair of Earthquake-Damaged RC Columns with FRP Wraps," *ACI Structural Journal*, Vol.94, No.2, Mar-Apr.
124. Saadatmanesh, H., Ehsani, M. R., EERI, M and Jin, L. (1997) "Seismic Retrofitting of Rectangular Bridge Columns with Composite Straps," *Earthquake Spectra*, Vol.13, No.2, May, pp.281-304.
125. Saadatmanesh, H. and Malek, A.M. (1998) "Design Guidelines for Flexural Strengthening of RC Beams with FRP Plates," *ASCE, Journal of Composites for Construction*, Vol.2, No.4, pp.158-164.
126. Sakai, Y., Ugata, Y., Akiyama, Y., and Ushijima, S. (1996) "Strength Characteristics of Reinforced Concrete Slab Strengthened with Carbon Fiber-Reinforced sheet."

- Proc. Japan Concrete Inst (JCI)*, Japan, Vol.2, pp.1445-1450. (In Japanese)
127. Samaan, M., et al. (1998) "Model of Concrete Confined by Fiber Composites." *ASCE, Journal of Structural Engineering*, Vol.124, No.9, Sep. pp.1025-1031.
128. Sano, M., Miura, T (1996) "Design Method for Strengthening Concrete Members By steel Plate Bonding," *Proc. of JSCE*, No.550, Vol.33, pp.117-129. (In Japanese)
129. Sato, Y., et al. (1997) "Ultimate Shear Capacity of Reinforced Concrete Beams with Carbon Fiber Sheets," *Proc. of the 3rd International Conference on Non-Metallic (FRP) Reinforcement for Concrete Structures*, Japan, Vol.1, pp.499-506.
130. Sato, Y., Kimura, K., and Kobatake, Y. (1997) "Bond Behavior between CFRP Sheet and Concrete; Part 1," *J.Struct. Constr. Eng, AIJ*, No.500, pp.75-82. (In Japanese)
131. Scalzi, J.B., Munley, E., and Tang, B. (1999) "Will FRP Composites Change Bridge Engineering?," *Proc. of the 8th International conference and Exhibition, Structural Faults & Repair-99*, London, CD-ROM.
132. Seible, F. (1996) "Advanced Composite Materials for Bridges in the 21st Century," *Proc. of the 2nd International Conference, Advanced Composite Materials in Bridges and Structures*, Montreal, Canada, Aug.
133. Seible, F., Priestley, M.J.N., Hegemier, G.A., and Innamorato, D. (1997) "Seismic Retrofit of RC Columns with Continuous Carbon Fiber Jackets," *ASCE, Journal of Composites for Construction*, Vol.1, No.2, pp.52-62.
134. Seible, F. (1997) "Advanced Composites for Bridge infrastructure Rehabilitation and Renewal," *Proc. of the IABSE Conference Composite Construction-Conventional and Innovative*, Innsbruck, Austria, pp.741-746.
135. Sharif, A. M. et al. (1994) "Strengthening of Initially Loaded Reinforced Concrete Beams Using FRP Plates," *ACI Structural Journal*, Vol.91, No.2, pp.160-168.
136. Sharif, A., Al-Sulaimani, G.J., Basunbul, I.A., Baluch, M.H., and Husain, M. (1995) "Strengthening of Shear-damaged RC Beams by External Bonding of Steel Plates," *Magazine of Concrete Research*, Vol.47, No.173, Dec. pp.329-334.
137. Sonobe et al. (1997) "Design Guidelines of FRP Reinforced Concrete Building Structures," *ASCE, Journal of Composites for Construction*, Vol.1, No.3, pp.90-115.
138. Soudki, K.A, et al. (1996) "Performance of CFRP Retrofitted Concrete Columns at Low Temperature", *Proc. of the Second International Conference on Advanced Composite Materials in Bridges and Structures*, Canada, Aug, pp.427-434.
139. Soudki, K.A. and Green, M.F. (1997) "Freeze-Thaw Response of CFRP Wrapped Concrete", *Concrete International*, ACI, Aug, Vol.19, No.8, pp.64-67.
140. Spadea, G., et al. (1997) "Behavior of Fiber Reinforced Concrete Beams under Cyclic Loading," *ASCE, Journal of Structural Engineering*, Vol.123, No.5, May, pp.660-668.
141. Spadea, G., Bencardino, F., and Swamy, R.N. (1998) "Structural Behavior of RC Beams with Externally Bonded CFRP," *ASCE, Journal of Composites for Construction*, Vol.2, No.3, Aug, pp.132-137.
142. Spoelstra, M.R., and Monti, G. (1999) "FRP Confined Concrete Model," *ASCE, Journal of Composites for Construction*, Vol.3, No.3, Aug, pp.143-150.
143. Steiner, W. (1997) "Strengthening of Structures with Carbon Fiber Laminates," *Proceedings of the IABSE Conference Composite Construction-Conventional and Innovative*, Innsbruck, Austria, pp.723-728.
144. Swamy, R.N., Jones, R., and Bloxham, J.W. (1987) "Structural Behavior of Reinforced concrete Beams Strengthened by Epoxy-Bonded Steel Plates," *The Structural Engineer*, Vol.65A, No.2, pp.59-68.
145. Swamy, R.N., Jones, R., and Sharif, A. (1989) "The Effect of External Plate Reinforcement on the Strengthening of Structurally Damaged RC Beams," *The Structural Engineer*, Vol.67, No.2, pp.45-55.
146. Swamy, R.N., Hobbs, B., and Roberts, M. (1995) "Structural Behavior of Externally Bonded Steel Plated Reinforced Concrete Beams after Long-Term Natural Exposure," *The Structural Engineer*, Vol.67, No.2, pp.45-55.
147. Swamy, R.N., et al. (1999) "Strengthening for Shear of RC Beams by external Plate Bonding," *The Structural Engineer*, Vol.77, No.12, pp.19-30.
148. Takeda, T., et al. (1996) "Development of Retrofitting Methods for Enhancing Seismic Performance of RC piers and Base Isolation Method for Existing Bridges."

- Bridge and Foundation Engineering*, Aug, pp.119-122. (In Japanese)
149. Täljsten, B. (1997) "Strengthening of Beams by Plate Bonding," *ASCE, Journal of Materials in Civil Engineering*, Nov, pp.206-212.
150. Täljsten, B. (1998) "Strengthening of Concrete Structures for Shear with CFRP-Fabrics Test and Theory," *Proc. 2nd International Conference on Concrete under Severe Conditions, CONSEC'98*, Norway, pp.1298-1310.
151. Täljsten, B. (1999) "Concrete Beams Strengthened for Bending using CFRP-Sheets," *Proc. of the 8th International conference and Exhibition, Structural Faults & Repair-99*, London, CD-ROM.
152. Tan, K.H., Gary Ong, K.C., and Shao, Y.T. (1998) "Confinement of Beam-Column Connections with Carbon Fiber Sheets," *Proc. of the 8th KKNN Seminar on Civil Engineering*, Singapore, pp.254-259.
153. Teng, J.G et al. (1999) "Strengthening of Two-Way RC Slabs by External Bonding of Steel Plates," *Proc. of the 8th International conference and Exhibition, Structural Faults & Repair-99*, London, CD-ROM.
154. Teng. S., W.Ma, K.H.Tan, and F.K.Kong (1998) "Fatigue tests of reinforced concrete deep beams," *The Structural Engineer*, Volume 76/No8, 15 Sep.
155. Titman, D.J. (1999) "Applications of Thermography In NDT of Structures," *Proc. of the 8th International conference and Exhibition, Structural Faults & Repair-99*, London, CD-ROM.
156. Toutanji, H.A. and Rey, F. (1997) "Durability Characteristics of Concrete Columns Wrapped with FRP Tow Sheets," *Proc. 3rd International Symposium on Non-Metallic (FRP) Reinforcement for Concrete Structures*, Japan, Vol.2, pp.251-258.
157. Toutanji, H.A. et al. (1998) "Performance of Concrete Columns Strengthened with Advanced Composites Subjected to Freeze-Thaw Conditions," *Proc. of the First International on Durability of Fibre Reinforced Polymer Composites for Construction*, Canada, pp.351-359.
158. Toutanji, H., and Balaguru, P. (1998) "Durability Characteristics of Concrete Columns Wrapped with FRP Tow Sheets," *ASCE, Journal of Materials in Civil Engineering*, Vol.10, No.1, pp.52-57.

159. Triantafillou, T.C., and Deskovic, N. (1992) "Prestressed FRP Sheet as External Reinforcement of Wood Members," *ASCE, Journal of Structural Engineering*, Vol. 118, No.5, pp.270-284.
160. Triantafillou, T.C., and Plevris, N. (1992) "Strengthening of R/C Beams with Epoxy Bonded Fiber Composite Materials," *Mat. And struct.*, Vol.25, pp.201-211.
161. Triantafillou, T. C., et al. (1992) "Strengthening of Concrete Structures with Prestressed Fiber Reinforced Plastic Sheets," *ACI Structural Journal*, Vol.89, No.5, pp.235-244.
162. Triantafillou, T. C. (1997) "Shear Reinforcement of Wood using FRP Materials," *ASCE, Journal of Materials in Civil Engineering*, Vol.9, No.2, May, pp.65-69.
163. Triantafillou, T. C. (1998) "Shear Strengthening of Reinforced Concrete Beams using Epoxy Bonded FRP Composites," *ACI Structural Journal*, Vol.95, No.2, pp.107-115.
164. Uji,K., (1992) "Improving Shear Capacity of Existing Reinforced Concrete Members by Applying Carbon Fiber Sheets," *Transaction of the Japan Concrete Institute*, Vol.14, pp.253-266.
165. Van Gemert, D.A. (1980) "Force Transfer in Epoxy Bonded Steel-Concrete Joint," *Int, Jnl of Adhesion & Adhesive*, Vol.1, pp.67-72.
166. Wu, Z., Matsuzaki, T., and Tanabe, K. (1997) "Interface Crack Propagation in FRP-Strengthened Concrete Structures," *Proc. of the 3rd International Conference on Non-Metallic (FRP) Reinforcement for Concrete Structures*, Japan, Vol.1, 319-326.
167. Xiao, Y., and Ma, R. (1997) "Seismic Retrofit of RC Circular Columns using Prefabricated Composite Jacketing," *ASCE, Journal of Structural Engineering*, Vol. 123, No.10, Oct, pp.1357-1364.
168. Ziraba, I. N. et al. (1994) "Guidelines toward the Design of Reinforced Concrete Beams with External Plates," *ACI Structural Journal*, Vol.91, No.6, Nov.-Dec, pp. 639-646.
169. Zhao, W., Pilakoutas, K., and Waldron, p. (1997) "FRP Reinforced Concrete: Calculations for Deflections," *Proc. of the 3rd International Conference on Non-Metallic (FRP) Reinforcement for Concrete Structures*, Japan, Vol.2, pp.511-518.

炭素繊維シート補強 RC 床版の力学的挙動に関する研究

2000 年 3 月

朴 海 均

論文要旨

近年交通量の増加および過積載車の増加により、道路橋 RC 床版に設計値以上の荷重が載荷されており、これによる床版の損傷は著しく放置すると道路そのものの寿命を縮める状態となっている。このため、これらの床版は主に増し厚工法や鋼板接着工法で補強されてきている。しかし、これらの工法は施工が比較的困難であり、鋼板の腐食や上部工重量増加等のデメリットもある。これに対して炭素繊維シート工法はシートが軽量かつ高強度で良好な耐久性も有しており、また、施工も容易なため、今後の床版補強工法として期待される。

しかしながら、炭素繊維シートで補強した RC 床版のとくに曲げ疲労特性に関する研究はほとんどなく、この補強によって床版の寿命をどの程度伸ばせるかは不明である。

本論文は、炭素繊維シート補強した道路橋 RC 床版の力学的特性およびその補強効果を明らかにするために実施した床版の静的および疲労試験の実験的成果をまとめると共に、炭素繊維シートとコンクリート間の付着に着目した補強床版の曲げ耐力算定方法も提案したものである。

得られた主な研究成果は以下のとおりである。

- (1) 炭素繊維シート 2 層の補強によって、RC 床版の曲げ耐力を 2.4 倍程度増加させることができる。
- (2) 炭素繊維シートとコンクリート間の付着強度に基づく曲げ耐力算定式により、補強床版の曲げ耐力を十分なる精度で推定することが可能である。
- (3) 炭素繊維シート 2 層補強の寿命は、設計曲げモーメントの 3 倍の繰り返し荷重下においても湿潤状態で 5 倍程度、乾燥状態で 10 倍程度延伸させることができる。
- (4) 炭素繊維シート補強工法は道路橋 RC 床版補強に有効に適用できる。

AUTHOR'S RESEARCH ACTIVITY

1. Ono, K., Park, H.G. (1997) "Fatigue Strength of RC Bridge Slab Retrofitted with Carbon Fiber Sheet," *Proceedings of the 7th KAIST-NTU-KU Tri-Lateral Seminar on Civil Engineering*, Kyoto, Japan, pp.245-250.
2. Park, H.G., Ono, K. (1998) "Fatigue Strength of RC bridge Slab Strengthened by CFS under High Stress Level," *Proceedings of the 42th Japan Material Society Symposium*, Tokyo, Japan, pp.109-110.
3. Ono, K., Park, H.G. (1998) "Improvement of the Fatigue Strength of RC Slab in a Viaduct by Carbon Fiber Sheet," *Proceedings of the 5th International Conference on Short and Medium Span Bridges*, Canada, CD-ROM.
4. Ono, K., Park, H.G. (1998) "Retrofitting of RC Bridge Slab by CFRP Sheets," *Proceedings of the Annual Conference of JSCE*, Kobe, Japan, pp.710-711(In Japanese)
5. Ono, K., Park, H.G. (1998) "Strength Evaluation of a Laminated Composite Member," *Proceedings of the 8th KKNN Seminar on Civil Engineering*, Singapore, pp.171-176.
6. Ono, K., Park, H.G. (1998) "Fatigue behavior of RC and CFS Composite Slab under Very Large Loading," *Proceedings of the 8th KKNN Seminar on Civil Engineering*, Singapore, pp.117-121.
7. Ono, K., Park, H.G. (1999) "Strength Evaluation of RC Slab Strengthened by Carbon Fiber Sheet," *Proceedings of the 8th International conference and Exhibition, Structural Faults & Repair-99*, London, CD-ROM.
8. Ono, K., Park, H.G. (1999) "Fatigue of RC & CFS Composite Slab Under Large Repeated Load," *8th International conference and Exhibition, Structural Faults & Repair-99*, London, CD-ROM.
9. Ono, K., Park, H.G. (1999) "Interfacial Bond Behavior Between Concrete Surface and Carbon Fiber Sheet," *Proceedings of the 12th KKNN Seminar on Civil Engineering*, Korea, pp.141-146.
10. Ono, K., Park, H.G. (1999) "Flexural Strength Evaluation of a RC member Strengthened by Carbon Fiber Sheet," *Proceedings of the 12th KKNN Seminar on Civil Engineering*, Korea, pp.147-152.
11. Park, H.G., Ono, K. (1999) "Strengthening of RC Bridge Slab by CFRP Laminates," *Proceedings of the Annual Conference of JSCE, Kansai Chapter*, Kyoto, Japan. (In Japanese)
12. Park, H.G., Ono, K. (1999) "Retrofitting Effect on Damaged RC Bridge Slab by CFRP Sheets," *Proceedings of the Annual Conference of JSCE*, Hiroshima, Japan, pp.710-711(In Japanese)
13. Ono, K., Park, H.G. (2000) "Flexural Fatigue strength of RC bridge Slab Retrofitted with CFRP Sheets," *Proceedings of the 4th ACI International Conference on Repair, Rehabilitation and Maintenance of Concrete Structures, and Innovations in Design and Construction*, Seoul, Korea, Sep 19-22, 2000.
14. Koichi ONO., and H.G Park.(2000) "Flexural Fatigue Strength of Reinforced Concrete Slab in a Viaduct by Carbon Fiber Sheet," *Journal of Structural Engineering Vol.46A*, JSCE, March. (Submitted)